GIS Based Rainfall – Runoff Model for the Turasha Sub Catchment Kenya

Daniel Ochieng' Arwa
February 2001

Disclaimer

This document describes work undertaken as part of a programme of study at the International Institute for Aerospace Survey and Earth sciences. All views and opinions expressed therein remain the sole responsibility of the author, and do not necessarily represent those of the institute.

GIS Based Rainfall – Runoff Model for the Turasha Sub Catchment Kenya

By

Daniel Ochieng' Arwa

Thesis submitted to the International Institute for Aerospace Survey and Earth Sciences in partial fulfilment of the requirements for the degree of Master of Science in Water Resources and Environmental Management.

Degree Assessment Board

Prof. Dr. A.M.J. Meijerink	(Chairman)
Dr. T. Van Asch.	(External Examiner)
Drs. R. Becht	(Supervisor)
Ir. A.M. Van Lieshout	(Supervisor)

INTERNATIONAL INSTITUTE FOR AEROSPACE SURVEY AND EARTH SCIENCES ENSCHEDE, THE NETHERLANDS

Table of contents

List of Tables

List of Figures

This page is dedicated to
My Wife Lillian
And
Daughter Noella.

You were always there
To give me courage
And support

Acknowledgement

First I would like to thank the almighty for without whose blessings it would not have been possible for me to complete my studies.

I wish to extend my gratitude to my employer, Ministry of Water Resources for granting me the opportunity to study. I would like to single out the Director of Water Resources Mr. G. Chesang for his efforts to ensure that I was cleared in time to attend the course.

I am grateful to the Dutch government through the Netherlands Fellowship Program for granting me the financial support to enable me pursue the studies.

Special thanks to Drs. Robert Becht, whom besides being my supervisor, tirelessly worked hard to ensure that I managed to study at ITC and was constantly concerned about my family. He was always there for me. His commitment all through my studies was overwhelming.

I would also like to thank my other supervisor Ir. A.M. van Lieshout, Director of Studies, for his guidance and advice wherever I encountered problems in the course of my research. Thanks to Prof. A.M.J. Merjerink, Chairman of water Resources Department for his patronage. I am grateful to Dr. C. Mannaerts and Drs. N.H.W. Donker for their assistance wherever I was in need. I would also like to thank all the lecturers who were involved in disseminating the knowledge, which I am now proud of.

Mr and Mrs. Kees de Wijs, I do not know how much to thank you. You mean more to my family and me than I can express in writing. Without your support it would not have been possible for my wife to attend my graduation.

I would like to extend my thanks to the following people and organisations in Kenya

- WRAP teams both in Nakuru and Nairobi for their support in terms of Vehicles and personnel during and other logistics after the fieldwork
- Richard Okello of Panafcon for his assistance
- LNRA, KenGen, KWS, KSS, Kenya Meteorological Department and Ministry of Environment and Natural resources for providing the data
- Shell, Sulmac, Oserian, Kijabe, Sher agencies, and WWF for their financial support
- All the people within Turasha catchment who in one way or another made it possible for me to obtain the relevant data for my studies
- Staff of Wambuku Hotel, Dancing spoons and la Belle inn who provided us with the comfort during the fieldwork

Thanks to the Kenyan community in ITC who stood by me during times of sorrow and happiness especially Musyimi, Kithinji and Oduor who were always there, not forgetting Dr. Farrah who tirelessly advised me on the best approach to do scientific research

I would also like to thank my immediate family members especially my father and mother who understood the need for me to be away for studies.

Last but not least all my MSc. Colleague

Abstract

Lake Naivasha is a very important fresh water resource in Kenya. Turasha sub catchment is one of the basins within Lake Naivasha catchment contributing most of the recharge water into the lake. Almost 80% of the inflow into the lake drains from Malewa and Turasha sub catchment. Over the last decade, the lake levels have been going down and various reasons have been given as to why there is a downward trend in the levels. Some of the reasons are: over abstraction from the lake for horticultural production, inter-basin water transfer for domestic and industrial use, changes in Landuse practices in the upper catchment etc.

In order to understand the dynamics of water transfer from the upper catchment to the lake, a detailed study on the catchment characteristics was carried out to evaluate the response of streams to rainfall events in the Turasha sub catchment.

The objectives of the study was to develop a rainfall-runoff model which could be used as a tool to predict the impact of future changes in Landuse or soil characteristics to the total outflow from the Turasha sub basin given a particular amount of rainfall.

In this model, the following parameters were used as input data: Digital elevation model, Landuse map, Hydrological soil group map, and the Hourly rainfall events.

The program used was Watershed Modelling System with HEC-1 interface, and the losses were calculated based on US soil conservation services method.

To calibrate the model, hourly rainfall data within a period of 24 hours was entered into the model. The simulated output of the model was then plotted against the actual measured discharge at the gauge station until the best results were obtained.

Finally the model was applied in running different scenarios.

The study is expected to assist water use planners, decision-makers and stakeholders in the best ways to manage the available water resources within the Lake Naivasha catchment and also to predict the impact of storm runoff if there are changes in the Landuse or soil characteristics within the sub catchment.

Chapter 1 INTRODUCTION

1.1 Introduction

“Scarcity and misuse of fresh water pose a serious and growing threat to sustainable development and protection of the environment. Human health and welfare, food security, industrial development and the ecosystems on which they depend, are all at risk, unless water and land resources are managed more effectively in the present decade and beyond than they have been in the past” (ICWE 1992). These are the present and future challenges facing the water resources managers, as summarised in the Dublin statement on water and sustainable development (ICWE 1992) and adopted at the international conference on water and the environment (a preparatory conference for UNCED conference held in Rio de Janeiro in June 1992). (Abbott and Refsgaard 1996)

Rapid population growth and industrial development have caused an increasing pressure on land and water resources in almost all regions of the world. Due to increasing demand for water for domestic, agricultural, industrial, recreational and other uses and due to increasing pollution of surface and groundwater, water resources have become scarce.

The availability of good quality water is critical for human survival, economic development and the environment. Modern management approach requires improved water resources management tools based on sound scientific principles and efficient technologies. A watershed model should be seen in this context. As discussed later, watershed models are important and necessary tools in improving the water resources management.

1.2 Importance of study

According to (Clarke 1991) the total global water use was about 1000 km^3 per year in 1940. It had doubled in 1960 and doubled again in 1990. Most parts of the world will not have enough readily available water of sufficient quality and quantity at such rate of increase in consumption unless major improvements are made in water use efficiency.

Lake Naivasha is an important lake within the Kenyan rift valley system with enormous value since it

- Is a natural reservoir of fresh water
- Has a unique ecosystem
- Is a ramsar site
- Has high economic importance in terms of job creation, horticultural farming, tourism, recreation, and fishing.
- Indirectly contributes to geothermal power generation

Turasha River is a tributary to Malewa River, which is the main source of water draining into Lake Naivasha. Approximately 80% of the total inflow into Lake Naivasha is from the Malewa and Turasha sub catchment.

Besides Turasha river is the source of water to Nakuru town, which is a fast growing town both in terms of Industries and population.
Heavy and unconstrained extraction of water from Turasha River and the resulting changes in its quality and quantity can have irreversible effects on the flora and fauna in Lake Naivasha.

1.3 Research objectives

The main objective of the research is to develop a rainfall – runoff model for the Turasha catchment, which can be used as a tool for predictions and forecasting of storm events

> Predictions are estimates of the magnitude of some feature of stream flow response e.g. peak flow that is associated with a particular exceedence probability or produced by a hypothetical rainfall with a particular exceedence frequency on a given watershed.
> Forecasts are estimates of the stream flow response to an actual event that is occurring or forecast to occur, e.g. peak flow rate that will result form the rain that is forecast to occur in the next 24-h on a given watershed.

A rainfall – runoff model transforms a water input event of a given magnitude and spatial and temporal distribution into a quantitative description of stream response at a location of interest

1.4 Research approach

The rainfall runoff model for Turasha catchment is to be developed using hourly rainfall events over a 24-h period in the following steps

- Identify the type of model
- Investigate the catchment characteristics of the area i.e.
    - Rainfall intensity
    - Catchment area
    - Main stream length
    - Stream frequency
    - Catchment slope
    - Soil type and condition
    - Landuse / landcover
- Identify the software to use in analysis
- Construct the model
- Define the performance criteria
- Calibrate the model
- Validate the model
- Simulate different scenario
- Present results

Flow chart of research approach

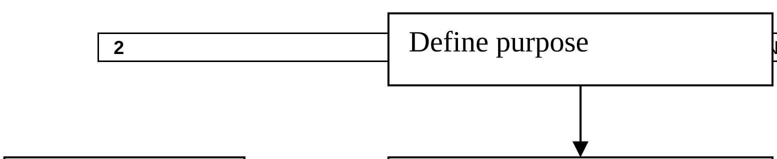

LAKE NAIVASHA BASIN

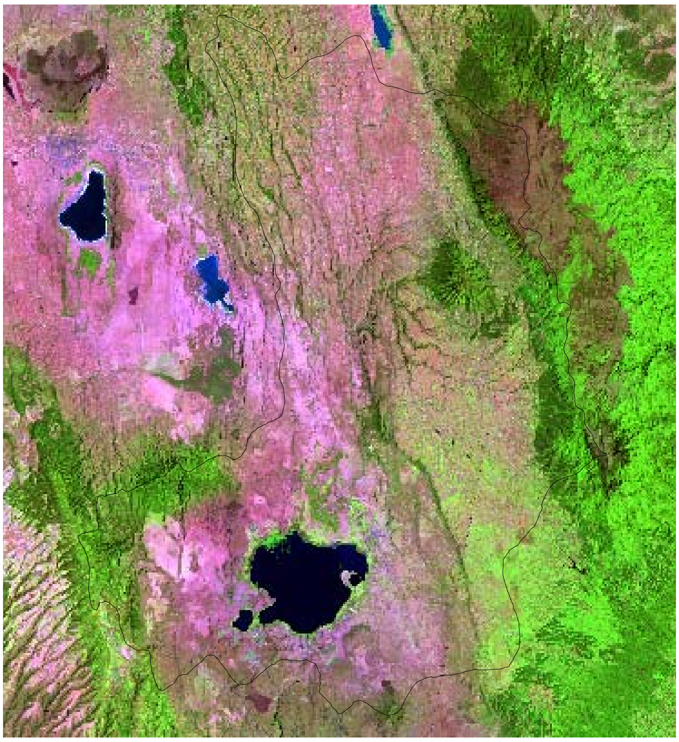

Chapter 2 GENERAL ASPECTS OF STUDY AREA

2.1 Location

The study area is situated in Nyandarua District, Central Province in Kenya within the east African section of the Great Rift Valley about 80km Northwest of Nairobi. The area is in UTM zone 37, lying between co-ordinates 210000, 245000 east, and 9919190, 9955600 north. The area is bounded by latitudes $0^0$24'04", $0^0$40'00" and longitudes $36^0$20'00, $36^0$40'00"

The study area is bounded by the Aberdare's range on the eastern side, the Kipipiri Mountain on the northeastern, the Karati escarpment to the west and the Kinangop plateau on the south.

Figure 2-1 the study area in national, Basin and sub basin contexts.

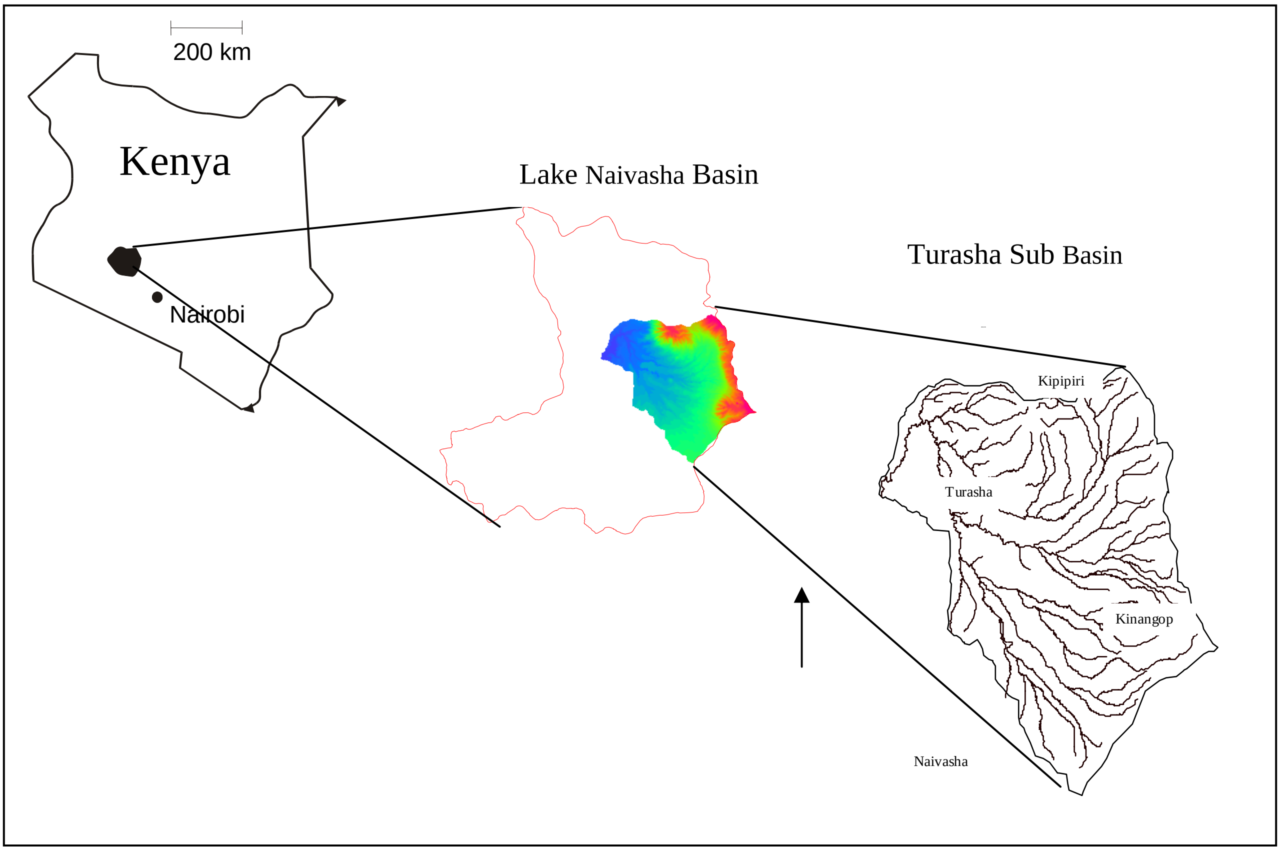

2.2 Topography and landforms

The combined geomorphological phenomena of volcanicity and other tectonic activities together with climate has resulted in the formation of extensive areas of plateau and scarps, mountains and hills in the area.

The southern part of the area is marked by the Kinangop plateau, which extends to the north ranging in elevation from approximately 2500m to 2680m. Although this landform is normally referred to as a plateau, it is a “step” on the side of the rift valley forming a plain or platform, which is approximately 16km wide. The surface of the Kinangop is conspicuously smooth. It is the marginal strip of a plain of accumulation, which formally extended from the foot of the Aberdare’s and Kipipiri across the rift valley region, and probably also eastwards across the northern end of the Aberdare’s (Shackleton 1945)

The plain is deeply dissected in the north western part of the area by the Mkungi, Kitiri, Turasha, En-gare mugutyu and other rivers all tributaries to the Malewa river which discharges to Lake Naivasha. This part of the plateau is characterised by a number of steps, which eventually form plateaus and scarps.

To the Northeast is the Kipipiri hill, which rises some 914m above the surrounding plains to 3347m. It stands apart from the main Aberdare range on the east, from which a saddle deeply trenched by the streams draining either side separates it from the Aberdare’s.

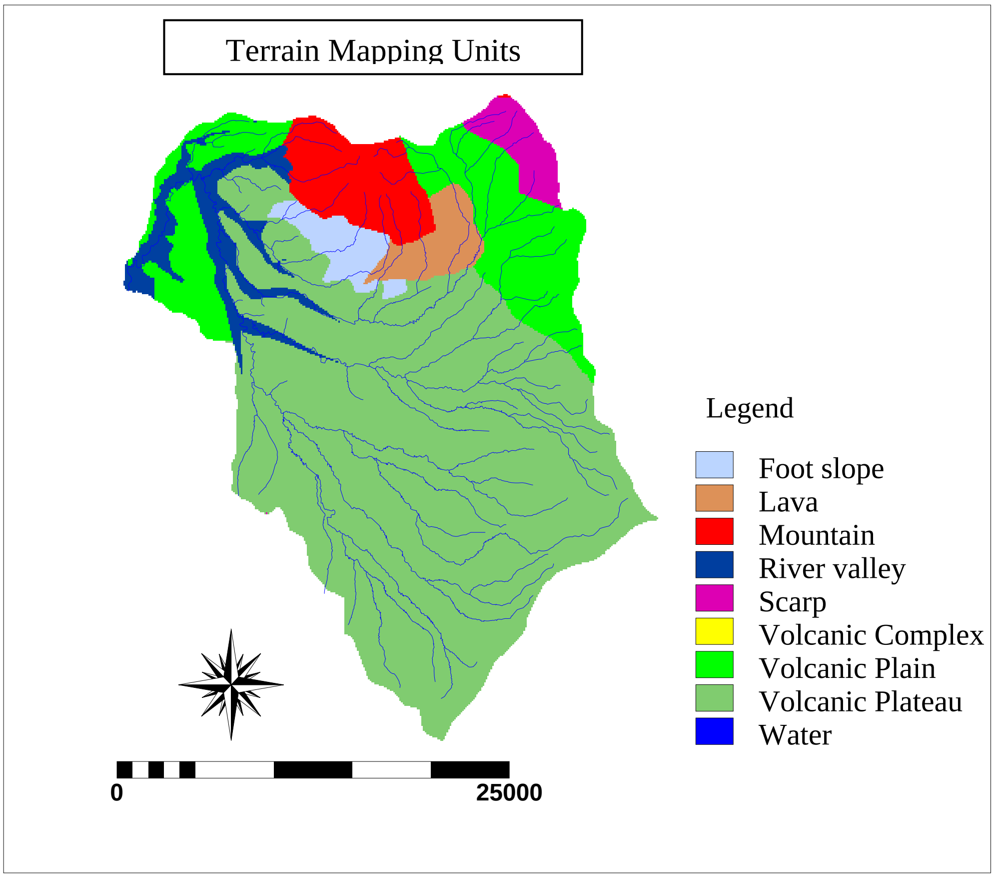

Figure 2-2 Terrain mapping units map.

2.3 Geology and paleo climate

The African rift valley is the most prominent morphologic and structural phenomenon in East Africa. In simple terms it is a deep graben divided into two clearly defined branches and the study area is located centrally in the eastern branch (also called the Gregory rift). The oldest rift structures are mid tertiary and immediately predate rift volcanism, which began in the Miocene, 23 million years BP (Chorowicz et al. 1999)

The Geology of the area is characterised by volcanic rocks and quaternary lacustrine deposits from large ancient lakes, which formed during pluvial periods, becoming shallow or completely drying during inter-pluvial

According to geological reports Numbers 12 (Shackleton 1945), 55 (Thompsons and Dodson 1958), 67 (Thompsons and Dodson 1964) and 78 (McCall 1967), the Geology of the area is mainly comprised of volcanic rocks dating back to the Miocene era.

Recent superficial deposits mainly cover the northern part of the study area. This is underlain by Pliocene tuff formations, which include citric pumice tuffs, ignimbrites and welded tuffs with lacustrine sediments, graded tuffs and diatomites. The Northeastern part consists mainly have Basalt, vesicular olivine basalt of Pliocene-Miocene era and Olivine Basalt of Miocene age, Basalt and Agglomerate of Simbara series (Predominantly in Kipipiri forest area) (Rachilo 1978). The other rocks within the study area include Trachytic tuffs and alluvial deposits along river valleys. Pyroclastics and sediments of upper to middle Pleistocene periods cover the central and southern parts of the area.

2.4 Climate

Climatic conditions in the study area are quite diverse due to considerable differences in altitude and landforms. Although the area is located within one degree of the equator and hence should experience Tropical type of climate, the altitude largely influences the relatively cool conditions.

2.4.1 Temperature

Air Temperatures are measured with Thermometers, Thermistors or Thermocouples mounted in the shelter. The shelters are designed to protect the instrument from direct exposure to solar heating. Electronic data loggers often sample air temperatures each minute and report hourly average in addition to 24-hour maximum and minimum values. The absolute maximum (Tmax) and absolute minimum (Tmin) temperatures are, respectively the maximum and minimum temperatures observed during the 24-hour period beginning at midnight.

2.4.1.1 Daily Temperature

Temperature data analysed from the automatic data loggers installed in the study area indicated the type and spatial variations of the temperature in the area. According to (Rachilo 1978), the main climatic problem in the area is the low night temperature, which is brought about by cold air, which flows from the Aberdare’s down to Kinangop during clear night causing night frost nearly every month.

Table 1: Temperature data for stations within the study area recorded within duration of two years between 1998 and 1999.

Station Name	Absolute Min. Temperature (°C)	Absolute Max. Temperature (°C)	Average Min. Temperature (°C)	Average Max. Temperature (°C)	Average Temperature (°C)
Geta Forest	1.6	31.9	5.5	24.9	13.0
Miharati Forest	3.7	29.1	7.0	23.4	13.1
Tulaga Forest	-0.2	30.7	5.6	23.6	13.0
North Kinangop	-2.0	29.1	4.5	23.3	13.3

Source: ITC temperature loggers

Table 2-1 Temperature data

NB.
Miharati data is for a short period (July 1998 – November 1998)

There are very little temperature variations within the area as shown in the table.

2.4.1.2 Monthly Temperature

From the monthly temperature data analysis for Kinangop and Tulaga weather stations for the period July 1998 to December 1999, it clearly showed very little variations.
The graph below indicates the monthly maximum and minimum values recorded in the two stations

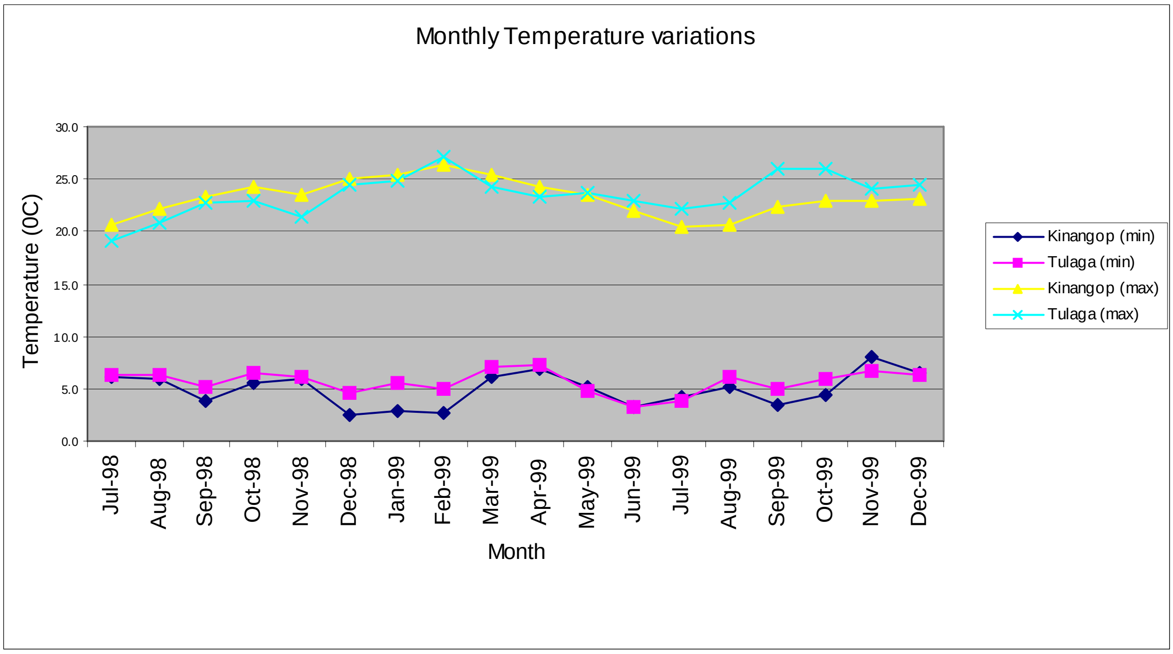

Source: ITC temperature loggers

Figure 2-3 minimum and maximum temperature graph

2.4.2 Air Humidity.

The water content of the air can be expressed in several ways. In Agronometeorology, vapour pressure, dew point temperature, and relative humidity are common expressions to indicate air humidity.

2.4.2.1 Vapour Pressure

Water vapour is a gas and its pressure contributes to the total atmospheric pressure. The amount of water in the air is related directly to the partial pressure exerted by the water vapour in the air and is therefore a direct measure of the air water content.

2.4.2.2 Dew point Temperature

The dew point temperature is the temperature to which the air needs to be cooled to make the air saturated. The actual vapour pressure of the air is the saturation vapour pressure at dew point temperature. The drier the air, the larger the difference between the air temperature and the dew point temperature

2.4.2.3 Relative humidity

The Relative Humidity (RH) expresses the degree of saturation of the air as a ratio of the actual vapour pressure to the saturation vapour pressure at the same temperature.
Relative Humidity is the ratio between the amounts of water the ambient air actually holds and the amount it could hold at the same temperature. It is dimensionless and is often given as a percentage. Although the actual vapour pressure might be relatively constant, throughout the day, the relative humidity fluctuates between a maximum near sunrise and a minimum around early afternoon. (Fig.2.4) The variation of the Relative Humidity is the result of the fact that the air temperature determines the saturation vapour pressure. As the temperature changes during the day, the relative humidity also changes substantially.

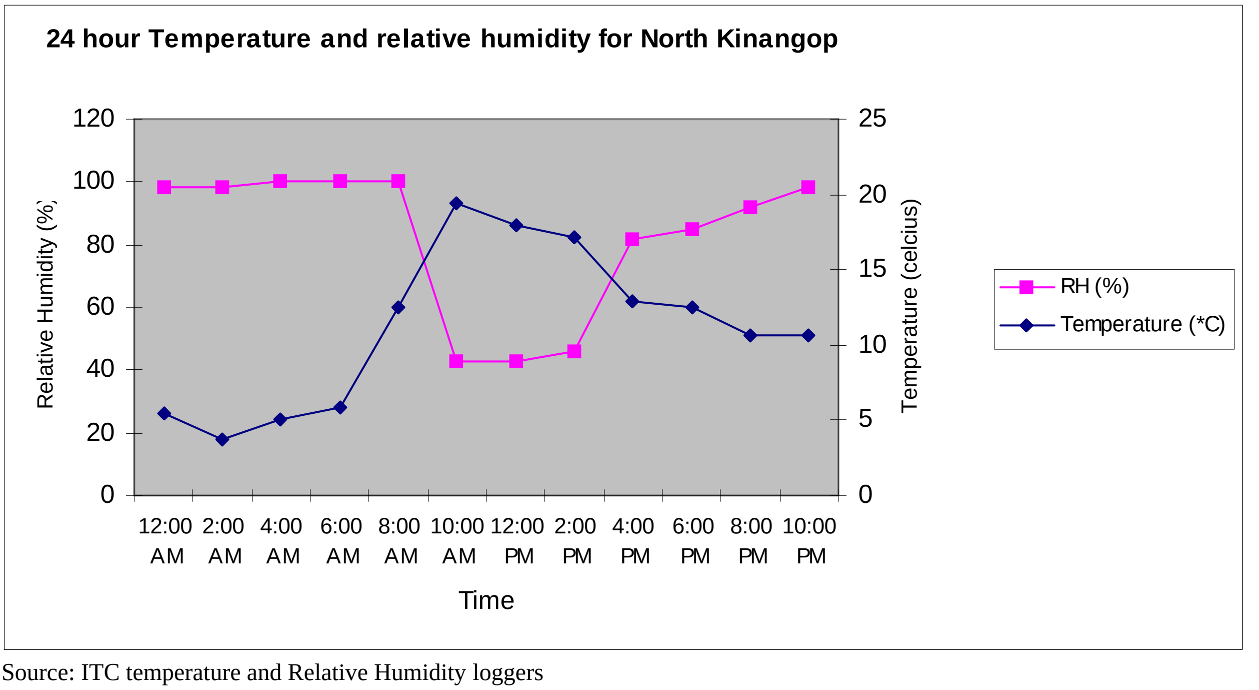

Source: ITC temperature and Relative Humidity loggers

Figure 2-4 daily fluctuations in Relative Humidity and Temperature

2.4.3 Precipitation

Precipitation is a major factor controlling the Hydrology of a region. It is the main input of water to the earth's surface and the knowledge of rainfall patterns in space and time is essential to an understanding of soil moisture, groundwater recharge and river flows. The study of precipitation is thus of fundamental importance to a hydrologist.

The rainfall pattern within the study area are subject to great spatial and temporal variations and are a subject of both the location of the area in the East African tropics (Macro-climate) and the particular topography of the region (Meso-climate). The macroclimate gives a regime of two rainy seasons per year, the "long rains" occurring in March, April and May and the "short rains" in October and November. In the study area the rainfall pattern is greatly influenced by relief with more rain falling at higher altitudes than in the valley floor.

Station Name	Station ID.	Alt. (m)	X	Y	Rain. (mm)	Data period
Naivasha WDD	9036281	2066	216172	9918875	591	1965-2000
N. Kinangop F. station	9036025	2629	236579	9935478	1075	1937-2000
Mawingo scheme	9036264	2481	223589	9944688	940	1964-1998
Geta Forest station	9036241	2588	234725	9948375	1052	1958-2000
Mutubio gate A.N.Park	9036272	3045	239876	9942222	1376	1965-1998
S. Kinangop F. Station	9036164	2588	242154	9920723	1256	1957-1998
Chokereria farmers co-op	9036129	2244	205019	9952060	707	1957-1974
Karati scheme	9036183	2618	227310	9918881	833	1957-1974
Olaragwai farm	9036262	2122	216168	9928090	639	1964-1998
Malewa farmers co-op	9036290	2481	216155	9959432	712	1969-1994
Wanjohi Chiefs camp	9036289	2466	225432	9961281	892	1969-2000

Source: Kenya Meteorological Department

Table 2-2 Rainfall stations used in analysis and the mean annual rainfall data

The study area is situated in the rain shadow of the Aberdare's hence the annual rainfall varies from 1000-1400mm per year in the eastern side to 600-800 on the western side as indicated in the graph below.

The table above gives a clear indication of the rainfall pattern within the study area. There is notably higher rainfall in stations located at higher altitudes compared to those situated at lower altitudes. For example Mutubio gate at 3045m above mean sea level receives on average above 1300mm of rain per year where as Naivasha WDD at 2066m above mean sea level receives less than 600mm per year.

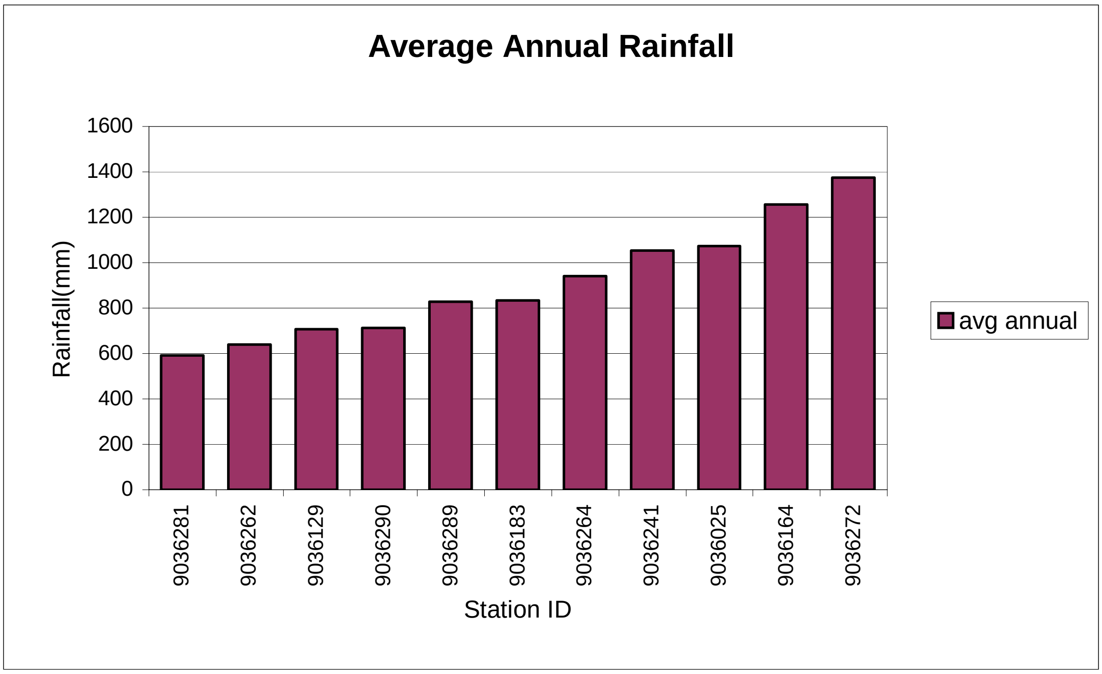

Source: Kenya Meteorological Department

Figure 2-5 Average annual rainfall for stations

2.4.4 Evapotranspiration

Evapotranspiration is the process of losing water from the soil surface by evaporation and from the crop by transpiration. In addition to knowing the amount of precipitation in an area, it is also important to know how much of it is lost through evapotranspiration. This is important in determining the water balance of an area. (Rachilo 1978)

In the study area (Turasha sub basin), the annual potential evaporation (Eo) ranges from 1400-1700mm from the eastern to the western part of the catchment (Jaetzold 1976). This puts the annual evaporation (0.8*Eo) to approximately 1100-1400mm.

Chapter 3 LITERATURE REVIEW

Remote sensing data and geographic information system are increasingly becoming an important tool in Hydrology and water resources development. This is due to the fact most of the data required for hydrological analysis can easily be obtained from Remote sensed images.

The greatest advantage of using Remote sensed data for hydrological modelling is its ability to generate information in spatial and temporal domain (Jagadeesha 1999), which is very crucial for successful model analysis, prediction and validation.

In the case of Lake Naivasha basin, remote sensed data has been used in classifying the different Geological and land cover types in the area. These data are crucial in the development of the rainfall – runoff model for the Turasha catchment within the lake Naivasha basin.

Remote sensed data could be used to monitor changes in land cover over time- temporal variation within the lake Naivasha basin. From the analysis of satellite images of the basin taken in 1996 and 2000 clearly indicate a lot of changes in land cover especially within the forested areas around the Aberdare’s. Part of the area, which was under forest cover, has since been converted to agricultural land. These changes have an impact in the flow regimes within the catchment. Reduction of area under forest cover implies a reduction in the groundwater recharge during the rainy season leading to a decrease in the base flow during the dry season.

Another important use of remote sensed data and application of geographic information system (G.I.S) is in the development of hydrological models. G.I.S provide input data for physically based hydrological models.

Hydrological modelling is a powerful technique of Hydrological systems investigation for both the research hydrologist and practising water resources engineers involved in the planning and development of integrated approach for the management of water resources (Seth et al. 1999).

According to a report by ASCE task committee on GIS modules and distributed models of the watershed (DeBarry and al. 1999), the increase in the availability of data and software for processing spatial information has changed the way people look at hydrological systems. With advances in computational power and the growing availability of spatial data, it is possible to accurately describe watershed characteristics when determining runoff response to rainfall input.

A lot of interest in distributed watershed modelling could be attributed to the invention of a number of software available in GIS for analysis such as

- Digital elevation models (DEM)
- Triangulated irregular networks (TIN)
- Digital line graphs (DLG)

Land cover maps derived from remote sensed images are the basis of hydrological response units for modelling (Seth et al. 1999). For the understanding of the hydrology of areas with little available data, a better insight into the distribution of the physical characteristics of the catchment are provided by image processing techniques.

The possibility of rapidly combining data of different types in a geographic information system has led to significant increase in its use in Hydrological applications. One of the typical applications is the use of digital elevation model for extraction of hydrological catchment properties such as elevation matrix, flow direction matrix, ranked elevation matrix and flow accumulation matrix.

From the paper by (De Silva and Taylor 1999) on spatiotemporal hydrological modelling, they argued that most of the hydrological models are numerical and computer based. They assume some form of spatial averaging process for parameter definition, where as geographic information systems models are well suited for spatial modelling with large and complex databases but have a limitation in temporal variations. Hence GIS and hydrological modelling can be considered as complimentary.

According to previous studies on the assessment of erosion in the Turasha catchment in the lake Naivasha area – Kenya by (Ringo 1999), remote sensing and GIS techniques were used. The assessment was carried out based on the terrain-mapping units (TMU), which combines the effect of rainfall, topography, soils, land cover and management practice.

A study by (Stuttard et al. 1995), on monitoring lakes in Kenya: an environmental analysis methodology for developing countries, data modelling techniques were found to be very effective in ensuring the GIS inputs to the hydrological model were correct. Maps were digitised, tabular data capture was carried out for meteorological data, Landsat images, soils and land use maps were integrated. Procedures were devised and implemented for creating a land reference unit (LRU) map and accompanying tables required for input to the hydrological model.

According to Swati Grover's paper on the perspective of GIS Modelling in Hydrology (Grover 1999), he mentioned that Modelling draws to greater or lesser degree upon the geographic tradition that hydrology; catchment and fluvial system interact closely and casually in time and space. The elements of hydrological Modelling predate GIS by more than a century. Geographic Information Systems (GIS) are highly specialised database management systems for spatially distributed data. Chow in his book. (Chow et al. 1988), offered a taxonomy of hydrological models based on the randomness (deterministic/ stochastic), spatial variation (lumped/ distributed; space independent/space dependent) and time variation (steady flow/ unsteady flow; time independent/time correlated) – thereby drawing the attention to the pivotal position of the spatial dimension explored the several possible applications of linking GIS with the hydrological models:

- Hydrological Assessment to represent hazard or vulnerability (through weighted and summed influences of significant factors rather than through physical laws)
- Hydrological Parameter Determination, whereby the GIS provide inputs to the model in terms of parameters such as surface slope, channel length, land use and soil characteristics.
- Hydrological Modelling within the GIS, provides feasible time snapshots or temporal averages are involved, not time – series.
- Linking the GIS and hydrological models to utilise the GIS as an input and display device, including real time process monitoring if the necessary (remotely sensed) observations are available.

Since GIS does not directly land itself to time varying studies, its features are utilised in hydrological studies by coupling it with hydrological models. Two types of approaches are possible for this purpose, the model driven, and data driven approach.

- In the model driven approach, a model or set of models is defined and thus the required spatial input for the preparation of the input data and output maps
- The data driven approach, it limits the input spatial data to parameters that can be obtained from generally available maps, such as topographic maps, soil maps etc.

" It is probably true that the factor most limiting hydrologic Modelling is not the ability to characterise hydrologic processes mathematically, or to solve the resulting equations, but rather the ability to specify values of the model parameters representing the flow environment accurately. GIS will help overcome that limitation."

(Ndege 1996), in an effort to examine sources of strain and water demand and supply directions in the most stressed systems of Eastern Africa, defined stressed system as a system where water quantity and quality have been jeopardised because of overuse or exploitation. The main factors that contribute to stress are population growth, irrigation and livestock watering. Others include drought, deforestation, poor land management, pollution from human activities and industry. The most critical issue in the study area is competition of the surface water not only for upstream and downstream users within the basin but also for domestic and industrial use in another basin (Nakuru).

The annual population growth in Kenya is about 2.5%-3%. This high growth rate combined with economic developments, results in ever-increasing demand for a finite resource. Hence water availability per capita is steadily decreasing.

Increased population pressure has led to deforestation and increased cultivation. This in turn is affecting the hydrological regime of the area, which may lead to increased flood and drought problems, as well as land degradation, soil erosion, and siltation problems.

In Kenya water for agricultural use commands the highest demand. It is projected that the national water demand will progressively increased from about $6*10^6$ m^3/day to $16*10^6$ m^3/day by 2010 (Ndege 1996). Of this 73% will be agriculture, 4% livestock development, 22% for domestic and industrial use, and 1% for inland fisheries and wildlife.

Chapter 4 HYDROLOGICAL DATA ANALYSIS

4.1 Precipitation

4.1.1 Introduction

All water enters the land phase of the Hydrologic cycle as precipitation. In order to assess, predict. And forecast hydrologic responses, one needs to understand how the amount, rate, duration, and quality of precipitation are distributed in space and time. Estimates of regional precipitation are critical inputs to water balance and other types of models used in water resource management. Sound interpretations of the predictions of such models requires an assessment of the uncertainty associated with their output which in turn depends in large measure on the uncertainty of the input values. (Dingman 1994)

The uncertainty associated with a value of regional precipitation consists of two parts

- That due to errors in point measurements
- That due to uncertainty in converting point measurements data into estimates of regional precipitation

4.1.2 Annual Rainfall data

Rainfall data used for the analysis was obtained from the Kenya Meteorological Department. A total of eleven rainfall stations were selected based on the aerial coverage of the area of study. The data were in a daily tabular format ranging from 1957 to 2000. This tabular data was converted into three columns of Station ID, Date, and Rainfall. The analysis of the data was done in Microsoft access where all the queries were written in SQL programming language and then exported to Microsoft excel spreadsheet for the generation of graphs and summaries. Quite often data sets containing weather variables observed at a given station are incomplete due to short interruptions in observation. The interruptions could be due to breakage or malfunction of the instrument during a certain period. Stations, which had missing data, had to be filled by using observations from a nearby and reliable station. However both data sets have to be homogeneous, in other words they need to represent the same conditions. The procedure for completing data sets is applied after the test for Homogeneity and any needed correction for no homogeneity has been performed

Below is a map of the rainfall stations within and around the study area, which have been used for analysis

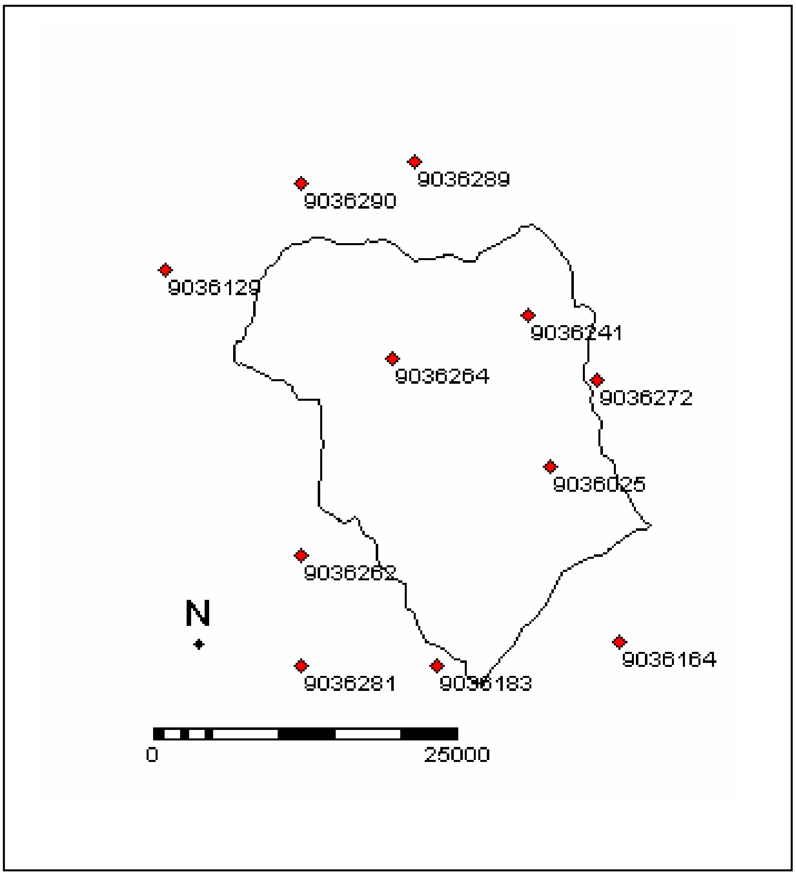

Figure 4-1 Map of Rainfall stations

4.1.2.1 Checking the consistency of the Rainfall data

Changes in the type, location, and or environment of the gauge associated with a weather station are quite common (Dingman 1994). It is therefore necessary for a hydrologist to determine whether the precipitation record are affected by such changes and to correct them if they are present so that they do not confound analysis of hydrologic relations.

The most common technique for detecting and correcting for inconsistent precipitation data is via a Double mass curve analysis. In the studies of Turasha basin, the double mass curve analysis was done specifically to check for the reliability of the rainfall data. The analysis involved plotting of successive cumulative annual rainfall collected at one-gauge verses the successive cumulative average annual rainfall for the same period of years collected at several gages in the same area. A change in the proportionality between the measurements at the suspect station and the rest of the stations is reflected in a change in the slope of the trend of the plotted points as indicated in the figures below

Once a double mass curve reveals a change in slope that is statistically significant, as in Fig 4-3 for the South Kinangop forest station (9036164), the annual values of the earlier portion should be adjusted to be consistent with the later portion before continuing with further analysis. The adjustment is done by multiplying the data for the period before the slope change with a factor K, where

K = (Slope for period after slope change/Slope for period before slope change)

Hence for the case of South Kinangop forest station the values would be multiplied by

K = (1.31/1.50) = 0.87 to produce a consistent record for the entire period of measurement.

This procedure was repeated for the rest of the stations that have details in appendix….

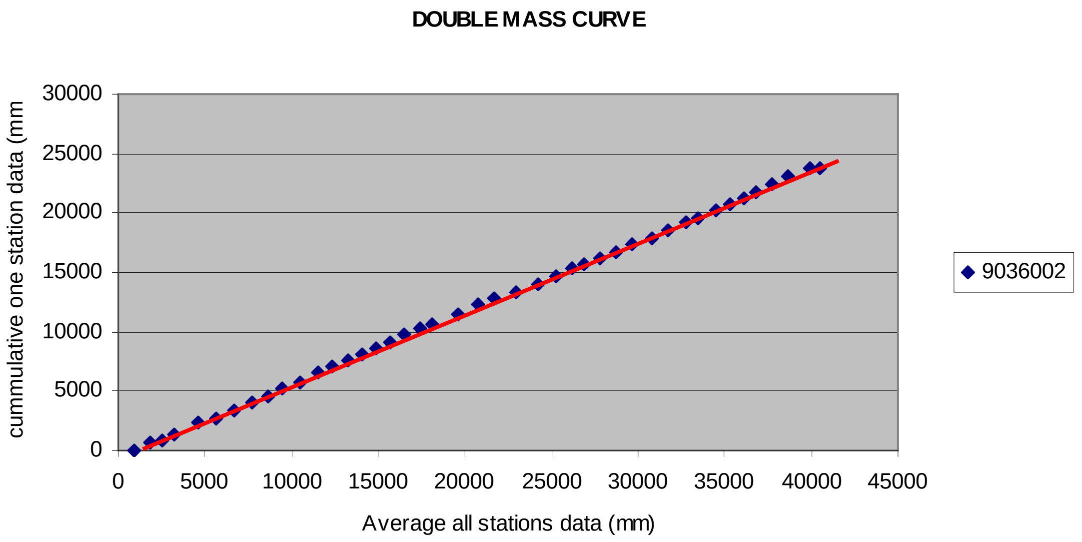

Figure 4-2 double mass curve for the Naivasha D.O. rainfall station from 1957 to 1999.

This graph shows no inconsistency, as there is no change in the trend for the plotted data.

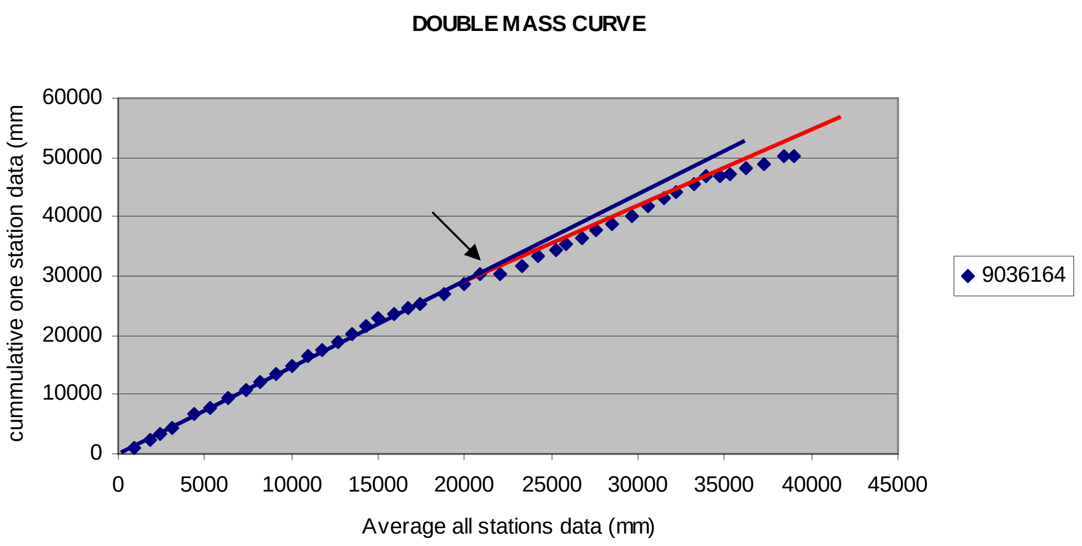

Figure 4-3 double mass curve for the South Kinangop forest rainfall station from 1957 to 1999.

This graph shows some inconsistency, as there is a change in the trend for the plotted data. The data is discontinuous. For adjustment the data before slope change should be multiplied by K=0.87.
The graph below shows both the original data and the adjusted data

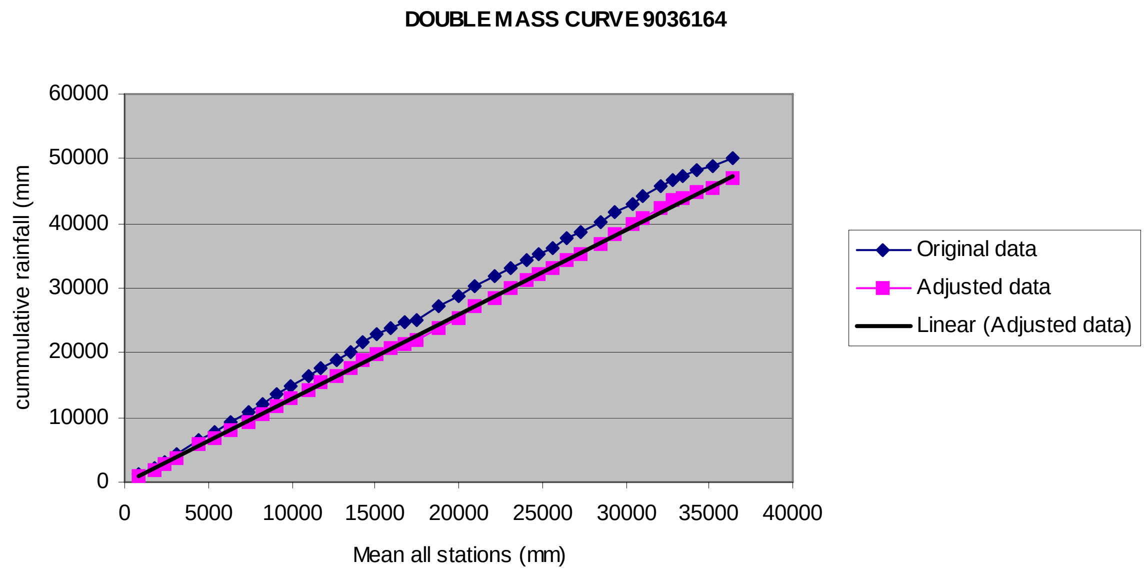

Figure 4-4 adjusted and original data for South Kinangop forest station

4.1.2.2 Missing data in the time series

Once the data had been checked for consistency and corrected for inconsistency, the data gaps had to be filled. There are many methods that exist, (Brouwer 1992) based on using the neighbouring stations such as:

- The station-year method
- The weighted average method
- The weighted distance method
- The isohyetal method

For this study the weighted average method was used for stations that had good correlation and are not far apart. The stations had data gaps not exceeding two years. Assume a station A with unknown rainfall P_A and known average rainfall $P_{avg\,A}$ and n surrounding stations with known rainfall P_n and known average $P_{avg\,n}$. the formula to estimate the missing rainfall at station A is:

$$P_A = \frac{1}{n}\left(\frac{p_{avgA}}{P_{avg1}} P_1 + \frac{p_{avgA}}{P_{avg2}} P_2 + \ldots\ldots + \frac{p_{avgA}}{P_{avgn}} P_n \right)$$

For rainfall stations with more than five years of continuous data missing, multi-regression analysis technique was applied. In the analysis station Y with missing data was plotted against six other stations X_1, X_2, $X_3 \ldots X_6$, and the linear equation obtained used to fill the missing data. Example of the analysis for station 9036281 is summarised below:

The equation is of the form

$$Y = a_1 X_1 + a_2 X_2 + a_3 X_3 + a_4 X_4 + a_5 X_5 + a_6 X_6 + C$$

SUMMARY OUTPUT
FOR 9036281

Regression Statistics

Multiple R	0.841
R Square	0.708
Adjusted R Square	0.640
Standard Error	88.225
Observations	33.000

ANOVA

	df	SS	MS	F	Significance F
Regression	6.000	490281.925	81713.654	10.498	0.000
Residual	26.000	202376.318	7783.705		
Total	32.000	692658.242			

	Coefficients	Standard Error	t Stat	P-value	Lower 95%	Upper 95%	Lower 95.0%	Upper 95.0%
Intercept C	-116.255	97.163	-1.196	0.242	-315.975	83.466	-315.975	83.466
X_1	0.227	0.125	1.815	0.081	-0.030	0.484	-0.030	0.484
X_2	0.034	0.048	0.712	0.483	-0.065	0.134	-0.065	0.134
X_3	0.066	0.059	1.126	0.270	-0.054	0.186	-0.054	0.186
X_4	0.075	0.066	1.146	0.262	-0.060	0.210	-0.060	0.210
X_5	0.032	0.084	0.386	0.703	-0.140	0.205	-0.140	0.205
X_6	0.439	0.181	2.420	0.023	0.066	0.812	0.066	0.812

Table 4-1 Multi Regression analysis results for Naivasha W.D.D. Station.

After all the analysis, below is the final summary of Annual Rainfall data for stations within and around the Turasha sub Catchment.
* Note that the station ID begins with 90…

Year	36002	36281	36262	36059	36025	36152	36164	36272	36241	36264	36129	36290	36289	36183	Grand
1957			766	695	943	1038	1165				684			680	853
1958	594	603	721	654	1096	1203	1110	1507	1153	887	792	684	892	859	911
1959	289	293	219	199	691	747	958	953	729	600	531	553	658	736	583
1960	540	548	254	230	767	839	1165	1051	804	654	462	576	699	563	654
1961	959	974	723	656	1487	1679	2222	1723	1318	1165	986	735	984	1301	1208
1962	241	245	512	464	1726	989	1262	1747	1336	1334	636	741	994	861	935
1963	721	732	767	696	1254	886	1529	1790	1369	1000	715	751	1012	819	1003
1964	676	686	730	921	1292	1230	1394	1616	1236	1027	1034	710	938	956	1032
1965	456	463	547	548	1027	1233	1398	1382	868	947	549	596	735	958	836
1966	691	447	694	484	1047	1189	1348	1292	1132	853	779	677	881	931	889
1967	627	611	804	772	1036	1070	1325	1384	923	845	581	613	765	858	872
1968	705	743	766	764	1023	1125	1582	1515	1057	836	824	654	839	892	952
1969	499	580	599	574	897	934	1208	1085	867	950	460	675	956	1015	807
1970	556	512	759	550	1063	940	1277	1329	1194	1076	959	708	860	779	897
1971	604	559	495	612	910	1046	1163	1324	1013	909	793	742	888	767	845
1972	472	486	586	456	1011	1197	1447	1188	909	956	788	543	717	943	836
1973	484	419	453	411	801	843	1244	1098	914	623	560	464	695	637	689

1974	634	574	764	693	1026	1195	955	1428	1092	872	597	479	850	812	855
1975	522	524	543	493	958	810	875	1357	1038	658	707	780	800	700	769
1976	432	331	524	475	972	935	562	1490	1140	800	770	381	610	776	728
1977	803	820	1109	1006	1659	1600	1912	2052	1570	1447	1038	852	1388	1182	1317
1978	838	890	928	842	1330	1441	1635	1680	1285	625	861	893	1060	1085	1099
1979	532	636	615	558	1008	1057	1679	1977	1076	609	731	532	748	850	901
1980	485	536	515	467	1004	1144	1297	1594	1098	822	745	609	765	904	856
1981	667	711	752	682	1358	1219	1376	1685	1344	1282	897	713	944	949	1041
1982	703	805	751	681	992	1282	1421	1640	971	1011	666	656	962	988	966
1983	560	624	600	544	1216	935	1152	665	1354	1175	904	823	1140	776	891
1984	423	420	579	525	884	764	963	950	727	489	514	500	564	672	641
1985	511	494	713	647	1188	1008	984	1515	1159	1054	782	502	567	821	853
1986	538	563	522	473	854	1472	1402	1009	779	931	546	555	662	1104	815
1987	572	528	558	506	887	2044	954	1270	557	857	408	505	573	1453	834
1988	485	527	677	614	1199	2047	1468	1616	1528	742	1012	824	1143	1455	1095
1989	656	603	636	577	1330	935	1506	1328	599	802	435	775	888	776	846
1990	695	716	713	647	1211	1079	1382	1164	1058	969	720	856	870	864	925
1991	403	479	456	414	869	717	1076	962	769	559	540	476	583	643	639
1992	667	598	616	559	1193	1202	1547	1223	1380	889	920	745	972	939	961
1993	445	437	538	488	816	967	1124	1111	647	656	464	651	653	796	699
1994	561	692	608	551	1275	1352	1532	1014	776	977	544	574	609	1030	864
1995	474	470	354	321	862	705	477	969	741	501	523	556	665	636	590
1996	691	708	498	452	864	913	959	1417	1046	891	712	651	833	763	814
1997	744	827	697	632	1041	1616	597	1656	983	722	673	631	798	1192	915
1998	687	695	670	608	1405	876	1421	1825	1401	1205	933	817	1130	740	1029
1999		512			736				576				614		610
2000															
Mean annual	582	586	627	575	1075	1131	1263	1380	1036	883	709	653	831	892	

Source: Kenya Meteorological Department

Table 4-2 Annual rainfall data

To clearly observe the long-term trend in the rainfall regime within the Turasha catchment, an annual plot for the average Rainfall for the stations was calculated from 1958 to 1999 and plotted below.

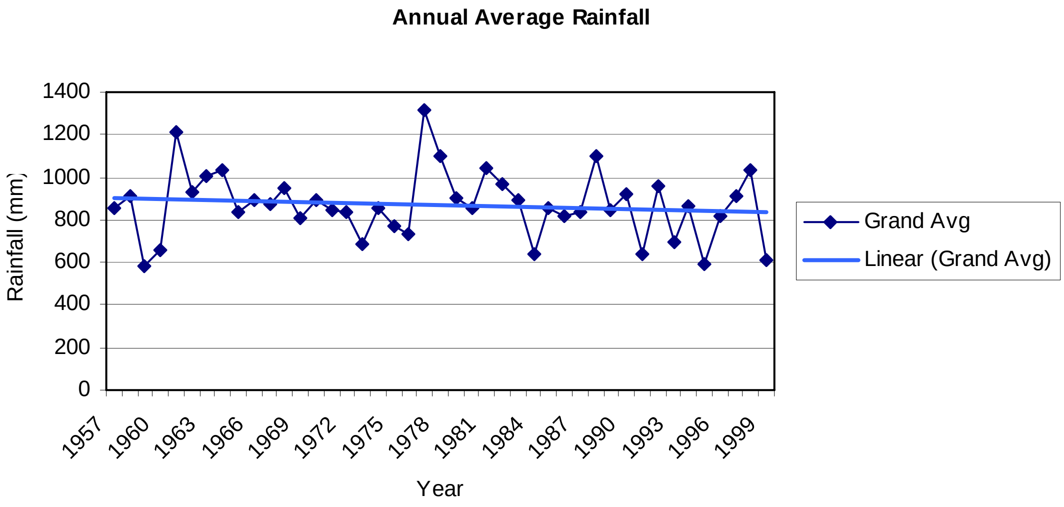

Figure 4-5 Annual rainfall trend from 1957-1999

From the graph it can be deduced that there has been a slight decrease in rainfall over the years since the trend line depicts a dip from around 900mm in 1957 to 850mm in 1999

4.1.3 Monthly Rainfall data

The rainfall within the study area is subject to great spatial and temporal variations. For clear understanding of the rainfall pattern within the study area, three rainfall stations covering the western, central and Eastern parts of the study area were selected for analysis. These stations have different elevations and geomorphology.

- Olaragwai-9036262 farm in valley bottom (2122m above sea level)
- Mawingo scheme-9036264 in the Kinangop plateau (2415m above sea level)
- Mutubio gate-9036272 in the Aberdare's mountain (3045m above sea level)

Month	9036262	9036264	9036272
January	36	43	61
February	44	35	73
March	53	46	109
April	111	159	184
May	76	148	159
June	55	97	133
July	38	71	108
August	51	88	129
September	36	74	130
October	56	196	160
November	65	77	131
December	40	44	64

Source: Kenya Meteorological Department

Table 4-3 Monthly Rainfall data

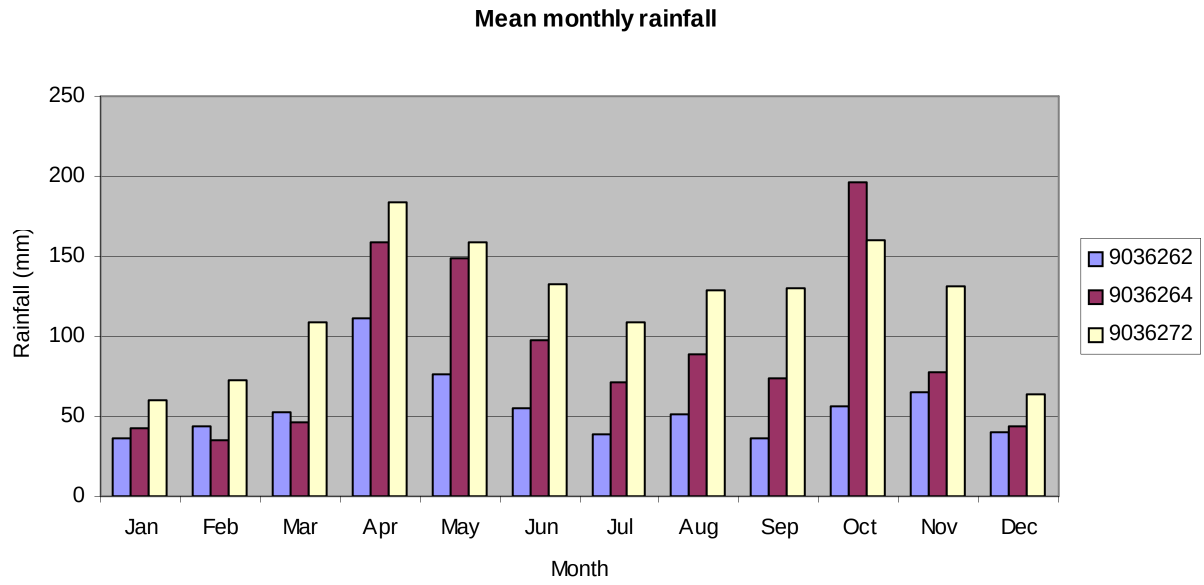

Figure 4-6 Graph of Long-term average rainfall

The figure above indicates clearly that the rainfall pattern differs widely across the study area, with notably higher levels of rainfall occurring at the stations located at higher altitudes compared with those situated in valley floor. The study area being in the East African tropics experiences macro-climatic conditions that give rise to two rainy seasons per year. The long rains occur in march- June and the short rains in October-November as shown in figure 4-6.

4.2 Stream flow analysis

4.2.1 Annual Stream flow analysis

Frequency analysis was done for the discharge data collected from Turasha River at station 2GC4, which is the outlet of the Turasha catchment. Daily discharge data from 1953 to 1999 was processed to obtain the annual maximum daily discharge as summarised in the table below (Discharge in m^3/sec). This analysis was done to predict the likely occurrence of a particular flood.

	0	10	20	30	40
1	2.50	65.71	7.15	14.90	45.58
2	16.03	13.47	51.00	12.59	66.59
3	20.58	12.79	25.81	24.32	64.83
4	48.76	26.32	8.60	62.25	63.96
5	16.81	62.25	63.96	19.70	107.53
6	65.71	39.08	47.30	56.46	117.29
7	13.82	16.03	30.62	19.70	8.29
8	6.61	28.43	21.94	63.10	
9	56.46	22.87	57.27	58.08	
10	53.30	18.85	64.83	41.71	

STATISTICS:
Number of observations: 47 Maximum Value: 117.29
Minimum Value: 2.50

	Untransformed Data:	LOG 10 transformed Data:
Mean	38.973	1.471
Standard Deviation	26.360	0.359
Skew Coefficient	0.819	-0.696

The Histogram of the maximum discharge data produced a skewed distribution, (the mean did not co-incide with the median), as shown in figure 4-7, hence Log Pearson Type III distribution was preferred in the analysis.

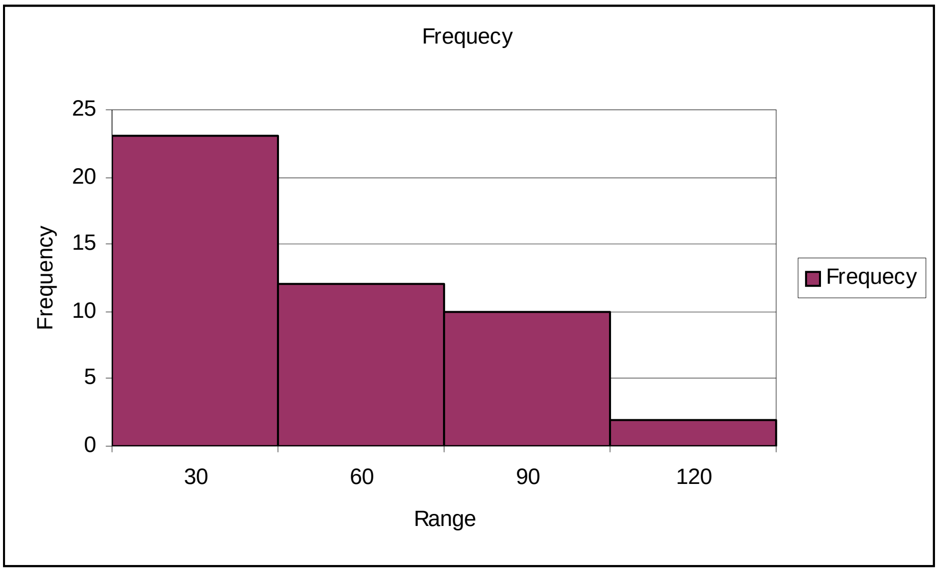

Figure 4-7 Frequency distribution of the maximum discharge data

- Mean = 38.9
- Median = 30.6
- Mode = 16.0

The analysis of the frequency distribution of the Hydrological data was done using the Rankplot program developed in ITC, ((Donker 1996)). The procedure used was based on Semi Graphical method and on Log Pearson III distribution as follows.

- The data are ranked from high (R=1) to low (R=N)
  - R = Rank, N = Number of observation
- The probability are calculated using R/(R+1)

- The data is then plotted on the Normal logarithmic graph paper
- A best fit line based on reduced major axis procedure is constructed through the data
- Once a fitted distribution is obtained, the best-fit line can be used to find the return period corresponding to a selected discharge

The figure below shows the result of the Turasha data

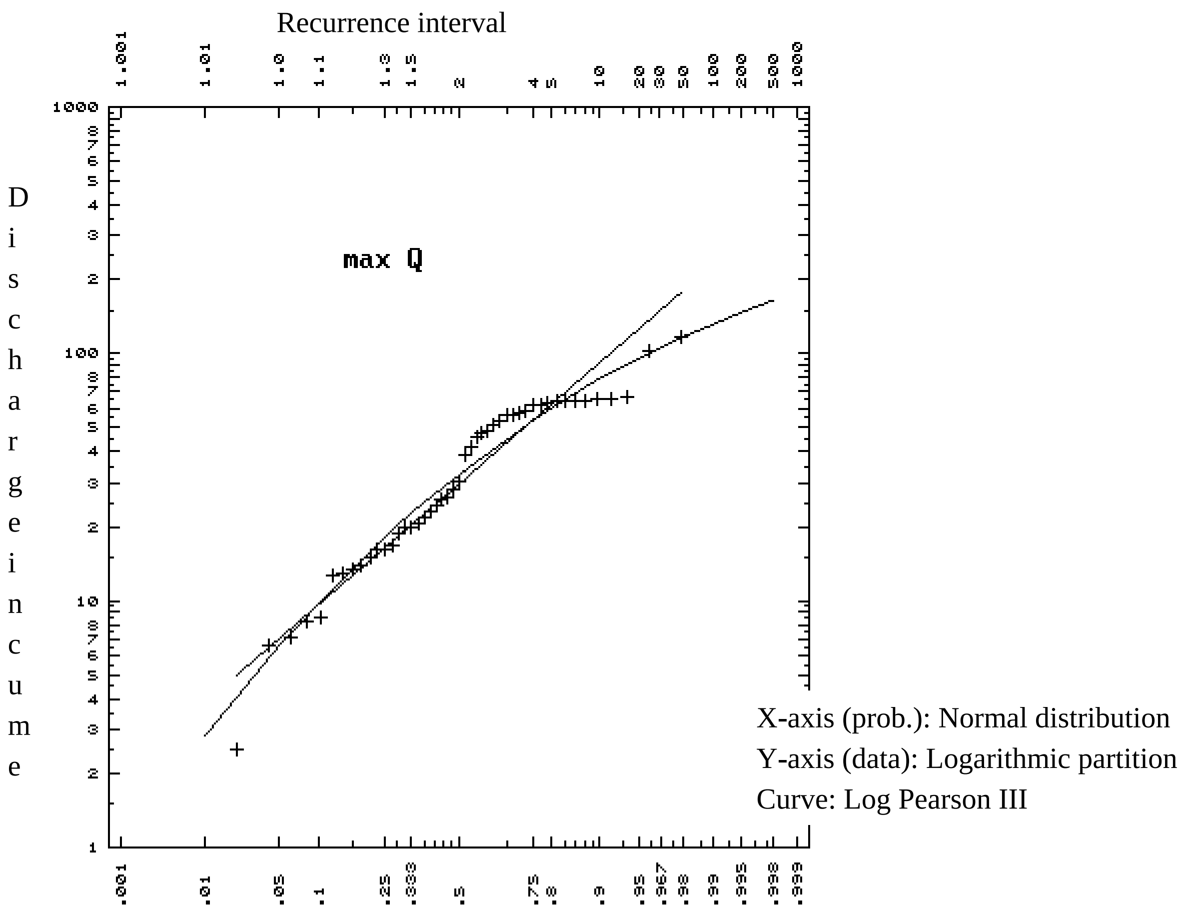

Figure 4-8 Annual maximum discharge data for Turasha River from 1953-1999

Since Log Pearson III distribution was used in the analysis, the magnitudes corresponding to the return periods are obtained by calculation and not by means of the "Graphical fit". The calculations are based on statistical moments of the distribution: mean, standard deviation, and skewness of the log transformed data. The equation used is as follows

$$Q_r = \mu_x + K^I \sigma_x \ldots (4.1)$$

Where

- Q_r = discharge corresponding with return period r
- μ_x = the average of the log transformed data
- σ_x = the unbiased estimate of the standard deviation of the log transformed data
- K^1 = selected from the table for the particular probability r and skew C_s.

This table is found in Chow (1988). In the program RANKPLOT the values for K^1 are calculated by the following approximation

$$K^1 = Z + (Z^2 - 1)k + \frac{1}{3}(Z^3 - 6Z)k^2 - (Z^2 - 1)k^3 + Zk^4 + \frac{1}{3}k^5 \quad \text{…. (4.2)}$$

Where

- $k = C_s/6$
- C_s = coefficient of skewness
- Z = the standard normal variable for the probability

Based on the above equation the program calculated the following values for the given return periods

Return Period	**Discharge (m^3/s)**
500 years	164.0
200 years	146.7
100 years	132.5
50 years	117.4
25 years	101.4
5 years	59.9

Table 4-4 Return period for maximum discharge of Turasha River.

4.2.2 Daily Stream flow analysis

The water level data recorded by the automatic logger at the gauge station in Turasha, 2GC4, was corrected for Barometric pressure difference before conversion to hourly discharge. The graph below shows the Diver data before and after correction for the atmospheric pressure difference. Note the effect of the corrections, the small sharp crests have been smoothened.
After correction for the Barometric pressure, the divers data was then plotted against the manually recorded data to try and see the behaviour of the two data sets in case they show a similar pattern. What was observed from this analysis is that there are times both data sets depict the same trend and at times they are not correlated at all. It was difficult to actually explain this kind of systematic difference since it could have resulted from the instrument or unreliable manual observation.

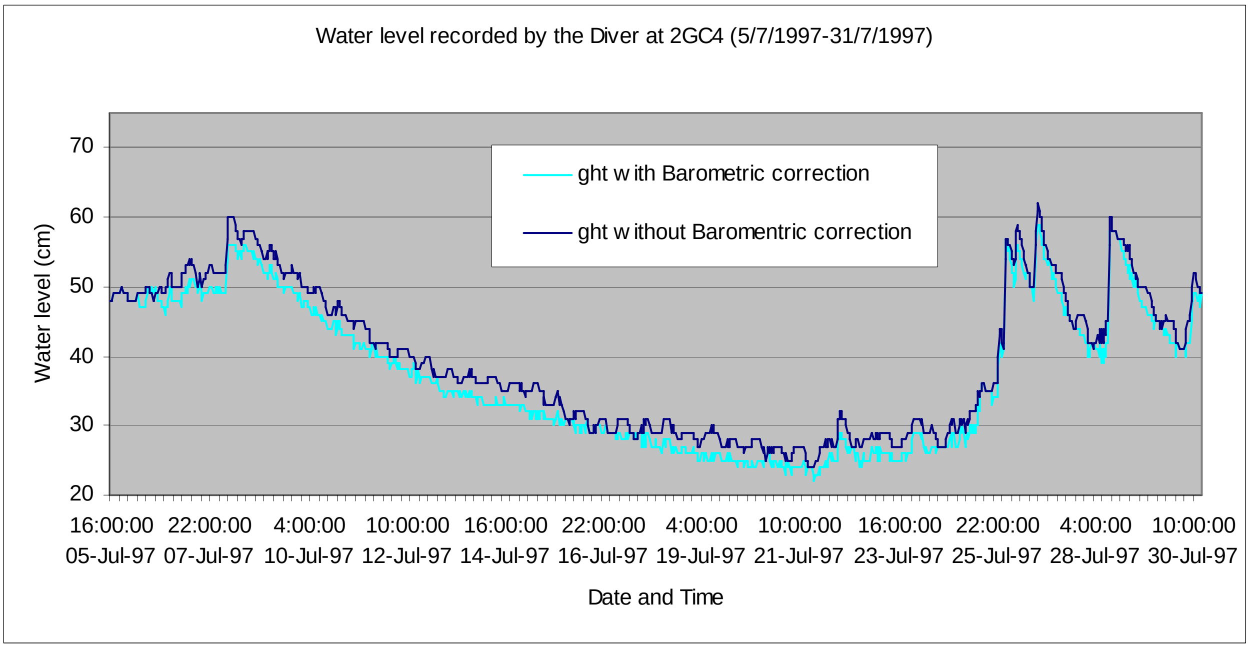

Figure 4-9 Comparison between corrected and raw data recorded at 2GC4.

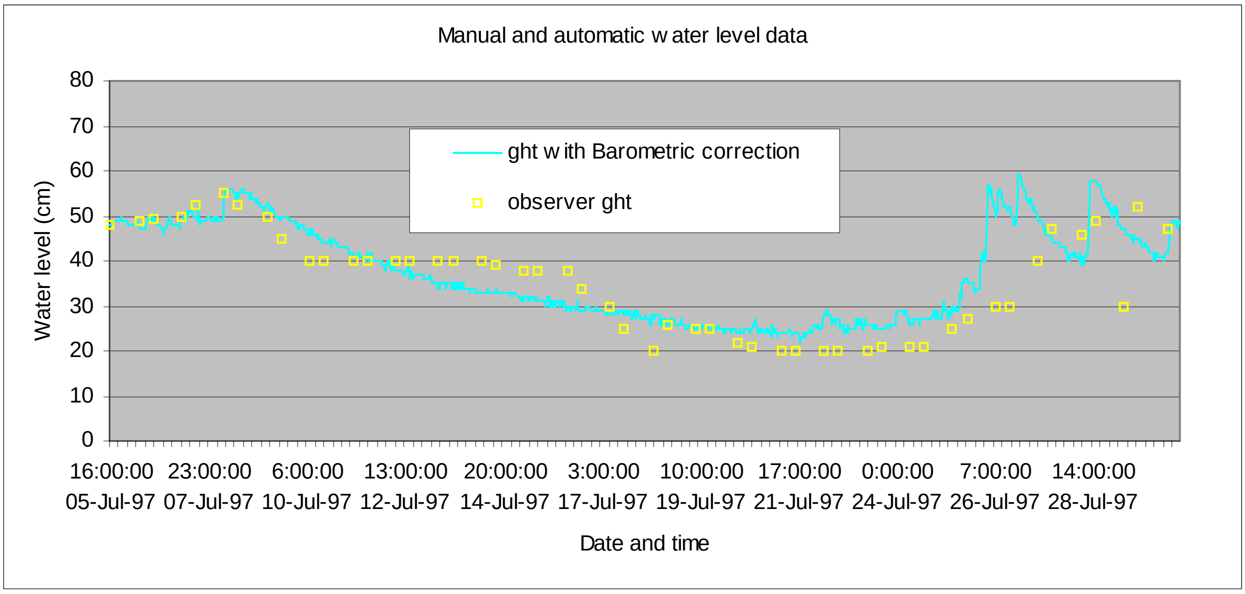

Figure 4-10 Manual and automatic water level data relation.

These hourly water column values were then converted to discharge values using the following rating equations.

$$Q = aH^{b} \quad \ldots(4.3)$$

Where

Q = Discharge (m^3/s)

a = A_constant
b = B_constant
H = water level (m)

Below is the rating table used for the conversion of hourly water levels to hourly discharges.

ID	RP	SDATE	EDATE	SEG	LWL	HWL	A_CONST	B_CONST	DH
2GC04	1	26-Jul-50	31-Dec-99	1	0	0.03	4.4478	1.4429	0
2GC04	1	26-Jul-50	31-Dec-99	2	0.03	0.46	5.656	1.5118	0
2GC04	1	26-Jul-50	31-Dec-99	3	0.46	0.91	16.2808	2.8627	0
2GC04	1	26-Jul-50	31-Dec-99	4	0.91	1.83	15.6462	2.4185	0

Table 4-5. Rating table for station 2GC4.

The computed flow data from the data loggers was compared with the daily flow data from the manual observations for the month of August 1997 to January 1998 as shown in the graph below.

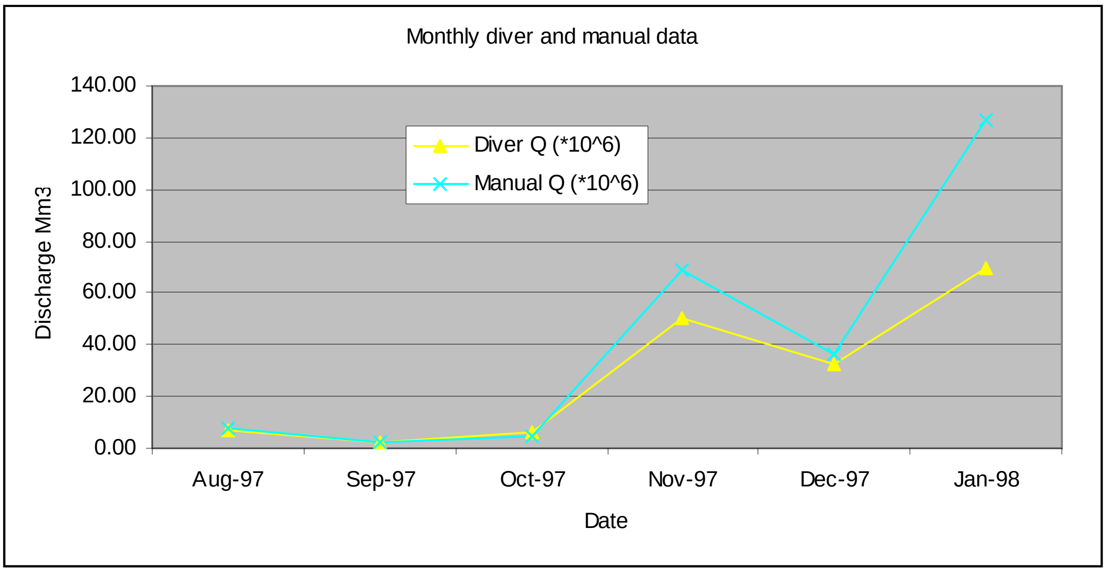

Figure 4-11 Monthly discharge data computed from the two data sets.

From the analysis one can deduce that there is either an over estimation by the manually observed data or an under estimation by the automatic data logger during the wet periods. But during the low flow season there seems to be less discrepancies in the two data sets.

.

4.3 Soils

The soils map was prepared by digitising the preliminary soils map of the Kinangop area from Report no.34 on the soils of the Kinangop area (Rachilo 1978). The map grids were in latitude/longitude and a scale of 1:100000. The map segments were then transformed to UTM and resampled to the correct orientation.
The description of the soils unit follows the legend as shown in the soil map below

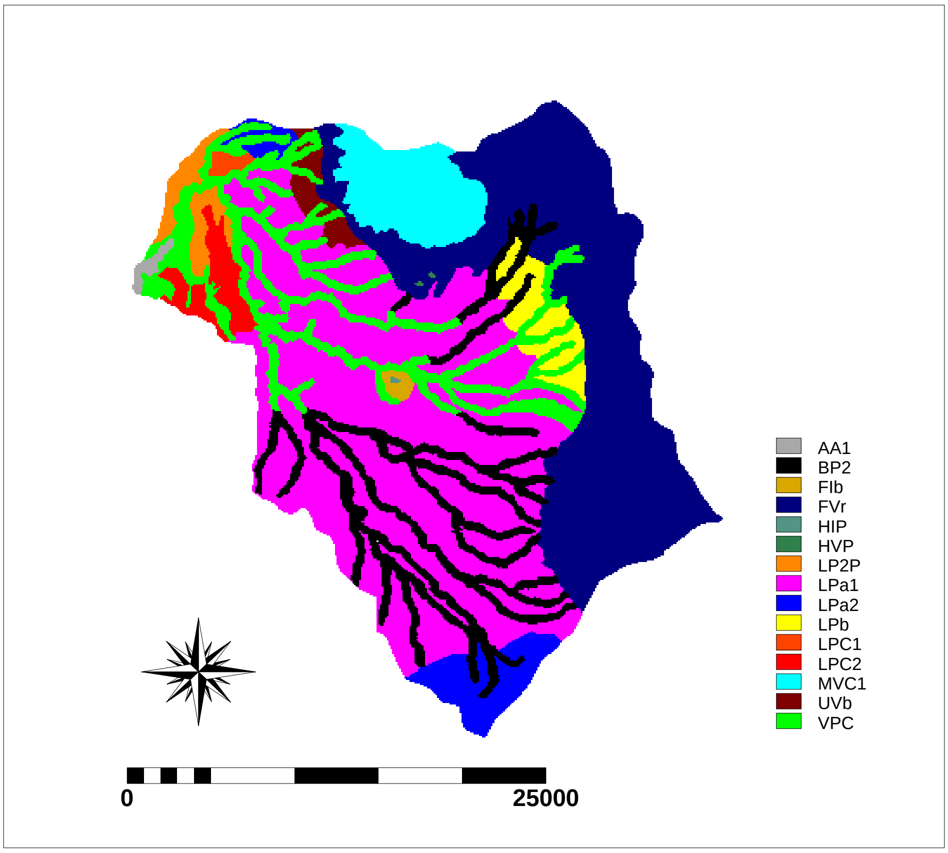

Source: Kenya soils survey

Figure 4-12 Soil map of the Turasha sub basin

Description of the soil units

- **Unit AA1 Soils of river alluvial plains and terraces**

These soils are developed on alluvium from undifferentiated volcanic rocks. They are moderately well drained, very deep, dark brown to very dark greyish brown, stratified, firm, calcareous clay

- **Unit BP2 Bottomland soils**

These soils are developed on alluvium/colluviums from pyroclastic rocks (tuffs). They are imperfectly drained to poorly drained, deep, very dark grey to greyish brown, mottled firm clay.

- **Unit F1b Footslopes**

These soils are developed on colluvium derived from trachytes. They are moderately well drained, very deep, dark reddish brown, firm clay

- **Unit FVr Footslopes**

These soils are developed on colluvium derived from undifferentiated volcanic rocks. They are well drained, deep to very deep, reddish brown, friable, clay to gravely clay.

- **Unit Hip Hills and minor scarps**

These are soils developed on trachytes. The soils are well-drained, shallow, dark reddish brown, rocky clay

- **Unit HVp Hills and minor scarps**

These are soils developed on undifferentiated volcanic rocks. They are well drained, shallow to moderately deep, dark brown to black, rocky, clay loam to loam

- **Unit LP2 Dissected plateau's**

These are soils developed on pyroclastic rocks (tuffs). They are well drained to moderately well drained, shallow to moderately deep, dark brown to dark greyish brown, firm clay, in places calcareous, stony and rocky.

- **Unit LPa1 Non dissected plateau's**

These are soils developed on pyroclastic rocks (tuffs). They are imperfectly drained to poorly, deep, very dark greyish brown, mottled, friable to very firm clay, abruptly underlying 45-55cm of silty clay loam to clay loam, with many iron-manganese concretions at transition.

- **Unit LPa2 Non dissected plateau's**

These are soils developed on pyroclastic rocks (tuffs). They are poorly drained, deep, very dark greyish brown to very dark grey, mottled, very firm clay, abruptly underlying 30-45cm of silty clay loam to clay loam, with common iron-manganese concretions at transition.

- **Unit LPb Non dissected plateau's**

These are soils developed on pyroclastic rocks (tuffs). They are moderately well drained, deep, dark reddish brown to strong brown, mottled firm clay.

- **Unit LPC1 Dissected plateau's**

These are soils developed on pyroclastic rocks (tuffs). They are complex of:

    - Moderately well drained, deep to very deep, dark brown to very dark greyish brown, very friable to friable, clay loam
    - Imperfectly drained, deep, very dark greyish brown to black, firm, calcareous cracking clay.

    - **Unit LPC2 Dissected plateau's**

These are soils developed on pyroclastic rocks (tuffs). They are complex of:

- Moderately well drained, deep dark brown to very dark greyish brown, firm calcareous cracking clay
- Moderately well drained to imperfectly drained, deep, very dark greyish brown to black, firm calcareous cracking clay.

- **Unit MVC1 Mountains and major scarps**

These are soils developed on undifferentiated volcanic rocks. They are well drained, shallow to moderately deep, stony and very rocky soils of varying colours and texture.

- **Unit UVb Uplands**

These are soils developed on undifferentiated volcanic rocks. They are well-drained, very deep, dark reddish brown to very dark greyish brown, friable clay.

- **Unit VPC Valleys**

These are soils developed on pyroclastic rocks. They are well drained, shallow to moderately deep, dark brown to very dark brown, friable clay loam to clay.

4.4 Classification of the soil map in terms of Hydrologic soil group

The soil type map was then reclassified using the slicing operation in ILWIS according to Hydrologic Soils Groups as defined by U.S. Soil Conservation Service (1964) [a].
The table below shows the SCS classification

Soil Group	Characteristics
A	Low overland flow potential, High minimum infiltration capacity even when thoroughly wetted (>0.76 cm/h), Deep, well to excessively drained sands and gravel
B	Moderate minimum infiltration capacity when thoroughly wetted (0.13-0.76cm/h) Moderately deep to deep, Moderately to well drained, Moderately fine to moderately coarse grained (e.g. sandy loam)
C	Low minimum infiltration capacity when thoroughly wetted (0.13-0.38cm/h) Moderately fine to fine grained soils or soils with an impeding layer (fragipan)
D	High overland flow potential: Very low minimum infiltration capacity when thoroughly wetted (<0.13cm/h) Clay soils with high swelling potential, Soils with permanent high water table, Soils with a clay layer near the surface, Shallow soils over impervious bedrock.

[a] Minimum infiltration capacities given should approximate saturated hydraulic conductivities.
Source: Dingman, S.L (1993). Physical hydrology.

Table 4-6 hydrologic soil groups

The final map is shown in appendix A.

4.5 Landuse

4.5.1 Introduction

In its simplest form, the hydrological cycle involves precipitation, evaporation and condensation. However, this simple cycle is in reality modified in many ways depending on the ground surface (Ward and Robinson 1990). Hydrological models therefore do not only require meteorological data, but also spatially distributed data about topography, hydrology, soil physics and land use. These can be used to derive model parameters like slope, soil moisture, surface runoff, infiltration and Evapotranspiration.
Land use information is a basic input to the hydrological model describing the Turasha sub catchment

4.5.2 Preparation of the land use map

In the creation of the land use map, the following maps and data were used

- Satellite images

	Image_1	Image_2
Source	Landsat TM	Landsat TM
Bands	1,2,3,4,5,6,	1,2,3,4,5,6,
Date	February 2000	May 2000
Pixel size	30m*30m	30m*30m

- Topographic maps

Sheet	Title	Scale	Date
133/2	Naivasha	1:50000	1975
120/3	Kipipiri	1:50000	1975
119/4	Gilgil	1:50000	1975
134/1	Kinangop	1:50000	1975

These maps were scanned.

- Aerial photographs – scale 1:50000 dated 1984
- Ground truth data collected during the fieldwork period September/October 2000.

Procedure

4.5.2.1 Geometric correction

Digital images are usually not geo-referenced. The two images were geometrically corrected using a set of ground control points (GCP) identified on the images and on the scanned 1:50000 scale maps of the study area. A total of 40 GCP were identified and using the master and slave technique tied the points on the image to the points on the topographic maps. The images were then resampled by applying the nearest neighbour algorithm using the utilities of ERDAS-imaging software.
The two images were then glued together.

4.5.2.2 Cover classification using remote sensing and field data

The objective of automated classification is to group the spectral information contained in the bands of the multispectral imagery, in such a way that they coincide with known ground cover that have been defined for their hydrologic relevance. A false colour composite was used for the visual examination and interpretation as this band combination proved to be very suitable for visual distinction of all the classes. Several training samples were selected for the areas that had homogeneous land cover classes. The selection of the best performing training samples was iterative, using empirical (visual) criteria for the judgement of the discriminative potential of the spectral signature.
In areas where there was no distinct spectral signature within the land cover types as a result of mixed pixels, then the ground truth data was used and on screen digitising technique applied to clearly demarcate the classes. Seven classes were identified

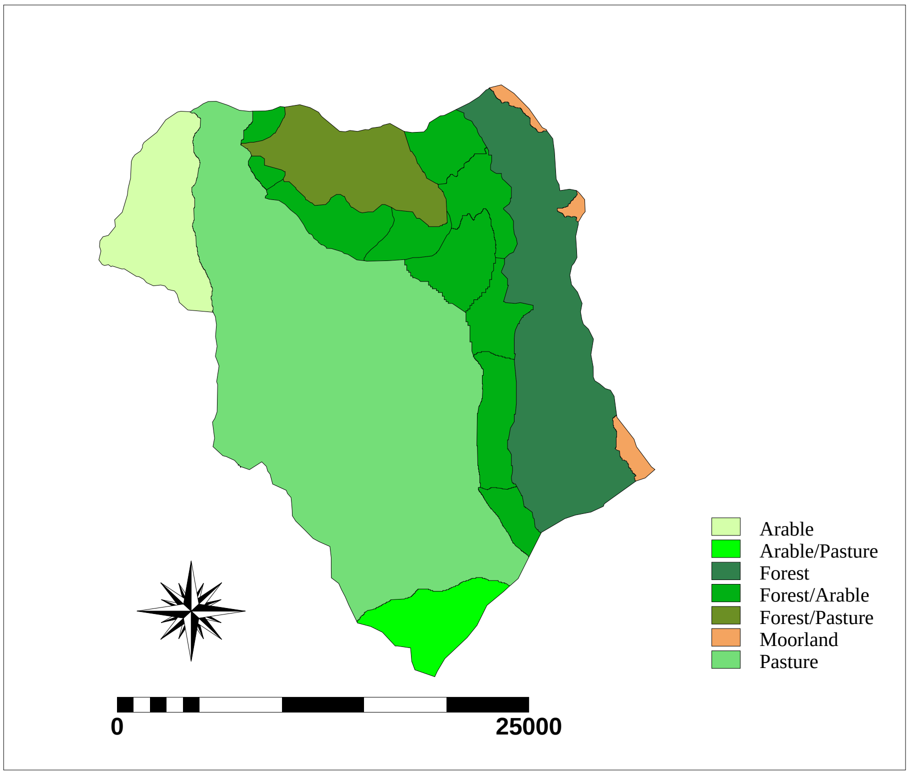

Figure 4-13 Land use map for Turasha sub catchment

4.5.2.3 Land Cover data as collected in the field

Arable	- Maize, potatoes, beans, peas, kale, castor, sunflower, wheat, onions
Arable/Pasture	- dairy cattle, sheep grazing, peas, potatoes and vegetable in some parts
Forest	- natural forests, bamboo
Forest/Arable	- where the forests are cleared, the unit is predominantly maize, carrots, onions, and potatoes
Forest/Pasture	- where the forests are cleared, peas and pyrethrum are cultivated, also cattle grazing
Pasture	- cattle and sheep grazing. In parts pyrethrum, peas, potatoes are cultivated.

- Also quarrying

Moorland - Peat, and peaty soils

The final map is shown in appendix A.

4.6 Infiltration tests carried out in the field

To clearly understand the dynamics of the soil, infiltration tests were carried around the catchment in selected sites with different hydrological characteristics. Infiltration is the process by which water arriving at the soil surface enters the soil. The main objective of carrying out the test was to estimate infiltration rate (f) as a function of time (t) during water input event. Infiltration rate varies between an initial high value and a lower constant value after some time of infiltration. Double ring infiltrometer and inverse auger methods ware used and below is a summary of the results obtained.

Site No.	X-co-ordinate	Y-co-ordinate	Land cover	Soil type	Lithology	Infiltration rate (cm/hr)	Date
1	222277	9949536	Cypress forest	Silt loam	Volcanic tuffs	12	30/9/2000
2	236666	9946298	Bamboo forest	Clay loam	Volcanic tuffs	Rainy	23/9/2000
3	221728	9930362	Pasture	Clay loam	Volcanic tuffs	2.4	18/9/2000
4	207473	9964142	Arable pasture	Clay loam	Volcanic tuffs	3.6	21/9/2000
5	213162	9964552	Arable pasture	Loam gravel	Volcanic tuffs	2.4	22/9/2000
6	211754	9964696	Arable	Loam	Volcanic tuffs	1.8	22/9/2000

Table 4-7 Infiltration tests

Infiltration of water into an unsaturated soil is influenced by both capillary and gravity forces, but the water applied within an infiltrometer ring moves laterally as well as vertically, hence the measured infiltration rate normally exceeds the rate that would be obtained if the entire surface were ponded. Also infiltration capacities of soils tend to have considerable spatial variability, so the value for a given soil should be the average of several measurements. Burgy (Burgy R.H and D.C. 1964) found that the average of six single ring infiltrometer measurements of infiltration capacity was within 30% of the true value for a soil with uniform characteristics. Due to the limited time available for the fieldwork, it was not possible to carry out as many infiltration tests within soils with the same characteristics so as to get the average value.
High infiltration rates recorded in the forest area (12cm/hr) could be as a result of organic surface layers. The ground surface usually consist largely of leaf litter, humus and other organic matter that has a large number of large openings, and hence a high hydraulic conductivity, regardless of texture of the mineral soil. Root growth and decay and the action of worms, soil insects, and burrowing mammals contribute to the surface porosity.

4.7 Digital elevation model

Topography plays an important role in the distribution and flux of water and energy in the natural landscape. Classical examples include surface runoff, evaporation, infiltration and heat exchange, which are hydrologic processes that take place at the ground-atmosphere interface. Quantitative assessment of these processes depends on the topographic configuration of the landscape, which is one of the several controlling boundary conditions.

Landscape topography can be digitised into an array of elevation values called a Digital Elevation Model (DEM). The DEMs can be visualised by means of Geographic Information Systems (GIS) and evaluated with specialised numerical algorithms.

Digital elevation models are generally produced by photogrammetric techniques from stereo-photo pairs, stereo satellite images or interpolation of digitised elevation data. For the development of the Digital Elevation Model for the Turasha catchment, topographic base maps of scale 1:50000 were manually digitised to produce a contour map. The contour maps were glued together using ILWIS operations. Contour interpolation was done with grid spacing of 100m by 100m, based on the Universal Traverse Mercator (UTM) projection. This pixel size was selected owing to the size of the catchment and the memory available to run TOPAZ (explained in detail in the next chapter)

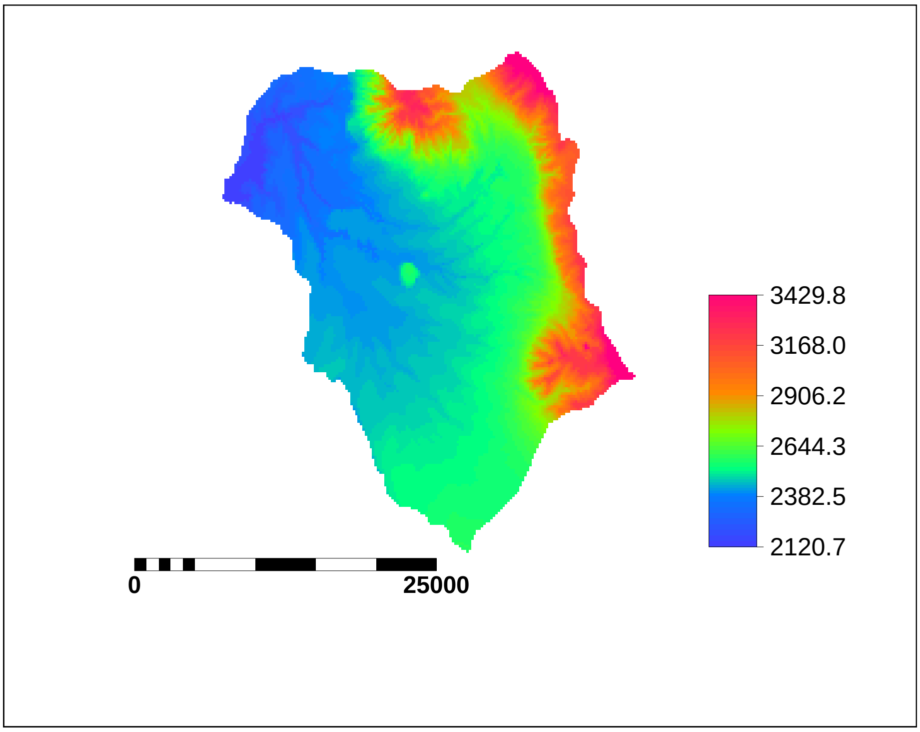

Figure 4-14 Digital Elevation model for Turasha sub Basin

Chapter 5 MODELLING

Modelling using Watershed Modelling Systems

5 Introduction

Inspired by the rapidly increasing power of computers and the development of geographic information systems and digital terrain maps, distributed models in Hydrology (and other areas such as ecology) have been developing rapidly since the first outline of a physics-based distributed model published by (Freeze and Harlan 1969).

The Watershed Modelling System (WMS) is a graphically based, comprehensive hydrologic modelling environment that was developed to address the needs of rainfall runoff computer simulations. Specifically, it has been designed to take advantage of watershed data developed and/or stored in geographic information system (GIS). WMS is a stand-alone programme and is capable of creating, reading and writing GIS data layers using the shape file format. WMS has the capability to delineate watershed and sub basin boundaries with TINs (Nelson et al. 1994), and also with digital elevation models grids, or use vector coverage of previously delineated basin boundaries and streams network stored in a GIS format. WMS can also process both grid (raster) and vector data for land use, soil type, rainfall zone, and flow path networks to develop modelling parameters such as curve numbers, infiltration parameters, rainfall intensities, and water course travel times (lag time and time of concentration). WMS uses the elevation to compute flow direction, and flow accumulation values. Also it has an interface for several different models including HEC-1, TR-55, TR-20, rational method, and other hydrologic calculations including detention basin design and curb and gutter analysis.

5.1 Steps in developing the watershed model

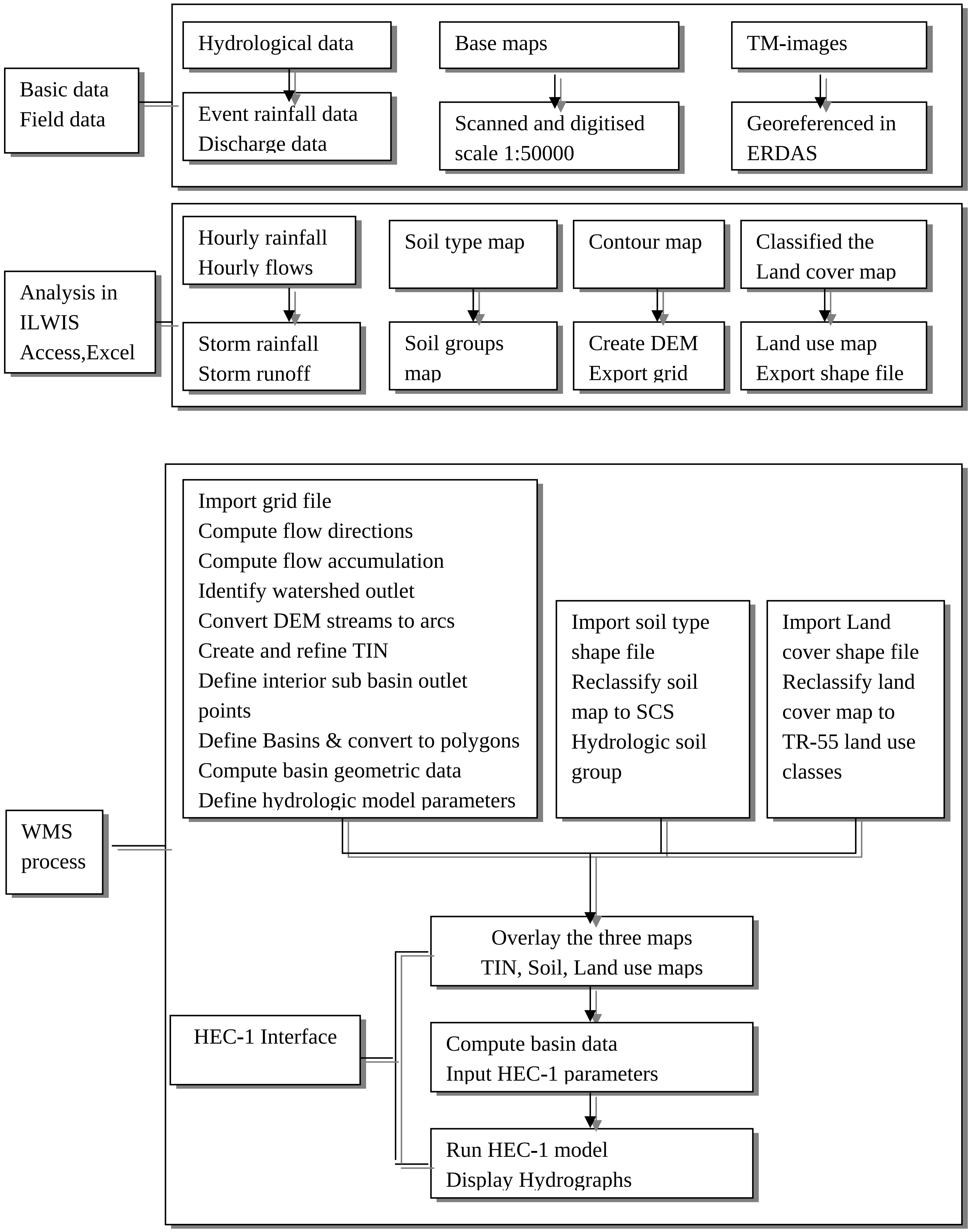

5.2 Model Components

This section discusses the conceptual aspect of using WMS program to formulate the stream network model for the Turasha river basin data.

5.2.1 Stream network model development

The Turasha river basin was subdivided into an interconnected system of streams network components using the DEM data and the watershed delineation functions of WMS as detailed below.

- A grid file for the Turasha sub basin was imported as an Arc-info ASCII file into WMS in the format summarised below

```
    ncols              711            : number of columns in the grid
    nrows              858            : number of rows in the grid
    Xllcorner          174000         : lower left X coordinate of grid
    Yllcorner          9898500        : lower left Y coordinate of grid
    Cellsize           100            : grid cell size
    Nodata_value       -32767.        : value of an empty grid cell
-32767.  -32767.  -32767.  -32767.  -32767.  -32767.  -32767.  -32767.  -32767.  -32767.
 2542.    2542.    2543.    2543.    2544.    2545.    2546.    2547.    2548.    2549.
 2551.    2552.    2553.    2554.    2555.    2551.    2551.    2551.    2551.    2550.
 2550.    2550.    2549.    2549.  -32767.  -32767.  -32767.  -32767.  -32767.  -32767.
```

- After importing the grid file, Topographic ParameteriZation (TOPAZ) program was run within WMS to compute flow directions and flow accumulation files for use in basin delineation
- A flow direction grid consists of a flow direction value for each DEM point. The flow direction identifies which neighbouring point has the lowest elevation. The TOPAZ program uses the variation of the eight-point pour model (HEC-1 users manual, 1999). The figure below illustrates how flow directions are computed. The flow direction value for the DEM points is then assigned an integer number representing the given direction

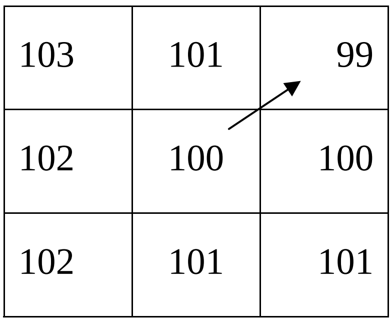

Figure 5-1 Eight-point pour model

- A flow accumulation grid consists of an integer value for each DEM point that represents the number of “upstream” DEM point whose flow path passes through. For the Turasha catchment a flow accumulation threshold value was set at 200. Higher values greater than the threshold value indicate points in the stream, whereas lower values represent areas of overland flow.

The primary data required to perform basin delineation and watershed characterisation with DEMs are the elevation and flow direction values for each DEM point. With the aid of Feature objects command

in WMS, stream networks and basin boundaries are defined. Arcs represent streams and nodes represent basin outlets. There after basins and sub basins are defined and converted to feature polygons. Basin data are then computed which include geometric values such as area, slopes, stream lengths etc. from the DEM data.
Each of the sub basins within the Turasha basin represents areas that on average have the same hydrologic properties. Since it is assumed that uniform precipitation and infiltration occurs within the sub basin, a better estimate of the averaged parameters is given in smaller sub basins than in larger ones.

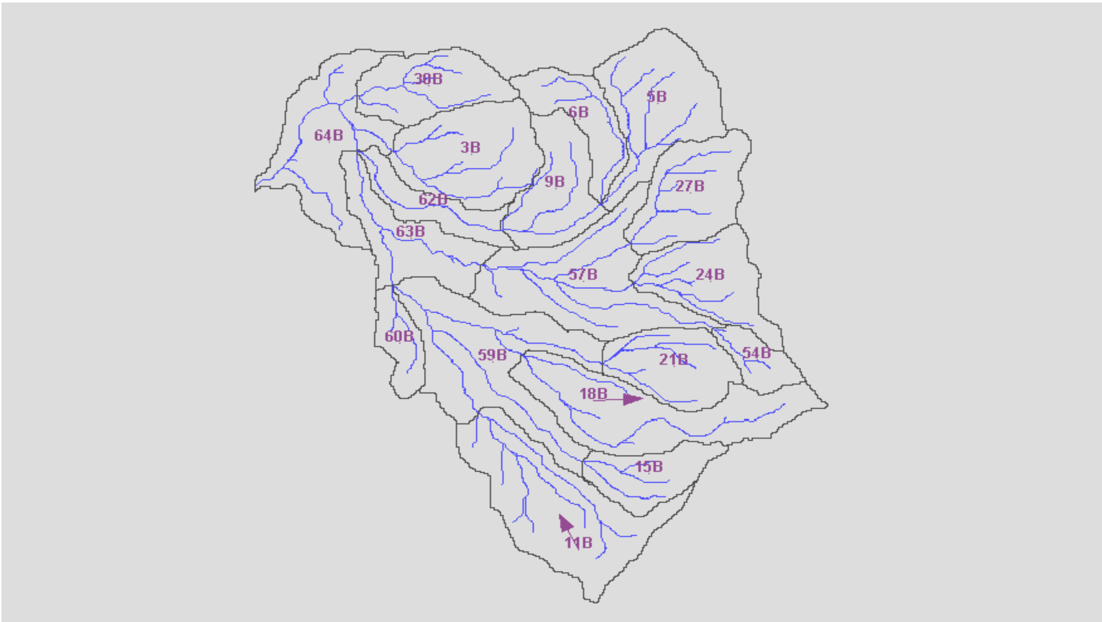

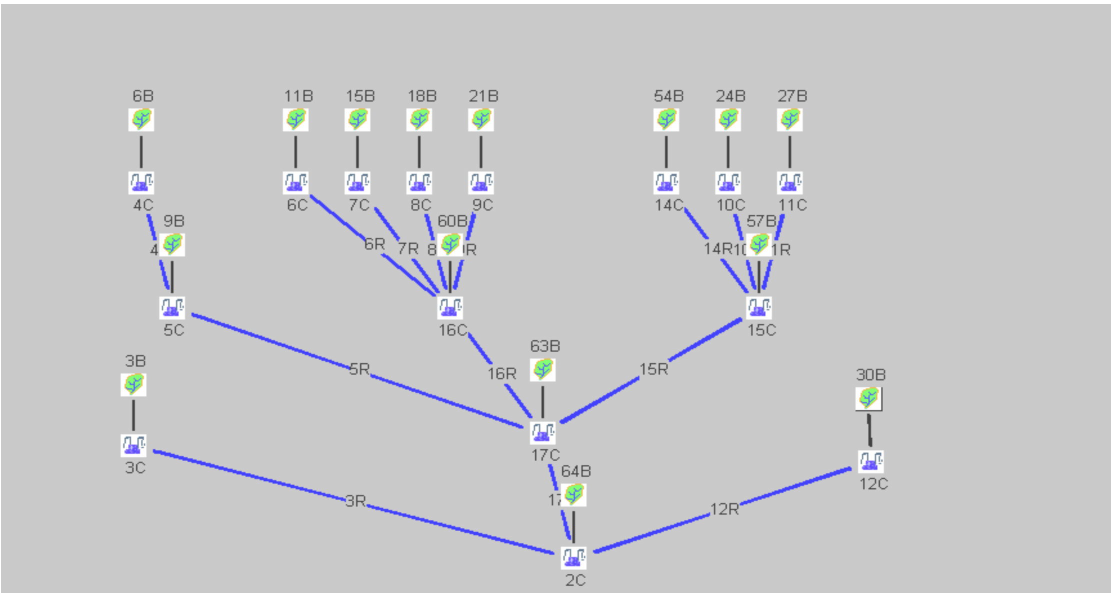

Figure 5-2 Sub basins of Turasha Catchment

Figure 5-3 Schematic diagram of the Turasha Sub basins

5.2.2 Land Surface Runoff Component

The sub basin land surface runoff component, such as sub basin 5B, 6B etc in figure 5.2 or its equivalent in figure 5.3, is used to represent the movement of water over the land surface and in the stream channels. The input to this component is a precipitation hyetograph. Precipitation excess is computed by subtracting infiltration and detention losses based on a soil water infiltration loss function. Note that the rainfall and infiltration are assumed to be uniform over the sub basin. The resulting rainfall excess is then routed by the unit hydrograph technique to the outlet of the sub basin producing a runoff hydrograph.

5.2.3 River Routing Component

A river routing component, element 3R, in figure 5.3, is used to represent flood wave movement in a river channel. The input to the component is an upstream hydrograph resulting from individual or combined contributions of sub basin runoff, river routings or diversions. The hydrograph is routed to a downstream point based on the characteristics of the channel.

5.3 Rainfall-Runoff Simulation

The HEC-1 model interface was used to simulate the rainfall-runoff process. The model components function based on simple mathematical relationships, which are intended to represent individual meteorologic, hydrologic, and hydraulic processes, which comprise the precipitation-runoff process. These processes are separated into precipitation, interception/infiltration, transformation of precipitation excess to sub basin outflow, addition of base flow and flood hydrograph routing. The subsequent sections describe the parameters and computation methodologies used by the model to simulate these processes. The equations are in metric units.

5.3.1 Precipitation

5.3.1.1 Precipitation Hyetograph

A precipitation hyetograph is used as the input for all runoff calculations. The specified precipitation is assumed to be basin average (i.e., distributed uniformly over the sub basin). The Hyetograph is as shown in the figure 5.4.

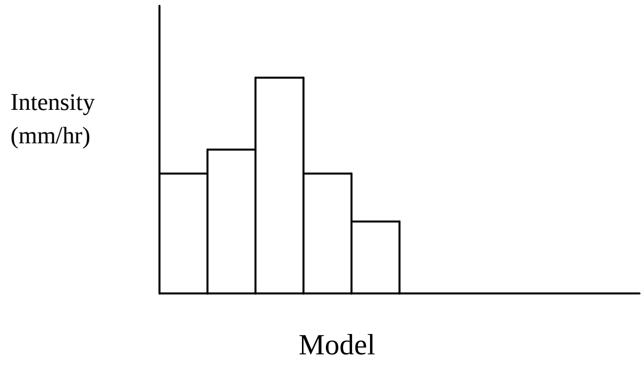

Figure 5-4 Rainfall Hyetograph

5.3.1.2 Storm data

Precipitation data for an observed storm event was computed as a weighted average of measurements from several gages within the Turasha catchment. Three rainfall gauging stations were selected which had recorded rainfall storms in November 1997. Mutubio, Olaragwai and Mawingo rainfall stations were entered in the terrain model and the appropriate gage weights (using the Thiessen polygon method) for each sub basin were computed. The following equations show how the averages were computed

$$PRCPA = \frac{\sum_{j=1}^{n} PRCPN(j) * WTN(j)}{\sum_{j=1}^{n} WTN(j)} \quad .....(3.1)$$

Where

- PRCPA is the sub basin average total precipitation
- PRCPN (j) is the total precipitation for gage j
- WTN (j) is the relative weight for gage j
- n is the number of gages

The Temporal pattern for the distribution of the storm total precipitation is computed as a weighted average of temporal distribution from recording stations

$$PRCP\ (i) = \frac{\sum_{j=1}^{n} PRCPR(i, j) * WTR(j)}{\sum_{j=1}^{n} WTR(j)} \quad . \quad ...(3.2)$$

Where

- PRCP (i) is the basin-average precipitation for the i^{th} time interval
- PRCPR (i, j) is the recording station precipitation for the i^{th} time interval
- WTR (j) is the relative weight for gage j

The sub basin- average hyetograph is computed using the temporal pattern, PRCP, to distribute the total, PRCPA.

- **Aerial Rainfall**

The rainfall data used for the analysis was processed for three Rainfall stations in the study area. (Mutubio, Olaragwai and Mawingo). These stations were selected based on their spatial distribution in the area. An attribute map of the station was generated in ILWIS and using the Distance calculation function prepared a Thiessen polygons map. A histogram of the map was generated which enabled the calculation of the relative weight for each of the rainfall station.

Station name	Station ID	Weight
Mutubio	9036272	0.32

Olaragwai	9036262	0.21
Mawingo	9036264	0.46

Table 5-1 Weights of the rainfall stations

Data for the wettest month in 1997 was used for the analysis. The daily rainfall data recorded in the three stations were recalculated using the weights to get the aerial rainfall. The result was then plotted against the Krigged data for the whole of Lake Naivasha basin to check the reliability of the data.

Date	9036262	9036264	9036272	Aerial rainfall	Krigged rainfall
01-Nov-97	0	5	26	10.6	7.1
02-Nov-97	0	6	11	6.3	5.6
03-Nov-97	7	14	34	18.8	13.6
04-Nov-97	13	12	73	31.6	20.1
05-Nov-97	4	7	21	10.8	11.9
06-Nov-97	3	12	6	8.1	15.1
07-Nov-97	4	0	6	2.8	9.6
08-Nov-97	0	0	2	0.6	3.2
09-Nov-97	10	0	10	5.3	7.8
10-Nov-97	0	0	5	1.6	1.5
11-Nov-97	1	0	7	2.5	3.9
12-Nov-97	0	5	0	2.3	1.8
13-Nov-97	6	19	6	11.9	6.1
14-Nov-97	25	13	2	11.9	6.7
15-Nov-97	5	7	5	5.9	6.9
16-Nov-97	9	15	0	8.8	11.4
17-Nov-97	32	16	41	27.2	14.3
18-Nov-97	4	0	28	9.8	11.1
19-Nov-97	1	5	0	2.5	6.8
20-Nov-97	5	8	10	7.9	9.1
21-Nov-97	2	2	21	8.1	5.4
22-Nov-97	10	4	5	5.5	8
23-Nov-97	21	6	1	7.5	4.9
24-Nov-97	2	13	5	8.0	7
25-Nov-97	3	0	0	0.6	4.4
26-Nov-97	0	0	3	1.0	3.3
27-Nov-97	3	0	10	3.8	4
28-Nov-97	1	0	4	1.5	5
29-Nov-97	6	0	8	3.8	4.1
30-Nov-97	0	1	5	2.1	3.2

Table 5-2 Rainfall data (mm)

The plotted data is as shown in the figure below. From the figure it can clearly be observed that there is a very good relationship between the calculated aerial rainfall in the sub catchment and the computed data for the whole of Lake Naivasha catchment.

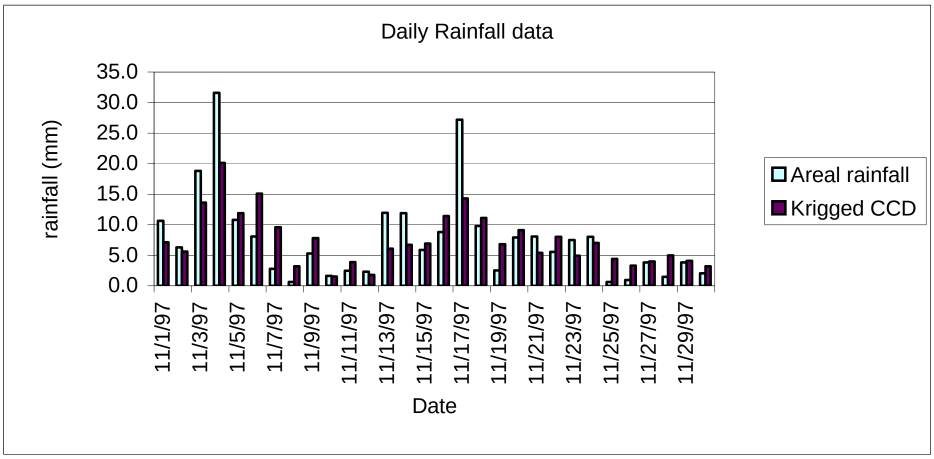

Figure 5-5 Graph of Krigged and calculated rainfall data of Turasha

- **Temporal distribution rainfall**

Hourly rainfall data for North Kinangop rainfall station was analysed to check on the temporal distribution of the daily rainfall in the area. The rainfall for 28/04/1999 was processed and the results are presented below

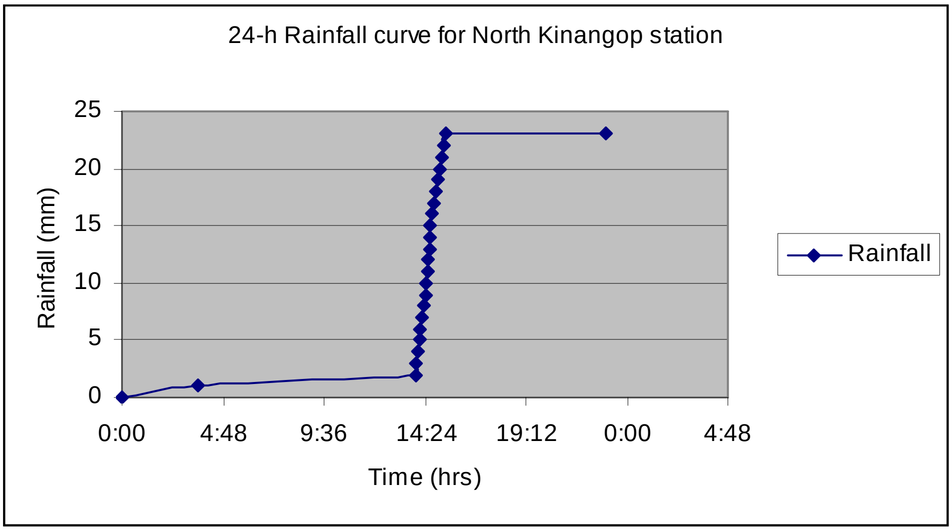

Figure 5-6 Type of rainfall for the Turasha catchment

This is Type II-24 hours rainfall that was used in as the type of temporal variation in the Model

5.3.2 Precipitation Losses (SCS Curve Number)

Land surface interception, depression storage and infiltration is referred in the HEC-1 model as precipitation losses. Interception and depression storage refer to surface storage of water by trees or grass, local depressions in the ground surface or in areas where water is not free to move as overland flow. Infiltration represents movement of water to areas beneath the land surface.

Two factors to note about precipitation loss computation in the model:

- Precipitation which does not contribute to the runoff process is considered to be lost from the system
- The equations used to compute the losses do not provide for soil moisture or surface storage recovery.

There are five methods, which can be used to calculate the precipitation loss. For the development of Turasha basin rainfall – runoff model, SCS curve number method was used.
The SCS curve number method (US Army Corps of Engineers 1990) relates soil group type to the curve number as a function of soil cover, land use type and antecedent moisture conditions. Precipitation loss is calculated based on Curve numbers and initial surface moisture storage capacity as shown in the equations below:

$$ACEXS = \frac{(ACRAN - IA)^2}{ACRAN - IA + S} \ldots(3.3)$$

$$S = \frac{1000}{CN} - 10 \ldots(3.4)$$

$$IA = 0.2*S \ldots(3.5)$$

Substituting equation 3.5 in equation 3.3 we get

$$ACEXS = \frac{(ACRAN - 0.2*S)^2}{ACRAN - 0.8*S} \ldots(3.6)$$

Where

- IA is an initial surface moisture capacity (mm)
- ACEXS is the accumulated excess (mm)
- ACRAN is the accumulated rainfall depth (mm)
- S is the currently available soil moisture storage deficit (mm)
- CN is the Curve Number

Since the SCS method gives total excess for a storm, the incremental excess for a time period is computed as a difference between the accumulated excess at the end of the current period and the accumulated excess at the end of the previous period.
In the WMS model the input parameters entered to compute SCS curve numbers were the Hydrologic soil type map (0-soil A, 1-soil B, 2-soil C, 3-soil D), and the Land use ID map. These two maps were developed for the Turasha catchment as indicated in sections 4.2, 4.3 and 4.4. The composite curve number table used was the one created from a table given in the Handbook of Hydrology.

5.3.3 Flood Routing

Flood routing is used to simulate flood wave movement through river reaches and reservoirs. Most of the flood routing methods available in HEC-1 are based on continuity equation and some relationship between flow and storage or stage. The Muskingum routing method was used to compute outflows from the river reaches in Turasha sub basins.
The Muskingum method models the storage volume of flooding river channel by combination of wedge and prism storage's, as described in the book by Chow, using the following equations:

$$Q_{OUT(2)} = (CA - CB) * Q_{IN(1)} + (1 - CA) * Q_{OUT(1)} + CB * Q_{IN(2)} \ldots(3.7)$$

$$CA = \frac{2 * \Delta t}{2 * AMSKK * (1 - X) + \Delta t} \ldots(3.8)$$

$$CB = \frac{\Delta t - 2 * AMSKK * X}{2 * AMSKK * (1 - X) + \Delta t} \ldots(3.9)$$

Where:

- Q_{IN} is the inflow to the routing reach in m^3/sec
- Q_{OUT} is the outflow from the routing reach in m^3/sec
- AMSKK is the travel time through the reach in hours
- X is the Muskingum weighting factor ($0 \le X \le 0.5$)

The routing procedure is repeated for several sub reaches (designated as NSTPS) so that the total travel time through the reach is AMSKK. To ensure computational stability and the accuracy of computed Hydrograph, the routing reach was chosen such that:

$$\frac{1}{2(1 - X)} \le \frac{AMSKK}{NSTPS * \Delta t} \le \frac{1}{2X} \ldots(4.0)$$

In order to enter the routing data into the WMS program the following assumptions were done:

- Channel velocity estimated at 3 m/sec
- X assumed to be 0.2

To determine the routing time (AMSKK in hours), the following equation was used

$$AMSKK = \frac{L}{(V * T)} \ldots(4.1)$$

Where:

- L is the channel length (m)
- V is the channel velocity (m/sec)
- T is the travel time conversion factor (3600 sec/hr)

To determine the number of time steps to route the flow through the channel segment (NSTPS), the travel time in minutes was divided by the computational time steps which was 15 for the Turasha sub basins

Hence the following parameters were entered in the WMS model for Muskingum routing method

Routine ID	Length (m)	NSTPS	AMSKK (hr)
17R	12804	4.7	1.2
12R	10631	3.9	1.0
3R	14270	5.3	1.3
4R	6913	2.6	0.6
5R	12040	4.5	1.1
6R	10889	4.0	1.0
7R	18047	6.7	1.7
8R	10057	3.7	0.9
9R	14755	5.5	1.4
16R	10483	3.9	1.0
14R	16307	6.0	1.5
10R	10186	3.8	0.9
11R	10383	3.8	1.0
15R	13873	5.1	1.3

Table 5-3 routing data

5.3.4 Base flow analysis

The stream Hydrograph is composed of direct runoff and the base flow, which results from releases of water from sub surface storage. In order to calibrate the Rainfall-Runoff model of the Turasha catchment, the base flow was separated from the storm runoff using the technique discussed by (Wilson 1990). The hydrograph of base flow is near to an exponential curve and the quantity at any time is represented very nearly by

$$Q_t = Q_0 e^{-\alpha t} \quad \text{… (4.2)}$$

Where

- Q_0 = Discharge at start period
- Q_t = Discharge at end of time t
- α = Coefficient of aquifer
- e = Base of natural logarithms

To analyse base flow for the Turasha catchment the storm runoff of 21/22 November 1997 was used. The data is summarised below.

Date	Time	Discharge (m^3/s)	Date	Time	Discharge (m^3/s)
21-Nov-97	19:00:00	43.064	22-Nov-97	07:00:00	109.761

21-Nov-97	20:00:00	45.680	22-Nov-97	08:00:00	101.066
21-Nov-97	21:00:00	57.220	22-Nov-97	09:00:00	90.821
21-Nov-97	22:00:00	88.312	22-Nov-97	10:00:00	83.059
21-Nov-97	23:00:00	120.446	22-Nov-97	11:00:00	77.510
22-Nov-97	00:00:00	140.029	22-Nov-97	12:00:00	70.476
22-Nov-97	01:00:00	154.955	22-Nov-97	13:00:00	67.089
22-Nov-97	02:00:00	154.949	22-Nov-97	14:00:00	60.109
22-Nov-97	03:00:00	151.349	22-Nov-97	15:00:00	57.037
22-Nov-97	04:00:00	140.005	22-Nov-97	16:00:00	56.530
22-Nov-97	05:00:00	133.297	22-Nov-97	17:00:00	54.544
22-Nov-97	06:00:00	121.979	22-Nov-97	18:00:00	53.086

Source: Data processed by Author from Data logger installed at station 2GC4

Table 5-4 hourly discharge data for 2GC4

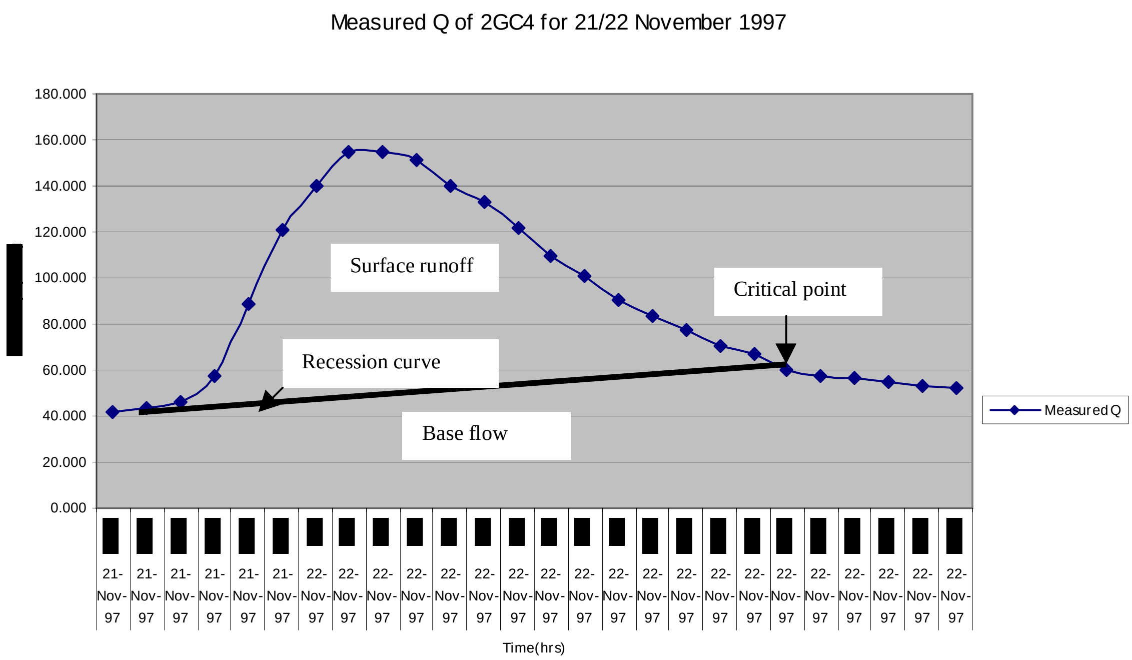

Figure 5-7 measured discharge data for 2GC4

- The first step in the separation of base flow was to establish the point of greatest curvature on the recession limb of the Hydrograph. This was done by computing the log Q of the recession limb verses time

Date	Time	Q (m^3/s)	Log Q (m^3/s)
22-Nov-97	8:00	101.066	2.005
22-Nov-97	9:00	90.821	1.958
22-Nov-97	10:00	83.059	1.919
22-Nov-97	11:00	77.510	1.889
22-Nov-97	12:00	70.476	1.848
22-Nov-97	13:00	67.089	1.827

22-Nov-97	14:00	60.109	1.779
22-Nov-97	15:00	57.037	1.756
22-Nov-97	16:00	56.530	1.752
22-Nov-97	17:00	54.544	1.737
22-Nov-97	18:00	53.086	1.725

Table 5-5 Computation to find the critical ratio

To obtain the critical point when recession begins, the logarithm of observed flows was plotted against time. The point at which there is a change in slopes in the graph, indicate the critical point.

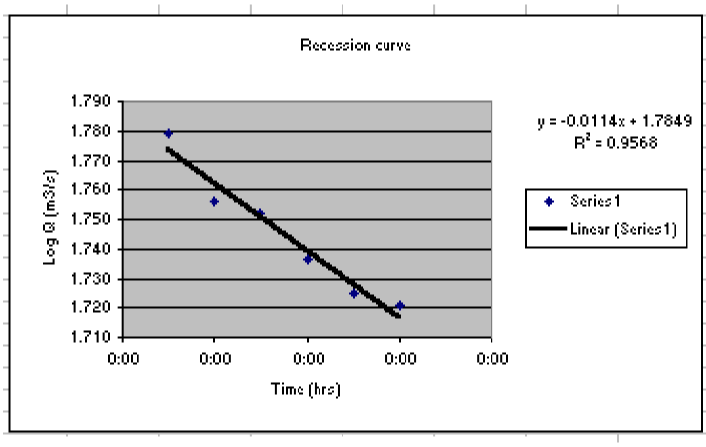

Figure 5-8a

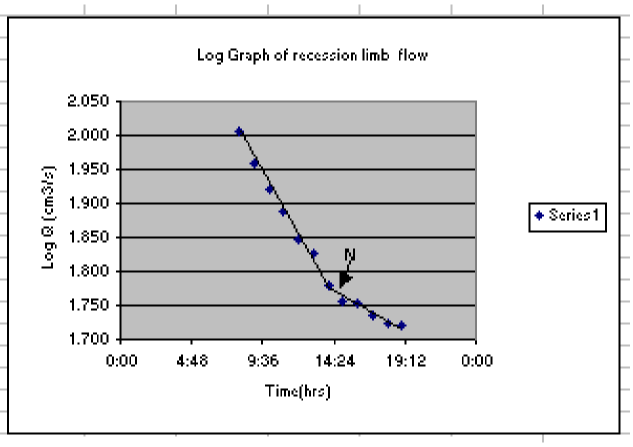

Figure 5-8b

Figure 5-8 Graph of the Log Q against time interval of the recession flow.

- From figure 5-8b, it can clearly been seen that two slopes are apparent, the upper being associated with runoff and the lower with ground water depletion. The critical point in this case is the first point beyond the region of intersection on the groundwater side marked N which is 22/11/1997 at 14.00 hrs.
- **The critical point indicates the flow at which the exponential recession flow began. In this case it is 1.779 and the value of Q_0 is inverse log of 1.779, which is 60.1.**
- **The slope of the straight line plotted in graph 5-8a for the recession limb is log (-0.0114), which is 0.974.**
- Once the critical point (initial flow) and the slope (ratio) had been identified, the values were substituted in the following equation to calculate the base flow

$$Q=Q_0(N)^{-n\Delta t} \quad \ldots(4.3)$$

Where:

- N is the Critical Ratio of Q to Q_{+1} (slope of the straight line)
- $n\Delta t$ is the time in hours since recession was initiated
- Q is the recession flow
- Q_0 is the initial flow in the river

The results of the base flow analysis for the storm of 21/22 November 1997 is summarised in the table below

Date	Time	Measured Q (m^3/s)	Base flow (m^3/s)	Storm runoff (m^3/s)
21-Nov-97	18:00	41.8	41.8	0.0
21-Nov-97	19:00	43.1	43.1	0.0
21-Nov-97	20:00	45.7	45.7	0.0
21-Nov-97	21:00	57.2	57.2	0.0
21-Nov-97	22:00	88.3	60.6	27.7
21-Nov-97	23:00	120.4	60.7	59.7
22-Nov-97	0:00	140.0	59.2	80.8
22-Nov-97	1:00	155.0	59.3	95.7
22-Nov-97	2:00	154.9	59.3	95.6
22-Nov-97	3:00	151.3	59.4	92.0
22-Nov-97	4:00	140.0	59.5	80.6
22-Nov-97	5:00	133.3	59.5	73.8
22-Nov-97	6:00	122.0	59.6	62.4
22-Nov-97	7:00	109.8	59.6	50.1
22-Nov-97	8:00	101.1	59.7	41.4
22-Nov-97	9:00	90.8	59.8	31.0
22-Nov-97	10:00	83.1	59.8	23.2
22-Nov-97	11:00	77.5	59.9	17.6
22-Nov-97	12:00	70.5	60.0	10.5
22-Nov-97	13:00	67.1	60.0	7.0
22-Nov-97	14:00	60.1	60.1	0.0
22-Nov-97	15:00	57.0	57.0	0.0
22-Nov-97	16:00	56.5	56.5	0.0
22-Nov-97	17:00	54.5	54.5	0.0
22-Nov-97	18:00	53.1	53.1	0.0
22-Nov-97	19:00	52.6	52.6	0.0

Table 5-6 Results of base flow analysis

After the separation of the base flow from the measured discharge at 2GC4, the following hydrograph was generated for the storm runoff that occurred on 21/22 November 1997.

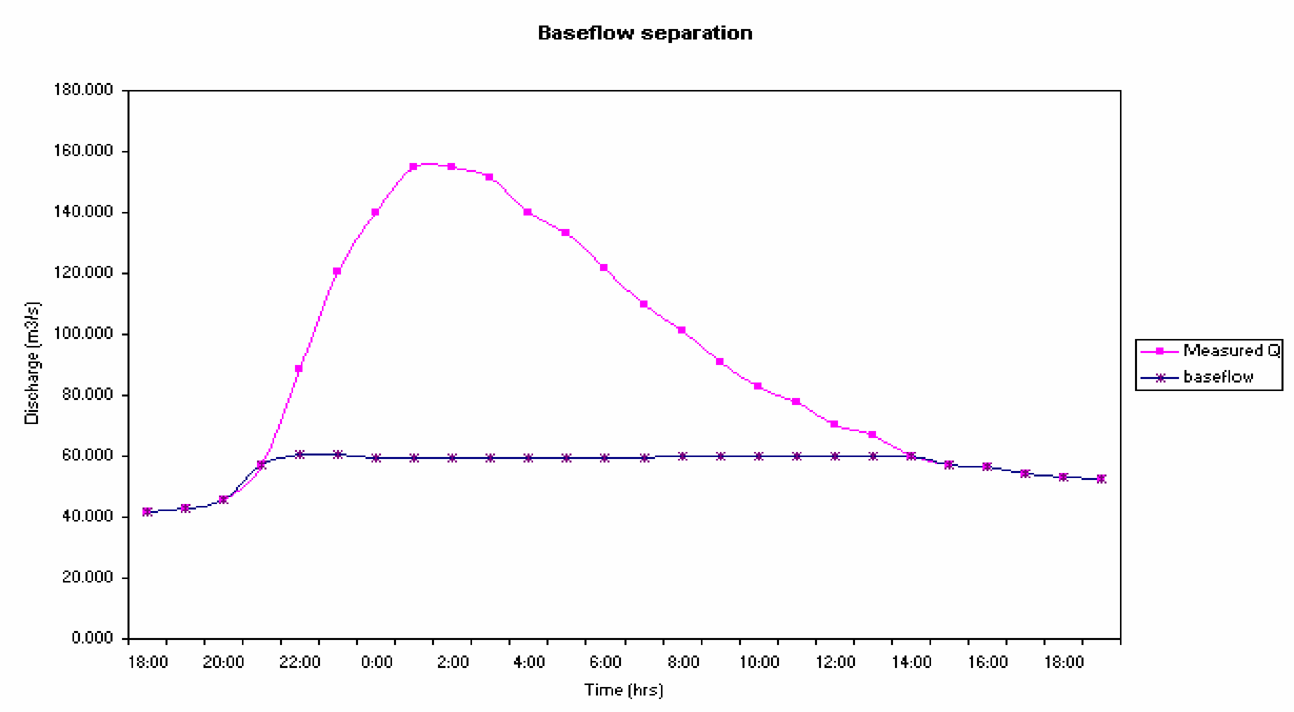

Figure 5-9 Base flow separation.

These results were used in the calibration of the model.

5.3.5 Model Calibration

Calibration and verification are important modelling processes. The Turasha rainfall-runoff model was calibrated to measured discharge for Turasha River measured at station 2GC4. The data used was recorded on 21/22 November 1997.

In order to calibrate the model the following parameters were adjusted in order to fit the model to the actual measured discharge:

- The hydrological soil group data
- Land cover data
- Curve Numbers to reflect the Antecedent moisture conditions of the sub basins

Since the Turasha catchment consists of more than one type of soil and Land cover complexes, the curve numbers are computed in the WMS program as weighted averages. As a result of changing these parameters, the computed curve numbers for the sub basins were automatically changed either upwards or downwards.

Every time one parameter was changed, the modelled flow was plotted against the measured flow (storm runoff). This analysis was repeated until the best-fit graph was obtained. The result of the measured and the modelled flow is presented in the graph. (This data is after base flow separation)

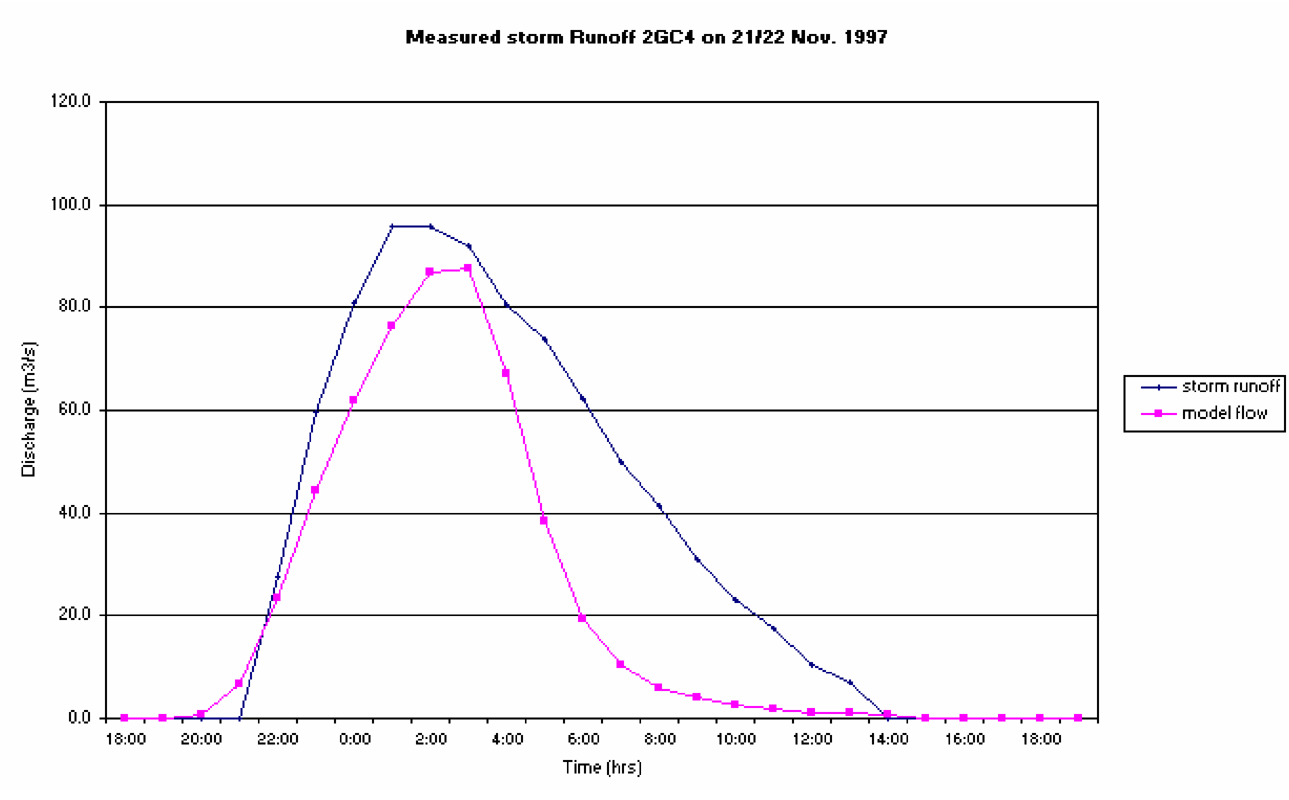

Figure 5-10 the graph of modeled and measured discharge of Turasha River 2GC4

5.3.6 Model results

After the model was calibrated, three scenarios were simulated Scenario 1 and 2 were based on a single days Rainfall event for different soil moisture characteristics. First scenario was simulated for the storm resulting from rainfall when the area had been continuously dry (Average antecedent moisture conditions), and the second scenario was when the area had been experiencing a wet weather conditions, saturated soils, prior to the storm date (Antecedent moisture condition III).
The third Scenario was based on simulating a whole month of daily rainfall redistributed to hourly rainfall events over the sub catchment.

- **Scenario 1 (Antecedent moisture condition II)**

The rainfall data used to run this scenario was recorded on 17 November 1997 in the following stations.

- Mutubio (9036272) – 41 mm
- Mawingo (9036264) – 16 mm
- Olaragwai (9036262) – 32 mm

Note: The positions of these stations are shown in figure 4.1 (chapter4)

The calculated aerial rainfall for this day was 27.2 mm
This data was entered into the WMS program and the simulation was run using the HEC-1 interface of the model. The input data resulting for the simulation of the model is detailed in appendix C.
Below is a summary of the results.

- Simulated Peak flow 32.8 m^3/s
- Time to peak 19 hrs
- Total area of the catchment 728 km^2

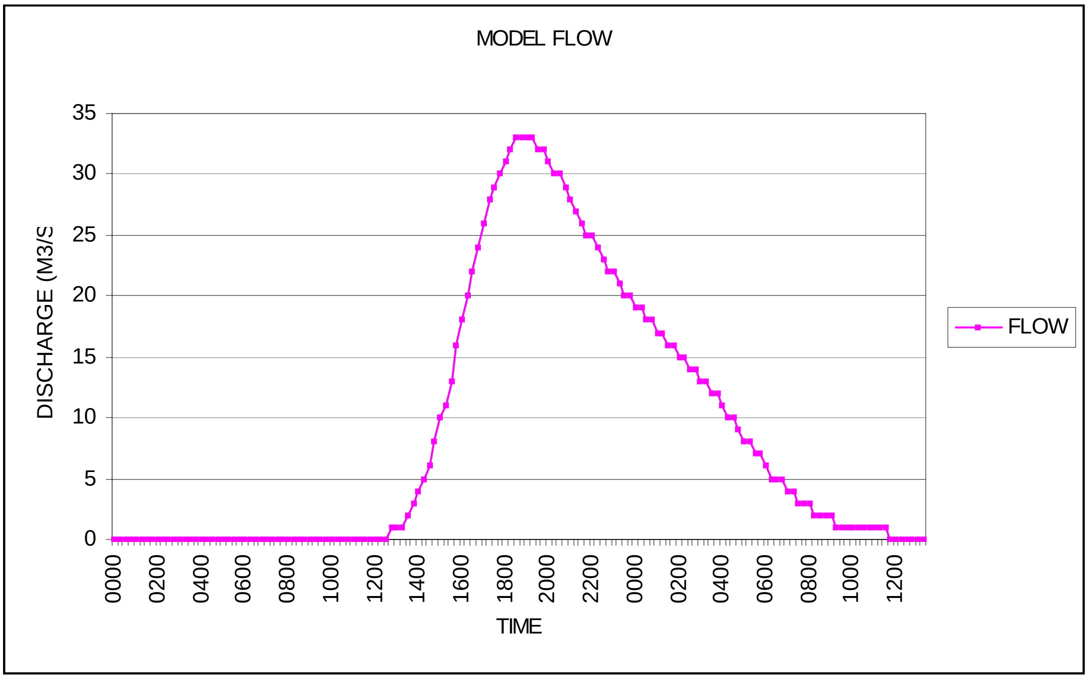

Figure 5-11 Simulated flow for average antecedent moisture condition

- **Scenario 2 (Antecedent moisture condition III)**

The same set of rainfall data was used to run this simulation. An assumption was held that the area was completely saturated before the storm and the results obtained are summarised below and detailed in appendix C.

- Simulated Peak flow 165.1 m^3/s
- Time to peak 17.5 hrs
- Total area of the catchment 728 km^2

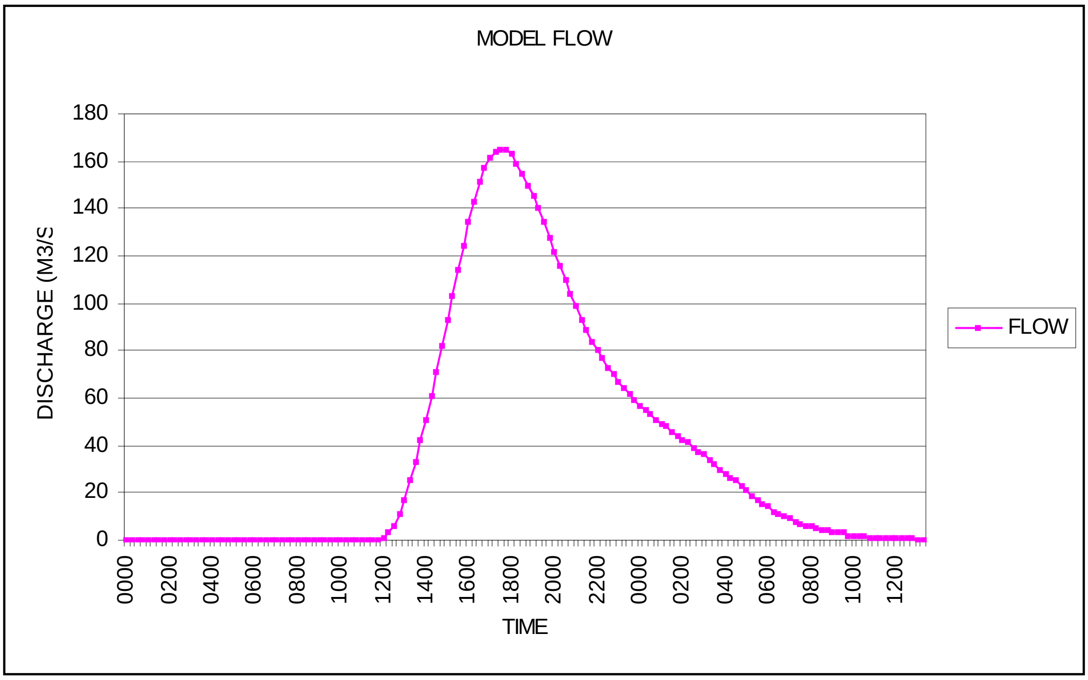

Figure 5-12 Simulated flow for saturated moisture condition

- **Scenario II1 (One month series with Average moisture condition)**

To run this scenario, three different types of Daily rainfall data sets for the month of November 1997 were used. Refer to table 5-2 for the different data sets.

- **Scenario III (a)**

Scenario III using aerial rainfall data computed from three rainfall stations, (Mawingo, Olaragwai and Mutubio). The daily aerial rainfall was calculated using weighted average method. The daily data was then redistributed to hourly rainfall based on the temporal distribution curve for the Kinangop station (refer to Figure 5-6). The hourly data was then entered into the WMS program in three-hour intervals for a whole month. The simulation was run in hourly intervals and the results obtained plotted against measured discharge at Turasha station 2GC4 as shown in the figure below.

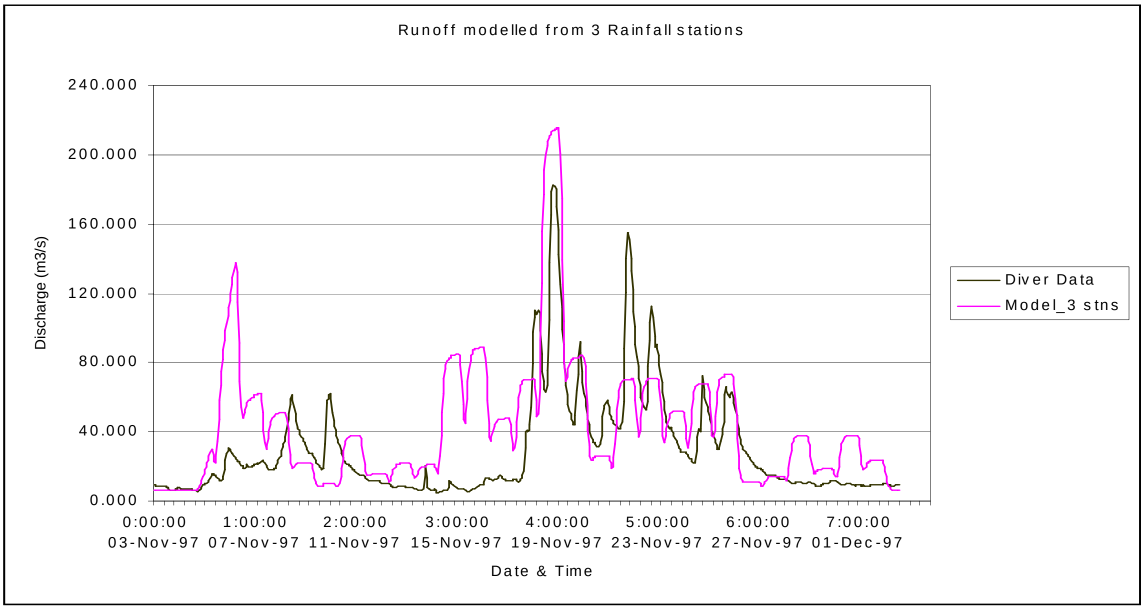

Figure 5-13 Graph of Modeled Runoff based on aerial rainfall 3 stations and actual diver data

From this analysis, one can clearly notice the influence of rainfall recorded at Mutubio station, which is in the Aberdare Mountains. On 4/11/1997 the rainfall recorded in the station was 73mm which was far much more than what was recorded in the other two stations. This rainfall appears as a peak in the modelled runoff data.

- **Scenario III (b)**

Scenario III was again run but this time using rainfall data recorded at the Mawingo Rainfall station, which is situated in the Kinangop plateau. Most of the runoff measured at the outlet of Turasha sub catchment from rainfall within the Kinangop plateau. The daily rainfall data was redistributed to hourly rainfall events and entered in the WMS program. The results of the simulation was then plotted with the actual measured data as shown below.

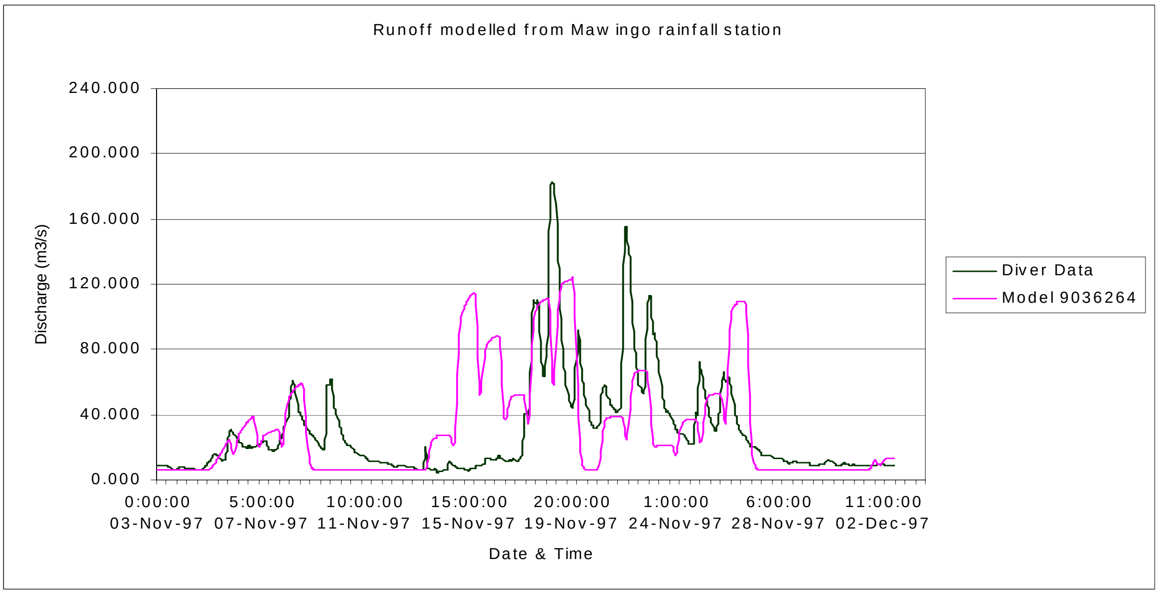

Figure 5-14 graph of modeled runoff from Rainfall at Mawingo scheme and diver data

From the analysis it can clearly be seen that the modelled and measured data are closely related apart from 14-15/11/1997 when the model over estimated the runoff.

5.3.7 Discussion of results

These results indicate how sensitive the model is to changes in hydrological conditions of the catchment. Based on the same amount of aerial rainfall produced a significant change in the peak discharge data.

The actual recorded discharge from the data logger installed at 2GC4 in Turasha River Indicated a peak discharge of 182.5 m^3/s on 19/11/1997 at 1.00am but the rainfall for that day was only 2.5mm, where as the peak flow recorded for 17/11/1997 was 17 m^3/s with a rainfall of 27.2mm. Below is the hydrograph of the recorded discharge from 17/11/1997 to 20/11/1997

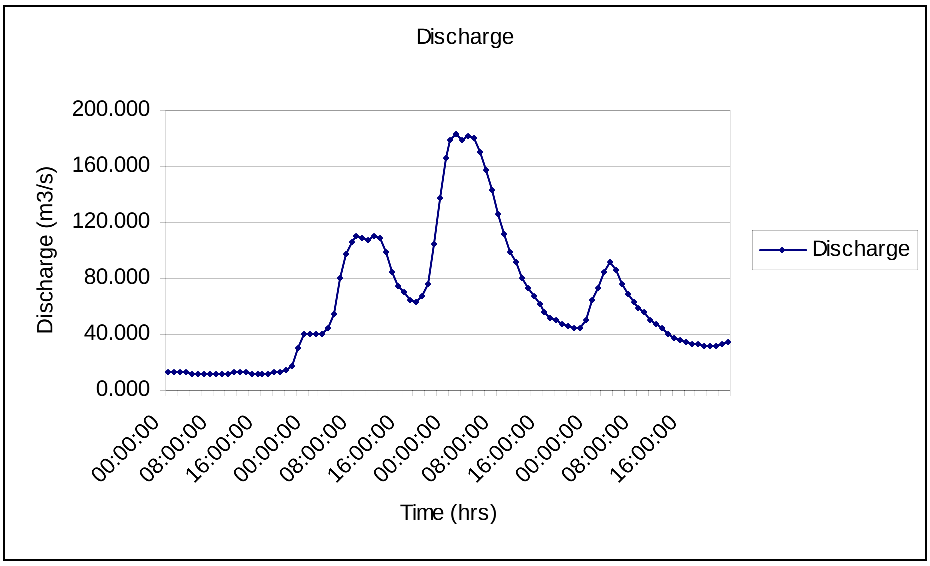

Figure 5-15 measured discharge processed from the data logger at 2GC4 station

Assuming the rainfall recorded on 17/11/1997 continued up to 18/11/1997 in the morning before 9.00 am. From our simulation the time to peak was almost 18 hours. This gives the actual time to record the maximum flow to be midnight 18-19/11/1997. This is clearly indicated in the graph above and also from the actual measured data table below.

Date	Time	Discharge (m^3/s)
18-Nov-97	17:00:00	64.353
18-Nov-97	18:00:00	63.271
18-Nov-97	19:00:00	66.534
18-Nov-97	20:00:00	75.799
18-Nov-97	21:00:00	104.824
18-Nov-97	22:00:00	137.596
18-Nov-97	23:00:00	165.182
19-Nov-97	00:00:00	178.621
19-Nov-97	01:00:00	182.560
19-Nov-97	02:00:00	178.595
19-Nov-97	03:00:00	181.550
19-Nov-97	04:00:00	180.559
19-Nov-97	05:00:00	169.853
19-Nov-97	06:00:00	156.792
19-Nov-97	07:00:00	142.621
19-Nov-97	08:00:00	125.153
19-Nov-97	09:00:00	111.981
19-Nov-97	10:00:00	99.002
19-Nov-97	11:00:00	90.821
19-Nov-97	12:00:00	80.584
19-Nov-97	13:00:00	72.193
19-Nov-97	14:00:00	66.534
19-Nov-97	15:00:00	61.154
19-Nov-97	16:00:00	55.532
19-Nov-97	17:00:00	51.644
19-Nov-97	18:00:00	50.698
19-Nov-97	19:00:00	47.015
19-Nov-97	20:00:00	45.680
19-Nov-97	21:00:00	43.924
19-Nov-97	22:00:00	44.359
19-Nov-97	23:00:00	49.342

Table 5-7 measured hourly discharge data analyzed from the logger installed at 2GC4

With these assumptions in mind, the daily measured rainfall from the catchment has a lag time of more than 18 hours before the whole catchment can effectively contribute to the measured runoff at the outlet. The total measured runoff includes:

- Direct overland flow
- Inter flow
- Base flow

The results of Scenario III (a) indicated an over estimation of the modeled runoff for the days when Mutubio rainfall station recorded high rainfall. As is the case on the ground the influence of rainfall from the Aberdare hills is usually very little compared to rainfall within the Kinangop plateau. Most of the rainfall in the Aberdare produces low runoff since:

- It is a very small area within the catchment
- The infiltration rates are very high due to the thick soils
- The area is mainly a dense tropical forest.

The daily measured Runoff and the modeled runoff within the catchment given a delay of one day when plotted together produced good relationship as shown below

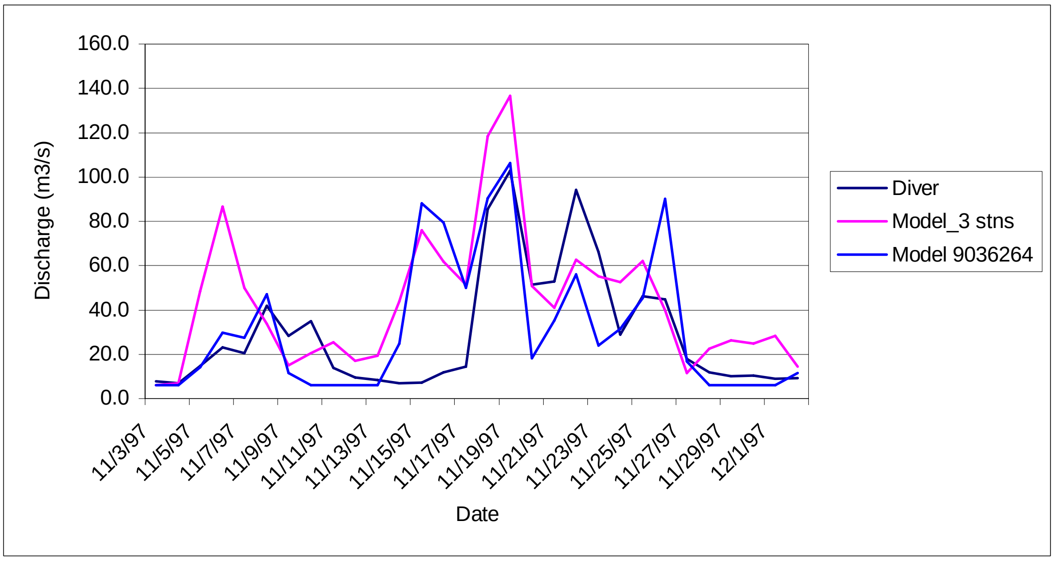

Figure 5-16 daily measured and modeled Runoff relationships for November 1997

Comparing the results of the modelled Runoff for 3 stations with the one simulated from Mawingo station (9036264), it can clearly be observed from the graph that Mawingo data produced a better estimate of the runoff than the aerial data of the three stations.

Chapter 6 CONCLUSION AND RECOMMENDATIONS

In this chapter a general discussion about the research and limitations of the study concerning the data and model are discussed. Conclusions on the achievements are drawn as well as recommendations for further research

General discussions

The aim of the study was to develop a model able to simulate Rainfall to stream Runoff events. The area of study was Turasha sub catchment within Lake Naivasha Basin in Kenya.
The model used was HEC-1 that was run within the Watershed Modelling System environment.
ILWIS-GIS was used for the generation of spatial components of the model such as the DEM, the Landuse and the Soil type maps. Also done in the GIS environment was the calculation of gage weights for the calculation of the aerial rainfall (Thiessen polygon map).
The DEM was imported in to the WMS program and used to delineate the sub basin boundaries and to generate the drainage system of the Turasha sub catchment. From the DEM, it was possible to compute the sub basin characteristics which included River length, maximum flow distance, mean basin slope, mean basin elevation, basin areas, etc.
The DEM was then integrated with the Landuse and the hydrologic soil group maps to produce a super file which was then used to calibrate and run different scenarios for the model. It was in the super file that the calculation of the composite curve numbers for each sub basin was carried out.

The calibration of the model was done using measured discharge at the outlet station, 2GC4, on Turasha River after separation of the base flow. The discharge data was processed from the pressure data logger installed in Turasha River. The logger measures the pressure exerted by a column of water above the logger together with the atmospheric pressure. The hourly logger data was corrected for the Atmospheric pressure using the barometric logger installed within the Lake Naivasha basin. The hourly data was then converted into daily data and plotted against the manually observed data. The corrected water levels from the data loggers was then computed into hourly discharge data using the rating equations for station 2GC4.

Optimisation of the model was not carried out since the input flow data for each sub basin is not available. This data is important because each sub basin in the Turasha catchment had different hydrological conditions and hence different initial flows before the storm runoff.

Frequency analysis was also done to compute the recurrence interval of different storms recorded for the period 1957 to 1999 in the Turasha River. From the analysis, it was evident that the floods, which occurred in 1997 and 1998, were extraordinarily high, but it was during this period that the area experienced the El-Nino rainfall phenomenon.

The model was run to simulate three different scenarios with the same rainfall input but with different hydrological characteristics. The results obtained compared relatively well with the actual measured data. On 4/11/1997, the measured rainfall was 31mm, but the Peak flow recorded at the gauge station was 30.6 m^3/s This rain was recorded after a duration of dry spell. On 17/11/1997, the measured rainfall was 27.2mm but the recorded peak flow was 183 m^3/s, which was recorded after a period of wet weather conditions in the catchment. From the model, the dry spell scenario gave 32 m^3/s, while the wet spell scenario gave 165 m^3/s.

Condition	Measured (+ Base flow)	Modelled (only storm runoff)
Aerial Rainfall – 27.2mm		
Antecedent moisture condition II	31.0 m^3/s	32.0 m^3/s
Antecedent moisture condition III	183.0 m^3/s	165.0 m^3/s

Table 6-1 Modeled and measured storm runoff values

The third scenario was simulated over a period of 30 days for the month of November 1997.

These were the only scenarios selected in this thesis although many other simulations are contained in the CD-ROM with all the databases.

Limitations in the study

- **Data Availability**

The daily rainfall data used for the analysis was questionable. There are days when the automatic loggers clearly indicated peaks in the discharge recorded where as the manual observed rainfall data indicates no rainfall. The rainfall loggers installed in some parts of the catchment further depicted this kind of discrepancy. For comparison, the Geta rainfall station was used. In this site there was both a manual and automatic rainfall logger. The measurements did not tally most of the times as indicated in Appendix E. with this kind of uncertainty, it was difficult to actually know which rainfall event produced the peak. In some instances, the manual observed rainfall was averaged over a period, which indicated the observer did not actually record the rainfall on a daily basis as required.

- **WMS Program (HEC-1 model)**

The HEC-1 program could only simulate rainfall data for a short period of time. The HSPF interface in the WMS program, which is capable of simulating long series of data, was only available in the last month of the research period and it was not possible to understand how the program works within the short period.

The computer capacity was not enough to generate a Grid file of pixel size 30m by 30m for the study area, hence the pixel size used for the DEM was 100m by 100m, which was not in the same format as the other maps processed from the satellite images.

There was no discharge data available for the sub basins. This made it difficult for the model to be optimised since each sub basin has different catchment characteristics.

The US SCS loss method used has a lot of limitations as discussed in the paper by (Kumar and Jain S.C 1982). In the paper, it was mentioned that SCS method was used to estimate effective rainfall for 11 storms on a research watershed in IOWA and the results obtained were not in agreement with values determined by Hydrograph separation. So this clearly gives an indication on how reliable the same method can be applied in a catchment, which has totally different characteristics as in the USA where the method was developed.

Conclusion

The differences between the recorded data and the simulated output data could be as a result of the following sources of uncertainty:

- Random or systematic errors in the input data i.e. Precipitation used to represent the input conditions in time and space over the catchment.
- Random or systematic errors in the recorded data
- Errors due to the type of loss method applied (SCS curve number)
- Errors due to biased model structure (influence of rainfall recorded in one station being spread over the entire catchment)
- Errors resulting from redistribution of daily data to hourly data

Despite all the limitations and errors, the model seems to have immediate potential for operational use as a decision support tool for watershed management in the area. It can be used to simulate rainfall events into runoff under different catchment wetness conditions.

Recommendations

A statistical analysis of the daily rainfall data should be carried in order to explain the relationship if any between the automatically recorded data and the manually recorded data at the same site.

The same model should be tried using the HSPF interface in WMS so as to Simulate long series of hourly data preferably from 1997 to 2001.

References

Abbott, M. B., and Refsgaard, J. C. e. (1996). *Distributed Hydrological Modelling*, Kluwer Academic publishers, Dordrecht, The Netherlands.

Brouwer, H. (1992). "Basic Hydrology, Precipitation.", International Institute for Aerospace Survey and Earth Sciences, Enschede, The Netherlands.

Burgy R.H, and D.C., L. (1964). "Hydrologic Balance from an Experimental Watershed." *Journal of Hydrology*, 2, 197-212.

Chorowicz, J., Anglier, J., and Saintot, A. (1999). *Mechanical Significance of Structural Patterns identified by Remote Sensing studies : A multiscale analysis of Techtonic structures in Crimea*.

Chow, V. T., Maidment, D. R., and Mays, L. W. (1988). *Applied Hydrology*, McGraw-hill, Inc, New York.

Clarke, R. (1991). *Water : The international crisis*, Earthscan Publications Ltd,, London.

De Silva, R. P., and Taylor, T. C. (1999). "Spatioltemporal Hydrological Modelling." *Asia's first GIS/GPS/RS/ monthly magazine*(November-December 1999).

DeBarry, P. A., and al., e. (1999). "GIS modules and distributed models of the watershed.", The American Society of Civil Engineers (ASCE), Reston, Virginia.

Dingman, L. S. (1994). *Physical Hydrology*, Prentice-Hall, Inc, New Jersey.

Donker, N. H. W. (1996). *Rankplot, Ananlysis of Frequency Distributions of Hydrologic Events, Users manual*,, Enschede.

Freeze, R. A., and Harlan, R. L. (1969). "Blue print for a Physically-Based digitally-simulated hydrological response model." *Journal of Hydrology*, 9.

Grover, S. (1999). "Perspective of GIS Modelling in Hydrology." *Asia's first GIS/GPS/RS/ monthly magazine*(November-December).

ICWE. "The dublin Statement and report of the conference." *International conference on water and the environment: Development issues for the 21st century*, Dublin, Ireland.

Jaetzold, R. (1976). "Climatic Situation of The Kinangop area." *International Publication*.

Jagadeesha, C. J. (1999). "Water Resources Development and Management." *Asia's first GIS/GPS/RS/ monthly magazine*(November-December).

Kumar, S., and Jain S.C. (1982). "Application of SCS Infiltration model." *Water Resources Bulleting*(18), 503 - 507.

McCall, G. J. H. (1967). "Geology of Nakuru-Lake Hannington." *78*, Geological survey of Kenya, Nairobi, Kenya.

Ndege, M. M. (1996). "Strain Water Demand, and Supply Directions in the most Stressed Water Systems of Eastern Africa." Water Mangement in Eastern Africa, Nairobi, Kenya.

Nelson, E. J., Jones, N. L., and Miller, A. W. (1994). "Algorithm for Precise Drainage basin delineation." *ASCE Journal of Hydraulic Engineering*, 120(No.3).

Rachilo, J. R. (1978). "Soil conditions in the Kinangop area - A preliminary investigations." *34*, Kenya soil survey,, Nairobi, Kenya.

Ringo, D. E. (1999). "Assessment of Erosion in the Turasha catchment in the Lake Naivasha area, Kenya.," Msc., International Institute for Aerospace Survey and Earth Sciences (ITC)., Enschede, the Netherlands.

Seth, S. M., Jain, S. K., and Jain, M. K. "Remote Sensing and GIS Application Studies at National Institute of Hydrology." *Map India 1999*.

Shackleton, R. M. (1945). "Geology of Nyeri area." *12*, Geological Survey of Kenya, Nairobi.

Stuttard, M. J., Hayball, J., Narsico, G., Carizi, G., Suppo, M., Catani, R., Isavwa, L., Baraza, J., and Oroda, A. (1995). "Monitoring Lakes in Kenya, An Environmental Analysis Methodology for developing Countries, final report.".

Thompsons, A. O., and Dodson, R. G. (1958). "Geology of the Naivasha area." *55*, Geological Survey of Kenya, Nairobi-Kenya.

Thompsons, A. O., and Dodson, R. G. (1964). "Geology of the Kijabe area." *67*, Geological Survey of Kenya, Nairobi, Kenya.

US Army Corps of Engineers. (1990). *HEC-1, Flood Hydrograph Package User's Manual*.,, Davis, California.

Ward, R. C., and Robinson, M. (1990). *Principals of Hydrology*, McGraw_Hill Book Company Europe, London.

Wilson, E. M. (1990). *Engineering Hydrology*, Macmillan Education Limited, Hampshire.

Appendix

Appendix A. WMS input maps

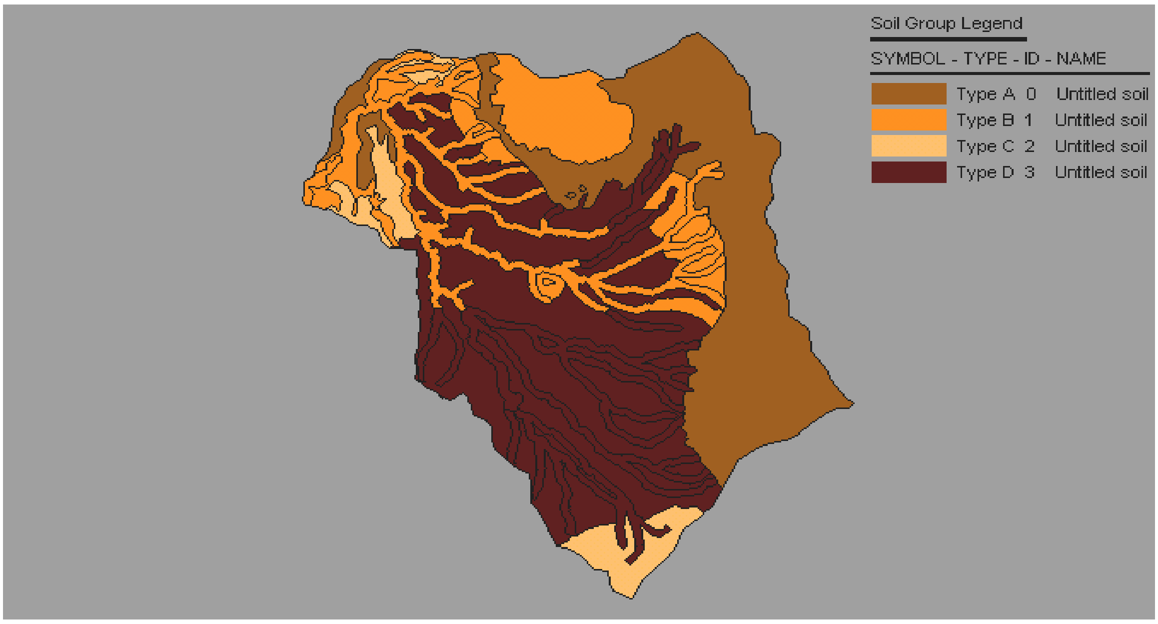

Plate 1.1 Hydrological soil group map.

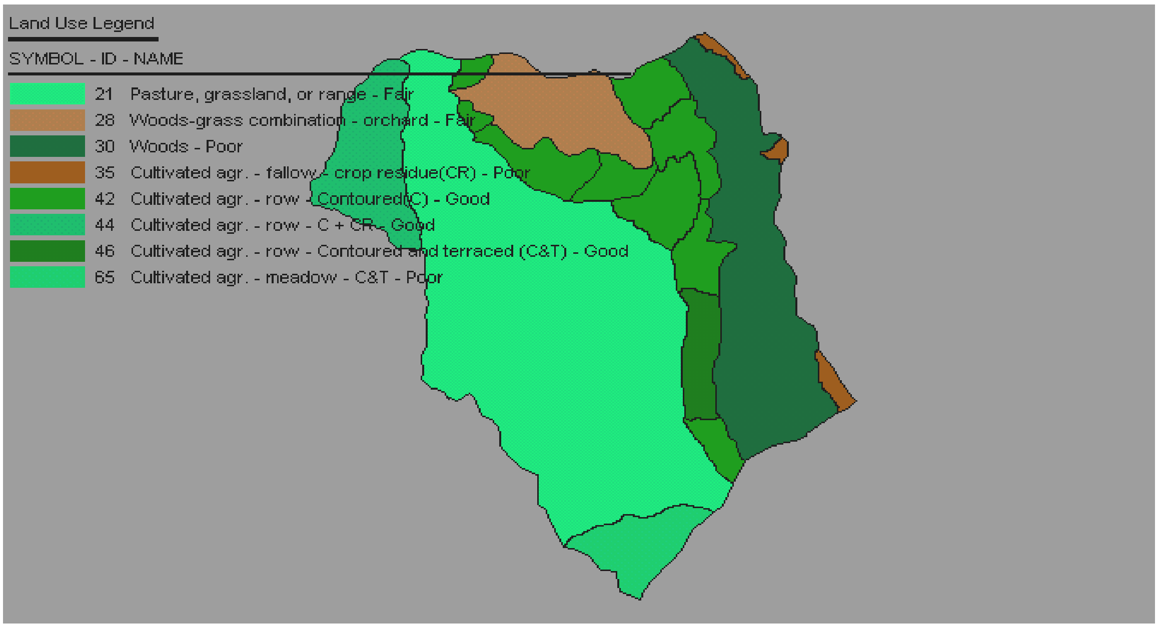

Plate 2.2. Land use map

Appendix B. HEC-1 Input and Output files

(B.1) HEC-1 INPUT File for Scenario I

```
  1          ID  Rainfall - Runoff Model
  2          ID  Turasha Sub Catchment
  3          ID  Lake Naivasha Basin
             *DIAGRAM
  4          IT      15 21NOV97    1800     300
  5          IO       0
  6          IM
             * Gage XY Position 223589.00000 9944688.00000 1
  7          PG    Mawi      10
             * Gage XY Position 236575.00000 9946540.00000 1
  8          PG    Mutu      31
             * Gage XY Position 216168.00000 9928090.00000 1
  9          PG   Olara      17
             * Gage XY Position 213270.00000 9946340.00000 0
 10          PG   Gage4
 11          IN       6 21NOV97       0
             * typeII-24hour

 36          PC       1

 37          KK      3B
 38          KO       0       0       0       1      22
 39          BA   50.02
 40          PR   Gage4
 41          PW       1
 42          PT    Mawi
 43          PW   51.66
 44          LS       0   86.05       0
 45          UD  1.6199
 46          KK      3R   CNAME      3C
 47          KO       0       0       0       0      22
 48          RM       5    1.32     0.2

 49          KK      5B
 50          KO       0       0       0       1      22
 51          BA   49.95
 52          PR   Gage4
 53          PW       1
 54          PT    Mutu
 55          PW   52.14
 56          LS       0   76.36       0
 57          UD  1.9158

 58          KK      6B
 59          KO       0       0       0       1      22
 60          BA   25.36
 61          PR   Gage4
 62          PW       1
 63          PT    Mutu    Mawi
 64          PW   17.99    8.28
 65          LS       0   82.33       0
 66          UD  1.5483

 67          KK      4C   CNAME      4R
 68          KO       0       0       0       0      22
 69          HC       2

 70          KK      4R   CNAME      4C
 71          KO       0       0       0       0      22
```

72	RM	2	0.64	0.2		
73	KK	9B				
74	KO	0	0	0	1	22
75	BA	33.85				
76	PR	Gage4				
77	PW	1				
78	PT	Mawi	Mutu			
79	PW	29.99	5.54			
80	LS	0	87.13	0		
81	UD	1.5332				
82	KK	5C	CNAME	5R		
83	KO	0	0	0	0	22
84	HC	2				
85	KK	5R	CNAME	5C		
86	KO	0	0	0	0	22
87	RM	4	1.115	0.2		
88	KK	11B				
89	KO	0	0	0	1	22
90	BA	70.82				
91	PR	Gage4				
92	PW	1				
93	PT	Olara				
94	PW	73.61				
95	LS	0	92.8	0		
96	UD	4.6325				
97	KK	6R	CNAME	6C		
98	KO	0	0	0	0	22
99	RM	4	1.008	0.2		
100	KK	15B				
101	KO	0	0	0	1	22
102	BA	24.14				
103	PR	Gage4				
104	PW	1				
105	PT	Olara	Mutu			
106	PW	20.42	5.09			
107	LS	0	89.03	0		
108	UD	2.0442				
109	KK	7R	CNAME	7C		
110	KO	0	0	0	0	22
111	RM	7	1.67	0.2		
112	KK	18B				
113	KO	0	0	0	1	22
114	BA	63.09				
115	PR	Gage4				
116	PW	1				
117	PT	Mutu	Olara	Mawi		
118	PW	32.92	24.73	8.38		
119	LS	0	83.69	0		
120	UD	2.8123				
121	KK	8R	CNAME	8C		
122	KO	0	0	0	0	22
123	RM	4	0.93	0.2		
124	KK	21B				
125	KO	0	0	0	1	22
126	BA	33.39				
127	PR	Gage4				
128	PW	1				

```
129            PT    Mutu    Mawi
130            PW   33.45    1.13
131            LS       0   77.71       0
132            UD  1.4248
133            KK      9R   CNAME      9C
134            KO       0       0       0       0      22
135            RM       5   1.366     0.2

136            KK     59B
137            KO       0       0       0       1      22
138            BA   68.86
139            PR   Gage4
140            PW       1
141            PT   Olara    Mawi
142            PW   36.71   33.73
143            LS       0   93.27       0
144            UD  3.8716

145            KK     60B
146            KO       0       0       0       1      22
147            BA   14.35
148            PR   Gage4
149            PW       1
150            PT   Olara    Mawi
151            PW   12.41    2.82
152            LS       0   93.05       0
153            UD  2.5776

154            KK     16C   CNAME     16R
155            KO       0       0       0       0      22
156            HC       6

157            KK     16R   CNAME     16C
158            KO       0       0       0       0      22
159            RM       4  0.9707     0.2

160            KK     54B
161            KO       0       0       0       1      22
162            BA   13.09
163            PR   Gage4
164            PW       1
165            PT    Mutu
166            PW    14.1
167            LS       0   68.75       0
168            UD  1.0808

169            KK     14R   CNAME     14C
170            KO       0       0       0       0      22
171            RM       6    1.51     0.2

172            KK     24B
173            KO       0       0       0       1      22
174            BA   36.74
175            PR   Gage4
176            PW       1
177            PT    Mutu
178            PW   38.46
179            LS       0   73.13       0
180            UD  1.7045

181            KK     10R   CNAME     10C
182            KO       0       0       0       0      22
183            RM       4   0.943     0.2

184            KK     27B
185            KO       0       0       0       1      22
186            BA   39.42
```

187	PR	Gage4				
188	PW	1				
189	PT	Mutu				
190	PW	40.96				
191	LS	0	74.47	0		
192	UD	1.9064				
193	KK	11R	CNAME	11C		
194	KO	0	0	0	0	22
195	RM	4	0.961	0.2		
196	KK	57B				
197	KO	0	0	0	1	22
198	BA	64.53				
199	PR	Gage4				
200	PW	1				
201	PT	Mawi	Mutu			
202	PW	37.09	30.37			
203	LS	0	89.88	0		
204	UD	3.0297				
205	KK	15C	CNAME	15R		
206	KO	0	0	0	0	22
207	HC	4				
208	KK	15R	CNAME	15C		
209	KO	0	0	0	0	22
210	RM	5	1.2846	0.2		
211	KK	62B				
212	KO	0	0	0	1	22
213	BA	20.29				
214	PR	Gage4				
215	PW	1				
216	PT	Mawi				
217	PW	21.23				
218	LS	0	90.99	0		
219	UD	1.5458				
220	KK	63B				
221	KO	0	0	0	1	22
222	BA	34.36				
223	PR	Gage4				
224	PW	1				
225	PT	Mawi				
226	PW	36.35				
227	LS	0	90.74	0		
228	UD	1.8688				
229	KK	17C	CNAME	17R		
230	KO	0	0	0	0	22
231	HC	5				
232	KK	17R	CNAME	17C		
233	KO	0	0	0	0	22
234	RM	4	1.1856	0.2		
235	KK	30B				
236	KO	0	0	0	1	22
237	BA	33.46				
238	PR	Gage4				
239	PW	1				
240	PT	Mawi				
241	PW	34.92				
242	LS	0	83.44	0		
243	UD	1.1486				

```
244         KK     12R   CNAME     12C
245         KO       0       0       0       0      22
246         RM       4   0.984     0.2

247         KK     64B
248         KO       0       0       0       1      22
249         BA    52.5
250         PR   Gage4
251         PW       1
252         PT    Mawi
253         PW   55.23
254         LS       0   89.28       0
255         UD  1.5808

256         KK      2C   CNAME      2R
257         KO       0       0       0       0      22
258         HC       4

259         KK      2R   CNAME      2C
260         KO       0       0       0       0      22
261         RN      2R
262         ZZ
```

(B.2) HEC-1 output file

RUNOFF SUMMARY, AVERAGE FLOW IN CUBIC METERS PER SECOND
AREA IN SQUARE KILOMETERS

			PEAK	TIME OF	AVERAGE FLOW FOR MAXIMUM PERIOD			BASIN
+					6-HOUR	24-HOUR	72-HOUR	
+	HYDROGRAPH AT	3B	.41	7.25	.17	.04	.01	50.02
+	ROUTED TO	3R	.37	8.50	.16	.04	.01	50.02
+	HYDROGRAPH AT	5B	9.99	7.00	5.42	1.44	.48	49.95
+	HYDROGRAPH AT	6B	5.74	6.75	3.02	.78	.26	25.36
+	2 COMBINED AT	4C	15.50	7.00	8.40	2.22	.74	75.31
+	ROUTED TO	4R	14.97	7.50	8.36	2.22	.74	75.31
+	HYDROGRAPH AT	9B	2.50	6.75	1.17	.30	.10	33.85
+	2 COMBINED AT	5C	16.94	7.50	9.52	2.52	.84	109.16
+	ROUTED TO	5R	16.16	8.50	9.43	2.52	.84	109.16
+	HYDROGRAPH AT	11B	14.35	9.00	11.73	4.26	1.42	70.82
+	ROUTED TO	6R	14.18	10.00	11.65	4.26	1.42	70.82
+	HYDROGRAPH AT	15B	6.56	7.00	4.14	1.14	.38	24.14
+	ROUTED TO	7R	6.26	8.50	4.09	1.14	.38	24.14
+	HYDROGRAPH AT	18B	10.53	7.75	6.99	2.03	.68	63.09
+	ROUTED TO	8R	10.27	8.75	6.94	2.03	.68	63.09
+	HYDROGRAPH AT	21B	8.45	6.75	4.21	1.08	.36	33.39
+	ROUTED TO	9R	7.82	8.00	4.17	1.08	.36	33.39
+	HYDROGRAPH AT	59B	10.88	8.25	8.42	2.81	.94	68.86
+	HYDROGRAPH AT	60B	3.71	7.25	2.60	.76	.25	14.35
+	6 COMBINED AT	16C	49.01	8.50	36.35	12.08	4.03	274.65

+	ROUTED TO	16R	48.08	9.50	36.09	12.08	4.03	274.65
+	HYDROGRAPH AT	54B	.94	6.50	.31	.08	.03	13.09
+	ROUTED TO	14R	.78	8.00	.31	.08	.03	13.09
+	HYDROGRAPH AT	24B	4.94	7.00	2.37	.61	.20	36.74
+	ROUTED TO	10R	4.66	8.00	2.36	.61	.20	36.74
+	HYDROGRAPH AT	27B	6.07	7.00	3.18	.84	.28	39.42
+	ROUTED TO	11R	5.80	8.00	3.16	.84	.28	39.42
+	HYDROGRAPH AT	57B	15.33	7.75	10.95	3.33	1.11	64.53
+	4 COMBINED AT	15C	26.33	8.00	16.71	4.85	1.62	153.78
+	ROUTED TO	15R	25.26	9.25	16.56	4.85	1.62	153.78
+	HYDROGRAPH AT	62B	1.49	6.75	.75	.19	.06	20.29
+	HYDROGRAPH AT	63B	2.14	7.00	1.14	.30	.10	34.36
+	5 COMBINED AT	17C	88.23	9.00	62.76	19.94	6.65	592.24
+	ROUTED TO	17R	85.59	10.25	62.09	19.94	6.65	592.24
+	HYDROGRAPH AT	30B	.00	.00	.00	.00	.00	33.46
+	ROUTED TO	12R	.00	.00	.00	.00	.00	33.46
+	HYDROGRAPH AT	64B	2.26	6.75	1.05	.27	.09	52.50
+	4 COMBINED AT	2C	85.88	10.25	62.57	20.25	6.75	728.22
+	ROUTED TO	2R	85.88	10.25	62.57	20.25	6.75	728.22

*** NORMAL END OF HEC-1 ***

Appendix C Output files for monthly simulations

OPERATION	STATION	PEAK FLOW CUMECS	TIME OF PEAK	MAXIMUM FLOWS 6-HOUR	24-HOUR	72-HOUR	BASIN AREA KM2
HYDROGRAPH AT	3B	0.7	18.3	0.7	0.3	0.1	50.0
ROUTED TO	3R	0.7	19.8	0.7	0.3	0.1	50.0
HYDROGRAPH AT	5B	0.0	0.0	0.0	0.0	0.0	50.0
HYDROGRAPH AT	6B	0.0	24.8	0.0	0.0	0.0	25.4
COMBINED AT	4C	0.0	24.8	0.0	0.0	0.0	75.3
ROUTED TO	4R	0.0	25.3	0.0	0.0	0.0	75.3
HYDROGRAPH AT	9B	0.8	16.0	0.7	0.3	0.1	33.9
COMBINED	5C	0.8	16.0	0.7	0.3	0.1	109.2
ROUTED TO	5R	0.8	17.3	0.7	0.3	0.1	109.2
HYDROGRAPH AT	11B	9.6	16.3	7.9	3.5	1.2	70.8
ROUTED TO	6R	9.5	17.3	7.9	3.5	1.2	70.8
HYDROGRAPH AT	15B	1.8	14.0	1.3	0.5	0.2	24.1
ROUTED TO	7R	1.6	15.8	1.2	0.5	0.2	24.1
HYDROGRAPH AT	18B	0.5	21.3	0.5	0.2	0.1	63.1
ROUTED TO	8R	0.5	22.3	0.5	0.2	0.1	63.1
HYDROGRAPH AT	21B	0.0	0.0	0.0	0.0	0.0	33.4
ROUTED TO	9R	0.0	0.0	0.0	0.0	0.0	33.4
HYDROGRAPH AT	59B	9.8	17.0	8.3	3.8	1.3	68.9
HYDROGRAPH AT	60B	3.3	14.0	2.1	0.8	0.3	14.4
COMBINED AT	16C	22.2	17.0	19.0	8.7	2.9	274.7
ROUTED TO	16R	22.0	18.0	18.8	8.7	2.9	274.7
HYDROGRAPH AT	54B	0.0	0.0	0.0	0.0	0.0	13.1
ROUTED TO	14R	0.0	0.0	0.0	0.0	0.0	13.1
HYDROGRAPH AT	24B	0.0	0.0	0.0	0.0	0.0	36.7
ROUTED TO	10R	0.0	0.0	0.0	0.0	0.0	36.7
HYDROGRAPH AT	27B	0.0	0.0	0.0	0.0	0.0	39.4
ROUTED TO	11R	0.0	0.0	0.0	0.0	0.0	39.4
HYDROGRAPH AT	57B	4.4	15.8	3.6	1.6	0.5	64.5
COMBINED AT	15C	4.4	15.8	3.6	1.6	0.5	153.8
ROUTED TO	15R	4.3	17.0	3.6	1.6	0.5	153.8
HYDROGRAPH AT	62B	2.1	15.3	1.6	0.7	0.2	20.3
HYDROGRAPH AT	63B	3.0	16.0	2.4	1.1	0.4	34.4
COMBINED AT	17C	30.5	17.8	26.6	12.3	4.1	592.2
ROUTED TO	17R	30.2	19.0	26.4	12.3	4.1	592.2
HYDROGRAPH AT	30B	0.2	24.0	0.1	0.0	0.0	33.5
ROUTED TO	12R	0.2	24.8	0.1	0.0	0.0	33.5
HYDROGRAPH AT	64B	3.0	15.0	2.4	1.1	0.4	52.5
COMBINED AT	2C	32.8	19.0	28.9	13.7	4.6	728.2
ROUTED TO	2R	32.8	19.0	28.9	13.7	4.6	728.2

c.1. Simulation result for average antecedent moisture conditions

OPERATION	STATION	PEAK	TIME OF	AVERAGE FOR MAXIMUM PERIOD			BASIN
		FLOW	PEAK	6-HOUR	24-HOUR	72-HOUR	AREA
HYDROGRAPH AT	3B	15.8	14.0	9.7	3.5	1.2	50.0
ROUTED TO	3R	15.0	15.5	9.6	3.5	1.2	50.0
HYDROGRAPH AT	5B	2.4	15.0	1.9	0.8	0.3	50.0
HYDROGRAPH AT	6B	4.3	14.5	2.9	1.1	0.4	25.4
2 COMBINED AT	4C	6.6	14.5	4.8	2.0	0.7	75.3
ROUTED TO	4R	6.4	15.3	4.8	2.0	0.7	75.3
HYDROGRAPH AT	9B	13.9	13.8	7.8	2.7	0.9	33.9
2 COMBINED AT	5C	18.0	14.3	12.1	4.6	1.5	109.2
ROUTED TO	5R	17.1	15.3	12.0	4.6	1.5	109.2
HYDROGRAPH AT	11B	35.4	15.8	27.0	10.3	3.4	70.8
ROUTED TO	6R	34.8	16.8	26.8	10.3	3.4	70.8
HYDROGRAPH AT	15B	15.0	13.3	7.2	2.4	0.8	24.1
ROUTED TO	7R	12.8	15.3	7.0	2.4	0.8	24.1
HYDROGRAPH AT	18B	11.1	15.3	8.3	3.3	1.1	63.1
ROUTED TO	8R	10.9	16.0	8.2	3.3	1.1	63.1
HYDROGRAPH AT	21B	2.8	13.5	1.8	0.7	0.2	33.4
ROUTED TO	9R	2.5	15.0	1.8	0.7	0.2	33.4
HYDROGRAPH AT	59B	32.3	16.3	26.1	10.5	3.5	68.9
HYDROGRAPH AT	60B	12.5	13.8	6.6	2.2	0.7	14.4
6 COMBINED AT	16C	92.7	16.0	73.7	29.3	9.8	274.7
ROUTED TO	16R	90.9	17.0	73.0	29.3	9.8	274.7
HYDROGRAPH AT	54B	0.1	23.8	0.1	0.0	0.0	13.1
ROUTED TO	14R	0.1	25.0	0.1	0.0	0.0	13.1
HYDROGRAPH AT	24B	0.8	15.8	0.7	0.3	0.1	36.7
ROUTED TO	10R	0.7	16.8	0.7	0.3	0.1	36.7
HYDROGRAPH AT	27B	1.2	15.0	1.0	0.5	0.2	39.4
ROUTED TO	11R	1.1	16.3	1.0	0.5	0.2	39.4
HYDROGRAPH AT	57B	28.1	14.8	19.2	6.9	2.3	64.5
4 COMBINED AT	15C	29.4	14.8	20.5	7.7	2.6	153.8
ROUTED TO	15R	28.4	16.3	20.3	7.7	2.6	153.8
HYDROGRAPH AT	62B	10.6	14.5	7.0	2.4	0.8	20.3
HYDROGRAPH AT	63B	15.4	15.0	11.0	4.0	1.3	34.4
5 COMBINED AT	17C	148.3	16.5	119.4	48.0	16.0	592.2
ROUTED TO	17R	145.3	17.8	118.1	48.0	16.0	592.2
HYDROGRAPH AT	30B	9.1	13.5	4.8	1.7	0.6	33.5
ROUTED TO	12R	8.1	14.5	4.7	1.7	0.6	33.5
HYDROGRAPH AT	64B	25.0	14.3	15.2	5.2	1.8	52.5
4 COMBINED AT	2C	165.1	17.5	137.6	58.4	19.5	728.2
ROUTED TO	2R	165.1	17.5	137.6	58.4	19.5	728.2

c.2. Results for simulation with antecedent moisture conditions III

Appendix D Double mass analysis

Double mass analysis was done for the stations which had long term annual data within the catchment. From the analysis it was clearly shown that most of the stations lacked continuity in data collected. The graphs below indicate the type of results.

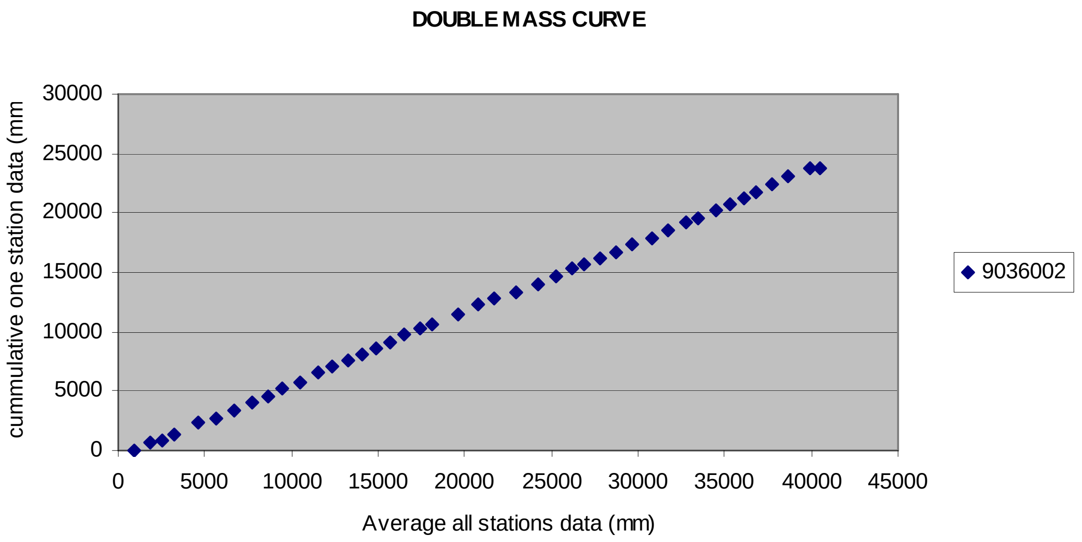
DOUBLE MASS CURVE
cummulative one station data (mm
30000
25000
20000
15000
10000
5000
0
0
5000
10000
15000
20000
25000
30000
35000
40000
45000
Average all stations data (mm)
9036002

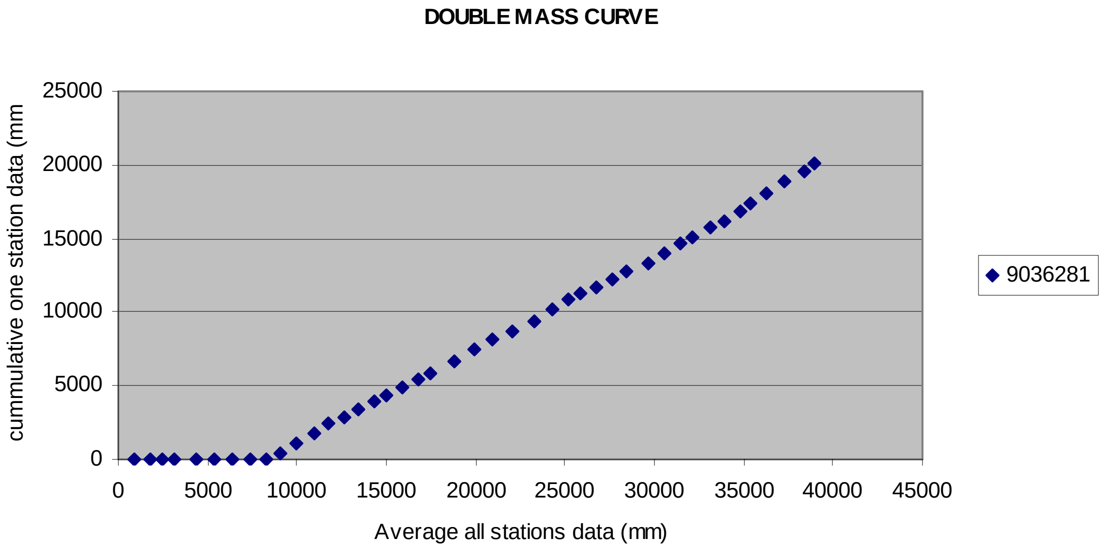
DOUBLE MASS CURVE
cummulative one station data (mm
25000
20000
15000
10000
5000
0
0
5000
10000
15000
20000
25000
30000
35000
40000
45000
Average all stations data (mm)
9036281

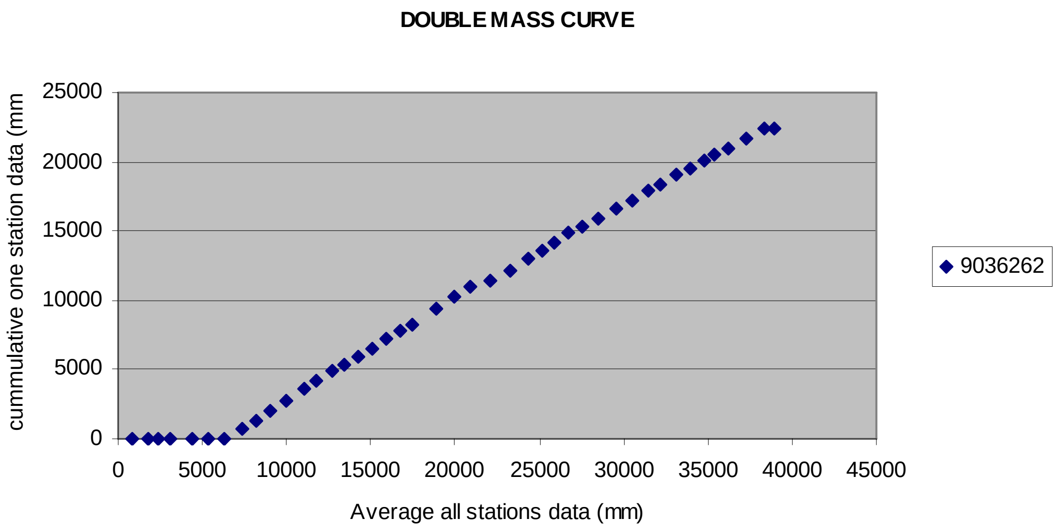
DOUBLE MASS CURVE
cummulative one station data (mm
25000
20000
15000
10000
5000
0
0
5000
10000
15000
20000
25000
30000
35000
40000
45000
Average all stations data (mm)
9036262

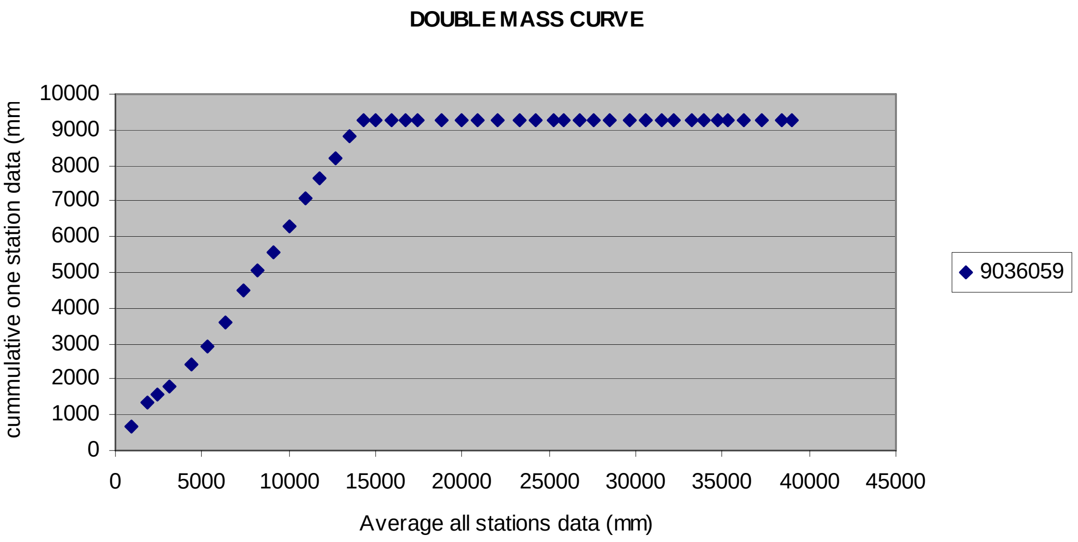
DOUBLE MASS CURVE
cummulative one station data (mm
10000
9000
8000
7000
6000
5000
4000
3000
2000
1000
0
0
5000
10000
15000
20000
25000
30000
35000
40000
45000
Average all stations data (mm)
9036059

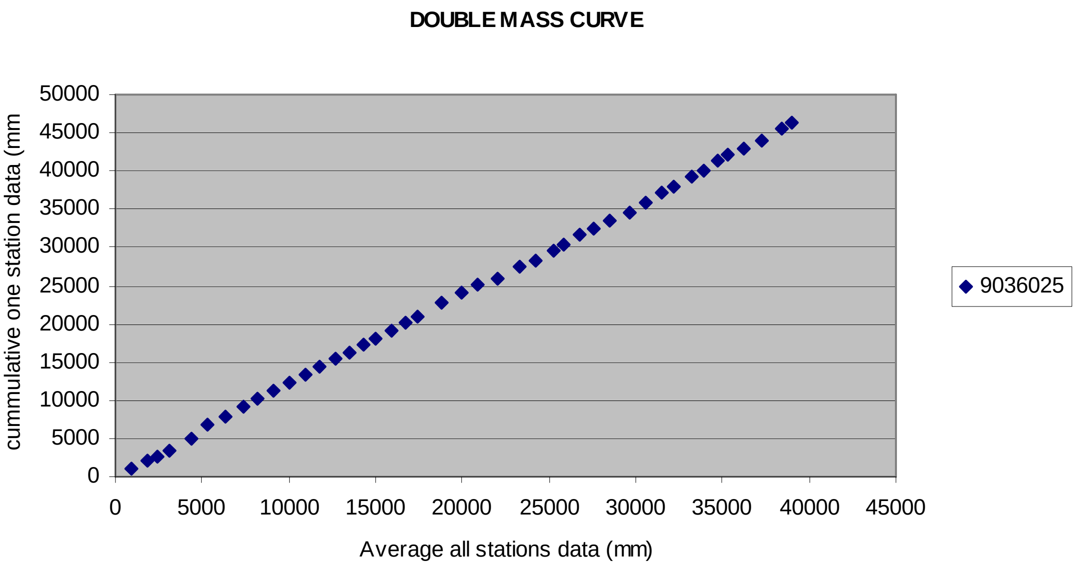
DOUBLE MASS CURVE
cummulative one station data (mm
50000
45000
40000
35000
30000
25000
20000
15000
10000
5000
0
0
5000
10000
15000
20000
25000
30000
35000
40000
45000
Average all stations data (mm)
9036025

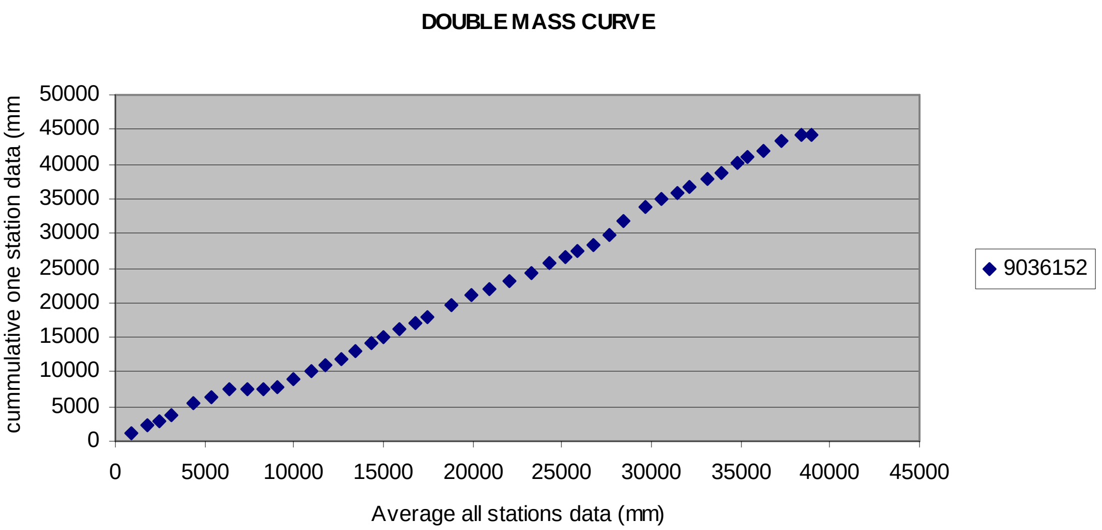
DOUBLE MASS CURVE
cummulative one station data (mm
50000
45000
40000
35000
30000
25000
20000
15000
10000
5000
0
0
5000
10000
15000
20000
25000
30000
35000
40000
45000
Average all stations data (mm)
9036152

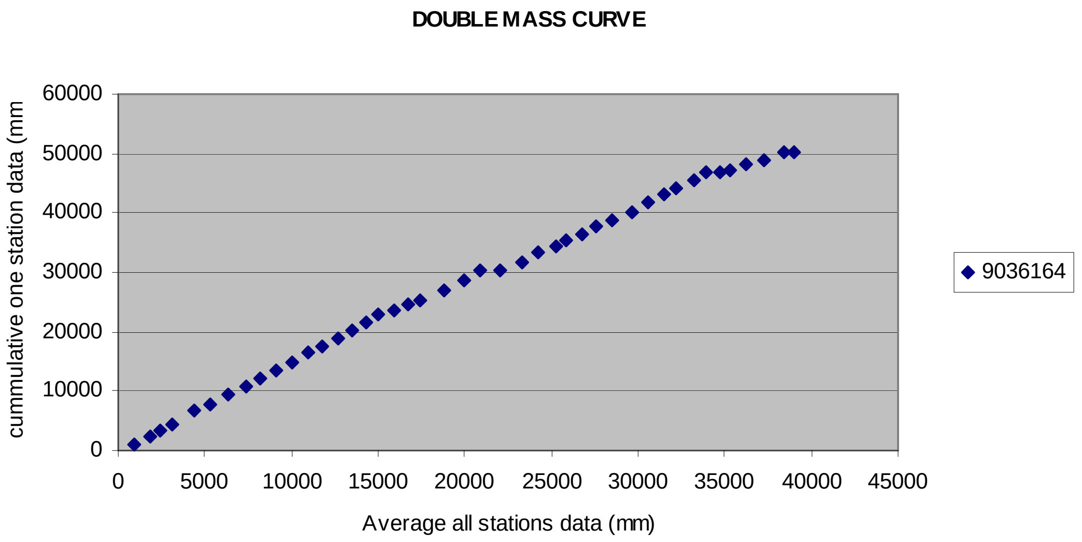
DOUBLE MASS CURVE
cummulative one station data (mm
60000
50000
40000
30000
20000
10000
0
0
5000
10000
15000
20000
25000
30000
35000
40000
45000
Average all stations data (mm)
9036164

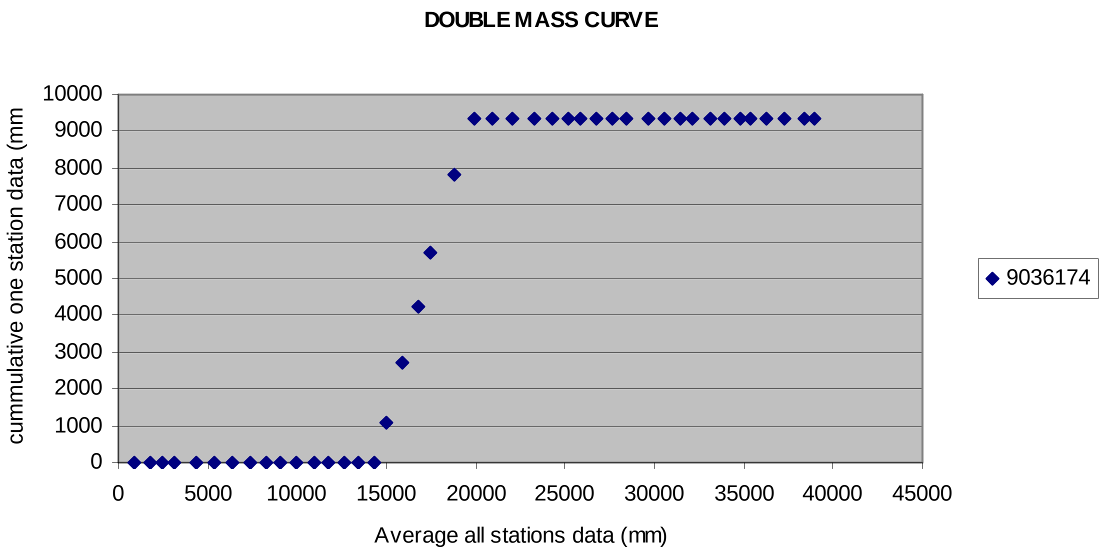
DOUBLE MASS CURVE
cummulative one station data (mm
10000
9000
8000
7000
6000
5000
4000
3000
2000
1000
0
0
5000
10000
15000
20000
25000
30000
35000
40000
45000
Average all stations data (mm)
9036174

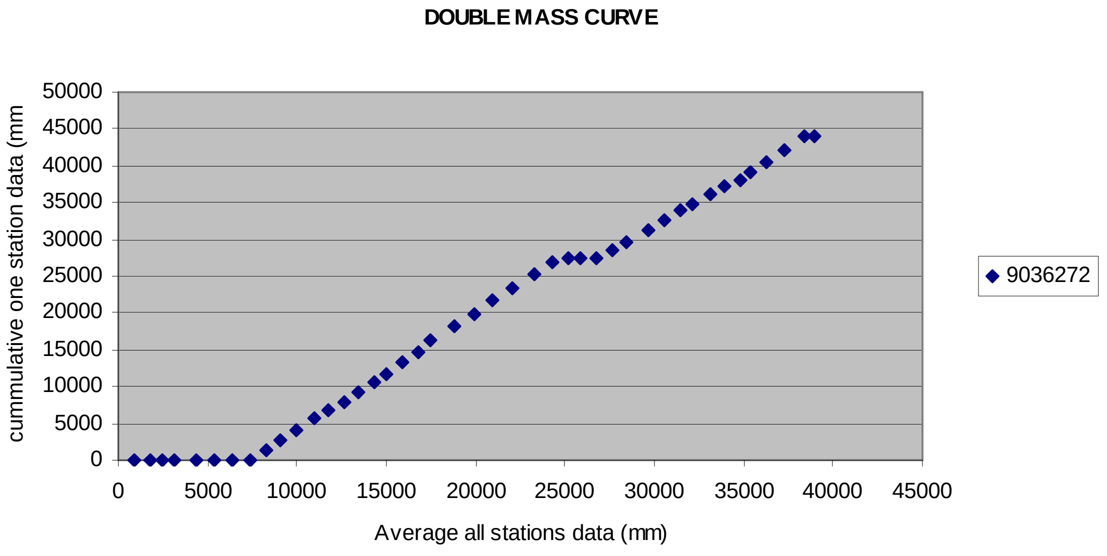
DOUBLE MASS CURVE
cummulative one station data (mm
50000
45000
40000
35000
30000
25000
20000
15000
10000
5000
0
0
5000
10000
15000
20000
25000
30000
35000
40000
45000
Average all stations data (mm)
9036272

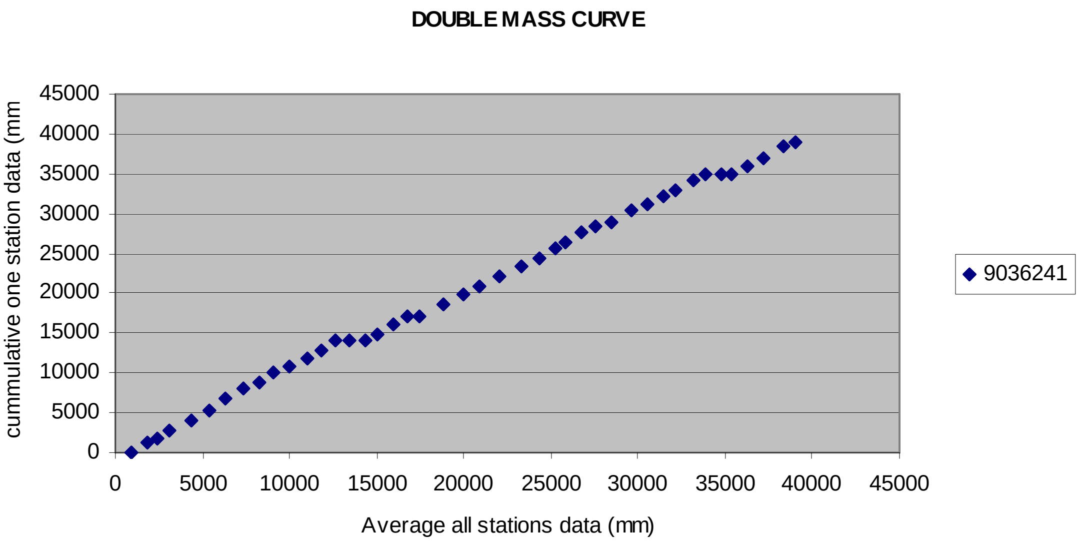
DOUBLE MASS CURVE
cummulative one station data (mm
45000
40000
35000
30000
25000
20000
15000
10000
5000
0
0
5000
10000
15000
20000
25000
30000
35000
40000
45000
Average all stations data (mm)
9036241

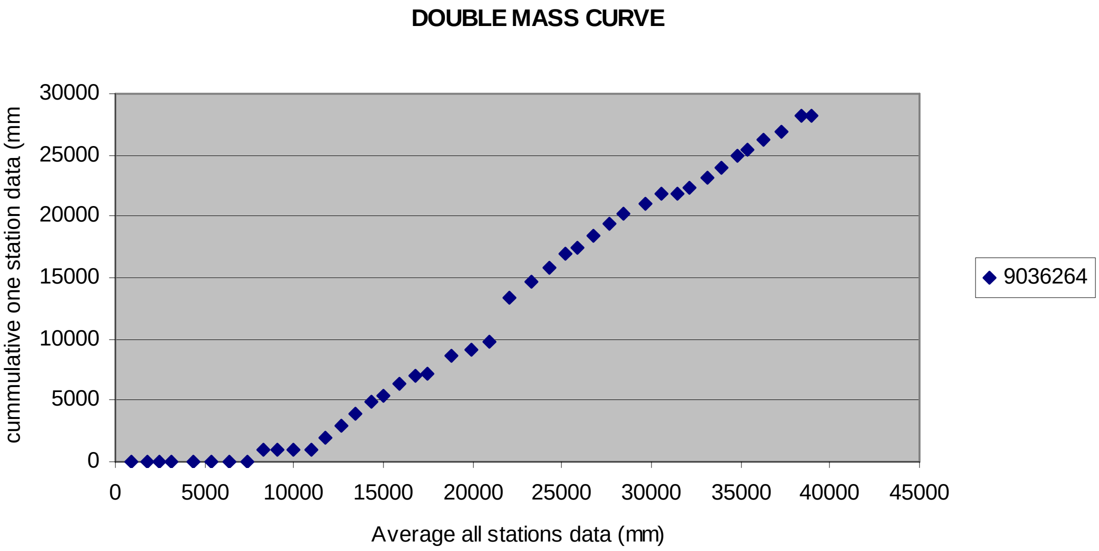
DOUBLE MASS CURVE
cummulative one station data (mm
30000
25000
20000
15000
10000
5000
0
0
5000
10000
15000
20000
25000
30000
35000
40000
45000
Average all stations data (mm)
9036264

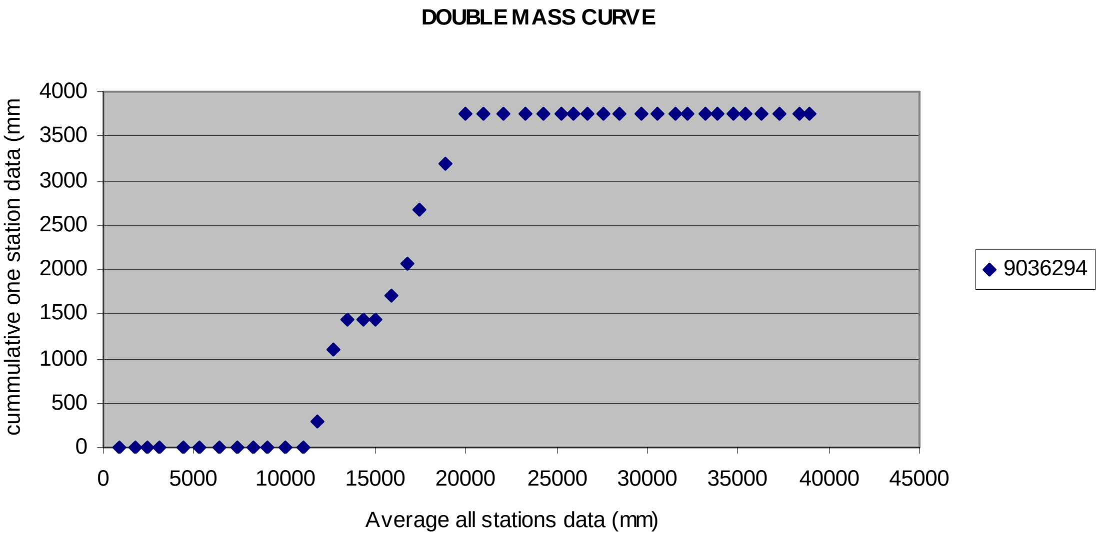
DOUBLE MASS CURVE
cummulative one station data (mm
4000
3500
3000
2500
2000
1500
1000
500
0
0
5000
10000
15000
20000
25000
30000
35000
40000
45000
Average all stations data (mm)
9036294

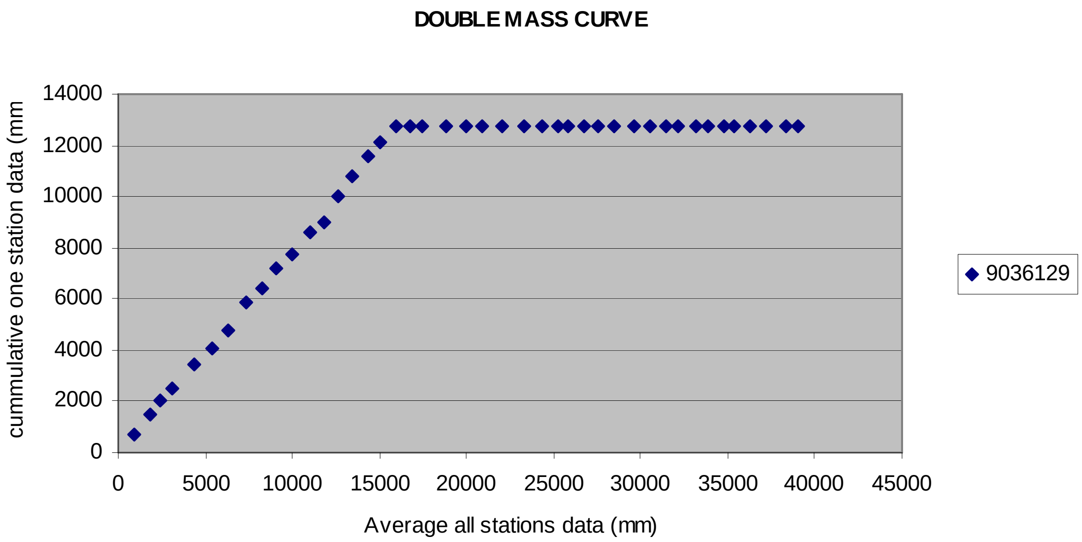
DOUBLE MASS CURVE
cummulative one station data (mm
Average all stations data (mm)
9036129
0
2000
4000
6000
8000
10000
12000
14000
5000
15000
20000
25000
30000
35000
40000
45000

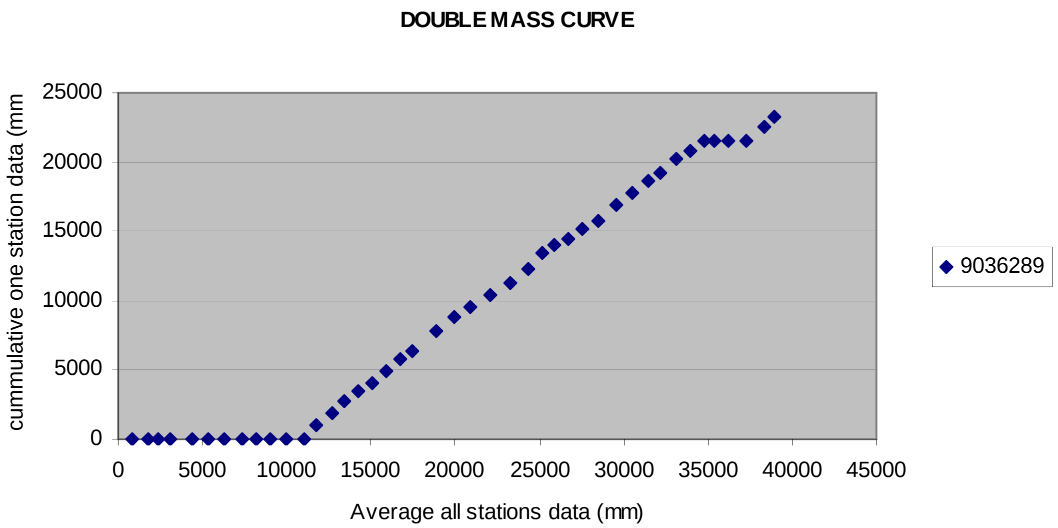
DOUBLE MASS CURVE
cummulative one station data (mm
Average all stations data (mm)
9036289
0
5000
10000
15000
20000
25000
30000
35000
40000
45000

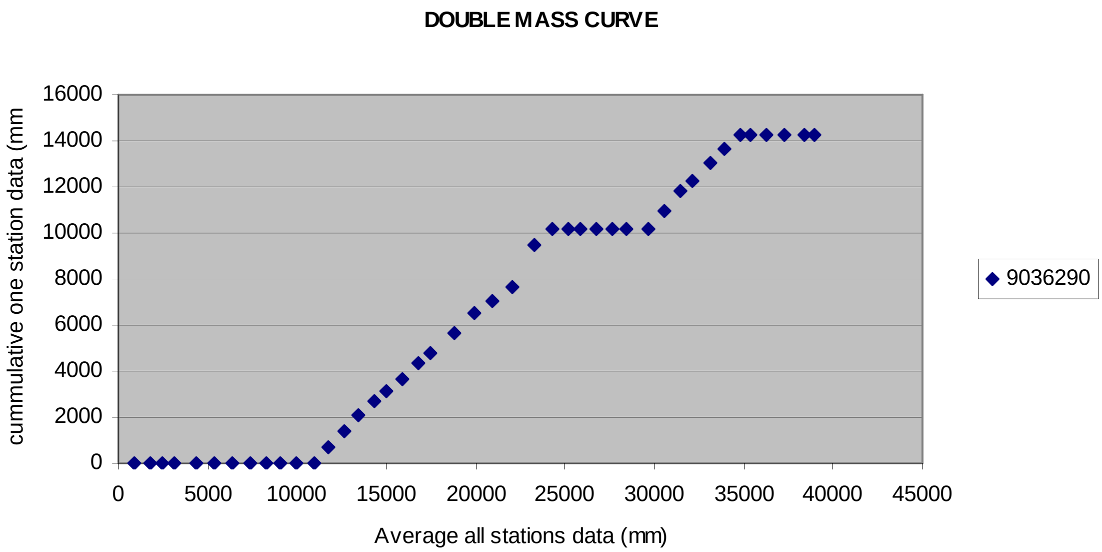
DOUBLE MASS CURVE
cummulative one station data (mm
Average all stations data (mm)
9036290
0
2000
4000
6000
8000
10000
12000
14000
16000
5000
15000
20000
25000
30000
35000
40000
45000

Appendix E Daily data from Geta Rainfall station

Rainfall data from Geta Rainfall station for October 1998

Date	Automatic rainfall record	Manual Rainfall record
1-Oct-98	0	0
2-Oct-98	0	0
3-Oct-98	0	0
4-Oct-98	0	0
5-Oct-98	0	0
6-Oct-98	6	3
7-Oct-98	6	0
8-Oct-98	4	10
9-Oct-98	0	0
10-Oct-98	0	0
11-Oct-98	1	0
12-Oct-98	4	5
13-Oct-98	7	5
14-Oct-98	3	6
15-Oct-98	1	11
16-Oct-98	10	0
17-Oct-98	0	0
18-Oct-98	0	0
19-Oct-98	0	0
20-Oct-98	1	0
21-Oct-98	0	0
22-Oct-98	0	0
23-Oct-98	0	0
24-Oct-98	0	0
25-Oct-98	0	0
26-Oct-98	5	8
27-Oct-98	0	15
28-Oct-98	14	0
29-Oct-98	6	7
30-Oct-98	1	0
31-Oct-98	21	0
Total	90	70

This table briefly shows the difference in Rainfall data collected in the same site but with different collection methods. As can be seen in the daily values, there occurs a lot of discrepancies e.g. on 7th and 8th of October there was rainfall recorded on the automatic logger but appeared as a single event in the Manual observation on 8th of the same month.

The graph below shows the variations between the manually observed rainfall data and the automatically recorded gauge for Geta rainfall station. It can be noticed that the data sets are not consistence most of the times which leads to the unreliability of the daily rainfall recordings.

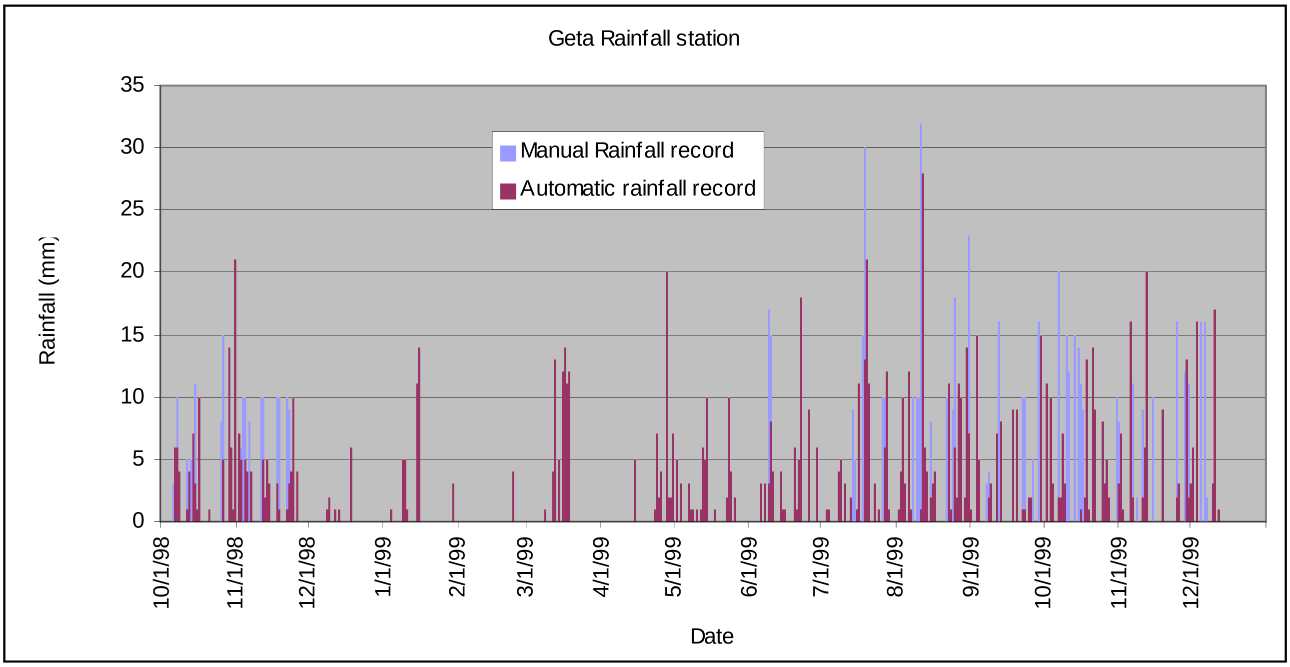
Geta Rainfall station
Manual Rainfall record
Automatic rainfall record
Rainfall (mm)
35
30
25
20
15
10
5
0
10/1/98
11/1/98
12/1/98
1/1/99
2/1/99
3/1/99
4/1/99
5/1/99
6/1/99
7/1/99
8/1/99
9/1/99
10/1/99
11/1/99
12/1/99
Date